Characterisation of a pair of copper storage proteins from pathogenic bacteria

Safa Abdullah Alsharif

Thesis submitted for the degree of Doctor of Philosophy

Newcastle University

Faculty of Medical Sciences

Biosciences Institute

January 2020

Abstract

Neisseria gonorrhoeae is a pathogenic Gram-negative bacterium that causes human gonorrhoeal disease. Its genome encodes a putative periplasmic homologue of a new family of copper storage proteins (Csp) recently described in methanotrophic bacteria. Although members of this protein family are abundant in pathogenic bacteria, the presence of this periplasmic Csp in *N. gonorrhoeae* is almost unique. Most Csp genes in pathogenic bacterial genomes lack a signal peptide and are therefore presumed to be cytosolic. For example, the Csp protein encoded in genomes of *Salmonella* sp. lacks a signal sequence. However, the *N. gonorrhoeae* Csp possesses a putative Tat signal for targeting it to the periplasm. *Salmonella enterica* is an important global pathogen, consisting of more than 2500 various serovars that can be host-specific or can have a broad range of hosts, whereas *N. gonorrhoeae* is highly specialised for infecting humans. Antibiotic resistance in both of these bacteria, *N. gonorrhoeae* and *S. enterica*, further enhances their risk to human health.

Copper is a redox active metal that is essential for several biological functions as a cofactor used by a number of copper-dependent enzymes. However, excess copper is toxic; thus, its homeostasis is carefully regulated through a system of protein transporters, sensors, trafficking proteins, and storage proteins. The Waldron lab is studying the form and function of these Csp proteins in pathogenic bacteria, as copper is known to play an important role in the innate immune system's ability to fight infection. It is anticipated that a putative role for *N. gonorrhoeae* Csp1 and *Salmonella* Csp3 in defending these pathogens from attack by the immune system would make these proteins potential therapeutic targets for future antibiotics.

This study explored the copper binding properties of Csp1 from *N. gonorrhoeae* and of Csp3 from *S. enterica*, in order to understand how they may be able to aid virulence, either through sequestration of excess copper, thereby reducing copper toxicity, or by storing copper during times of abundance and subsequent release of copper during copper deficiency. Copper binding by the Csp proteins was assessed, and the crystal structure of *Salmonella* Csp3 was determined. We concluded that Csps bind a large number of copper ions, likely as a storage mechanism, within a four-helix bundle structure that could be targeted in future drug discovery programmes.

Declaration

I declare that this thesis is outcome of my own research except where acknowledged. Under the guidance Dr.Kevin Waldron. It has not been previously submitted to support an application of any degree or certificate of this institute or other institute or university .

Safa Abdullah Alsharif

Acknowledgements

I am so glad to be part of Newcastle University and having the opportunity to work under Dr Kevin Waldron supervision. Thanks for making me feel confident in my abilities, for your support, positive guidance, encouragement, your patience and your help until the last minute. I would like also to thank Dr Arnaud Baslé for collecting crystallographic data and solving the crystal structure. Special thanks to louisa stewart and Abbi Kelly for their help and support. I would like also to extent my thanks to Dr. Paula Salgado and her group. I would like to appreciate all the members of the Institute for Cell and Molecular Bioscience, Newcastle University, and technical advice. In addition, I would like to thank my parents especially my beloved and supportive father for his kindness and unlimited support. Furthermore, I could not have completed this thesis without the support of my sister Bushra, and my brothers Bader and Omar, also my friends Tasneem, Reem, and Modi, who provided me joyful time to relax my mind outside of lab work stress. Finally, I would like to thank my husband Omar Al Attas from the bottom of my heart for supporting me spiritually and for his patience through tough times.

Safa Abdullah Alsharif

Table of contents

List of figures

List of tables

List of Abbreviations

(Csps)	Copper storage proteins
(PID)	Pelvic inflammatory disease
(ELISA)	Enzyme-linked immunosorbent assay
(iNOS)	Inducible nitric oxide synthase
(MMPs)	Matrix metalloproteinases
(WHO)	World health organisation
(ROS)	Reactive oxygen species
(TGN)	Trans-Golgi network
(Cys)	Cysteine
(FumA)	Fumarase-A
(TCA)	Tricarboxylic acid cycle
(PP)	Pentose phosphate
(RND)	Resistance/nodulation/cell division
(MCO)	Multi-copper oxidases
(Mct-B)	Mycobacterial copper transport protein B
(SR)	Sarcoplasmic reticulum
(TMH)	Transmembrane helices
(SOD1)	Superoxide dismutase
(MTs)	Metallothioneins
(pMMO)	Marticulate methane monooxygenase
(sMMO)	Moluble MMO
(Mbn)	Methanobactin
(STIs)	Transmitted infections

(AEC) Anion exchange chromatography

(SEC) Size exclusion chromatography

(Kan) Kanamycin

(CV) Column volume

(ε) Extinction coefficient ($M^{-1}cm^{-1}$)

(ICP-MS) Inductively coupled plasma mass spectrometry

(LB) Luria-Bertani

(OD) Optical density

(M9) Minimal medium

(IPTG) Isopropyl β-D-1-thiogalactopyranoside

(MW) Molecular weight

(Tris) tris(hydroxymethyl)aminomethane

(KDa) Kilo Dalton

(MW) Molecular weight

(SDS-PAGE) Sodium dodecyl sulfate–polyacrylamide gel electrophoresis

Chapter 1: Introduction

1.1 The bacterial pathogens under study

1.1.1 The pathogenicity of *Neisseria gonorrhoeae*

The obligate human pathogen *Neisseria gonorrhoeae* is the etiological agent causing the human disease gonorrhoea, which affects approximately 106.1 persons out of 100,000 per year in USA (Health and Services, 2012; Hill et al., 2016). This gonococcus species is a Gram negative bacterium, which was isolated for the first time by Albert Neisser in 1879. Infection rates by gonococcus is increasing in humans due to increasing resistance to antimicrobials (Knapp et al., 1994) that caused).

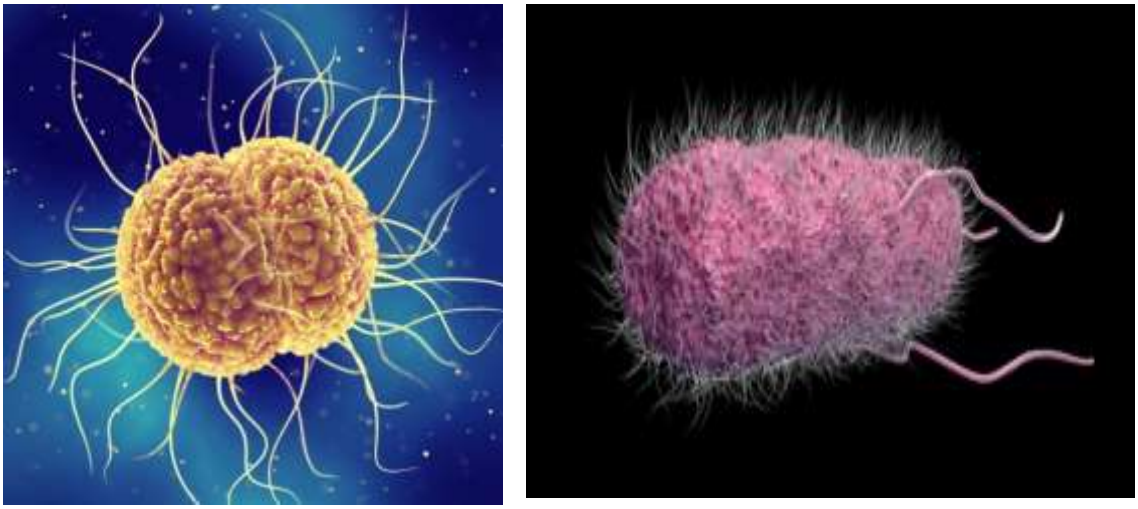

Figure 1.1. Cartoon diagram of Gram negative *Neisseria gonorrhoeae* and *Salmonella.*

Image attribution: Neisseria Gonorrhoeae Antigen - The Native Antigen Company; Salmonella Bacteria Isolated On Black Background. 3d Illustration Stock Photo, Picture And Royalty Free Image. Image 95013100. (123rf.com)

The bacterium arranges itself into pairs, termed diplococcus. As with all Gram negative bacteria, the cell envelope structure contains both an inner membrane and an outer membrane, with the peptidoglycan cell wall localized between the membranes. The bacteria have hair-like pili on their surface.

N. gonorrhoeae causes infections in humans primarily via sexual transmission. Gonorrhoea grows and multiplies rapidly in the mucous membranes of the mouth and anus of male and female, and especially in the uterus of human females. Infection of a human female with this organism often starts at the cervix, which is the dividing line between the lower and upper reproductive tract (Eschenbach et al., 1975). This infection at the cervix may be with or without symptoms, and infection of the fallopian tubes and upper reproductive tract occurs in approximately 10-20% of females without treatment. The infection in the fallopian tube can lead to the stage of pelvic inflammatory disease (PID), which can result in a high risk of ectopic pregnancy (2-9%), tubular factor infertility (3-16%), and severe chronic pelvic pain (36% of patients) (Waldron and Robinson, 2009; Weström et al., 1992).

N. gonorrhoeae infection is difficult to study because it is not easily adaptable to laboratory model animals because of its intense adaptation to specifically infect the human host. An experimental infection study was attempted in chimpanzees but this was expensive and unfortunately not suitable for large-scale study (Lenz and Dillard, 2018). Over the last 20 years, an innovative female mouse model has proven somewhat useful for understanding some of details of the complex immune response to *N. gonorrhoeae* infections, despite numerous morphological, physiological and biochemical differences between the human and murine female reproductive tract as well as between the human and murine immune responses. As an alternative, a technique using explants has provided an opportunity to understand the mechanisms of gonococcal infection on human female epithelial cells, the targeted site for this kind of infection (Lenz and Dillard, 2018; Quillin and Seifert, 2018). This particular study showed that gonococcal infection results in the production of numerous cytokines and chemokines by activating the nuclear transcription factor kappa-B (NF-κB), which were detected via enzyme-linked immunosorbent assay (ELISA) as early as after 3 hours of infection of the human cells with *N. gonorrhoeae* (Maisey et al., 2003).

The host also produces nitric oxide (NO) as a reaction to inflammation on mucosal epithelial cells via the enzyme inducible nitric oxide synthase (iNOS). The survival of gonococcal species decrease in correlation with the activity of iNOS within human cervical epithelial cells, although it is not clear if the damaging effects on the bacterium by NO in the fallopian tube is direct or indirect (Edwards, 2010). This kind of infection also induces the host to secrete matrix

metalloproteinases (MMPs) that function to degrade the extracellular matrix. Gonococcal infection of the fallopian tube induces intracellular accumulation of MMP2 and increases the secretion level of MMP9 (Lenz and Dillard, 2018; Van den Steen et al., 2003). The data demonstrated these enzymes as prime candidates for mechanistic damage of epithelial cells (Rodríguez-Tirado et al., 2012) .

1.1.2 The pathogenicity of *Salmonella enterica*

Salmonella enterica is a Gram-negative bacterium which is a facultative anaerobe (Santiviago et al., 2002; Hartman et al., 2014). The genus Salmonella is composed of two taxonomical species, *Salmonella bongori* and *Salmonella enterica*. *S. enterica* has the highest medical importance, consisting of more than 2500 various serovars (Lamas et al., 2018; Evangelopoulou et al., 2013). Isolates of this pathogen can be host-specific or can have a broad range of hosts. It is frequently present within the human food chain, which is the major source of human infections. It has flagella on its surface, which play an important role in its motility, attachment and penetration into the host cells, and its morphology is rod-shaped (Hedemann et al., 2005).

Salmonella has many serovars which are of great importance to human health. *S. enterica* sv. Typhi causes typhoid in humans, whereas *S. enterica* sv. Typhimurium infects a wide range of animals, including humans, and causes generally self-limiting diarrhoea (Jajere, 2019). *S.* Typhi is mainly host-specific, restricted to infection of humans, although is some evidence of other more primitive hosts that can be infected experimentally (Bäumler and Fang, 2013). Other serovars, e.g. *S. pullorum* and *S. galinarum*, are host-specific to birds, and there has been research on their infectivity in humans that suggest they can cause a typhoid-like disease as well (Chappell et al., 2009). Many animal models have been used to study the molecular mechanisms involved in pathogenicity of *S. enterica*, however these have focused most on gastrointestinal disease and least on typhoid fever. About ninety percent of the genome of *S. enterica* sv. Typhi, which is smaller than that of *S.* Typhimurium due to genome reduction processes, is homologous to other *Salmonella* serovars (Desai et al., 2013). Therefore, it is considered that the Typhi genome represents a kind of ‘core genome’ for Salmonella, and encodes genes associated with the infectivity and pathogenicity of all Salmonella species, including *S. enterica* sv. Typhi (Gerlach and Hensel, 2007).

Human typhoid fever has nonetheless been studied by using animal models that were infected with *S. enterica* serovar Typhimurium. This serovar induces typhoid-like disease in organisms such as mice, but only more localised and self-limiting gastrointestinal infections in humans. *S. enterica* sv. Typhimurium and *S. enterica* sv. Dublin have also been used in studies of intestinal diseases in human and other animals (Coburn et al., 2005; Dougan and Baker, 2014). These models have been helpful in understanding *Salmonella* pathogenicity at the genetic level, and many genes responsible for the intestinal diseases have been identified due to their association with infection of the epithelial tissues. These genes include invasion-associated genes responsible for inflammatory and secretory responses of the intestine in human (Khor et al., 2011; Wallis and Galyov, 2000). More serious systemic pathogenesis depends upon bacterial survival in intracellular niches within macrophages and intestinal epithelium cells (Takaya et al., 2004). The major primary sites for the invasion of *S. enterica* sv. Typhi are M cells of the ileal Peyer's patches (Lai et al., 2020). Later these can proliferate and migrate to spleen and liver via the reticuloendothelial system, resulting in typhoid fever in the host animal (Lai et al., 2020).

Various virulence systems have been identified from prior studies, including most notably those encoded within Salmonella pathogenicity island 1 (SPI1) and Salmonella pathogenicity island 2 (SPI2), based on the pathogenicity patterns in *Salmonella* isolates (Ibarra and Steele-Mortimer, 2009; Ochman and Groisman, 1996; Dieye et al., 2009). These horizontally acquired genomic islands encode a type III secretion system (T3SS), capable of secreting bacterial proteins into the host cell (Galán, 2001). Experimental data suggest that SPI2 is responsible for intracellular survival and systemic proliferation of *Salmonella enterica* into the target organs i.e. liver and spleen, while SPI1 plays a major role in the invasion of the bacterium into the intestinal epithelium cells (Miao et al., 1999; Dieye et al., 2009; Jones et al., 2007).

1.1.3. Antibiotic resistance

Antibiotic resistance is one of the key threats to human health worldwide. As pathogens become resistant to clinically important antibiotics through the spread of resistance genes under selection pressure caused by non-selective use of antibiotics in medicine and farming, these drugs become progressively less useful therapeutics.

Neisseria gonorrhoeae is a severe human pathogen that has the ability to adapt successfully to exist within the reproductive tract of *Homo sapiens*. It is believed that gonorrhea is an old disease, which demonstrates a remarkable relationship with humans over centuries. The gonococcus has also displayed a remarkable ability to develop resistance against many clinically useful antibiotics. Gonococcus can adopt multiple mechanisms to adapt to the innate and adaptive modes of immunity within humans. After successfully escaping from the immunological response, gonococcus has an ability to undergo phase variation of its outer membrane, which helps it to block antibodies and inhibit the induction of apoptosis. This adaptive nature of this pathogenic bacteria provides an image to help in \understanding the evolutionary mechanism used by gonococci to fight against myriad antibiotics (Unemo and Shafer, 2011).

For complete and successful elimination of *N. gonorrhoeae* infection, it is important to treat high-risk patients immediately with suitable antibiotics. In most countries, single dose therapy is considered sufficient against *N. gonorrhoeae* infection because of its efficiency and assures enough treatment. Recently, however, a large number of *N. gonorrhoeae* isolates obtained from patients have been reported to be antibiotic resistant. More and more identified clinical isolates are found to be resistant to at least one clinically applicable therapy, whereas particularly troubling strains have been identified that are resistant to several antibiotics (colloquially termed 'super gonorrhoea'), which are a major medical concern as they are extremely difficult to treat. Precise antimicrobial selection based on resistance testing against gonorrhea would potentially enable a 95% cure rate, according to recommendations of the World Health Organisation (Organization, 2012).

Moreover, the antibiotic resistance situation is becoming worse, especially in developing countries, because of poorly regulated use of antibiotics. In recent year, antibiotic resistance among gonococci has become a series issue and has led to further extensive investigation of this bacterium in an effort to identify novel targets for the development of future antibiotics capable of killing 'super gonorrhea'. Monitoring of resistance has become one of the most important aspects of healthcare, for numerous pathogenic bacteria, including *N. gonorrhoeae*. In developed countries, such data is frequently collected due to availability of sufficient resources, but these data are

frequently lacking in developing countries because of a lack of diagnostic and analytical laboratory facilities, especially in very poor areas.

Salmonella antibiotic resistance is also a major concern for public health (Eng et al., 2015; Ugboko and De, 2014) and there is a pressing need to target them with new antibiotics. It is becoming increasingly difficult to eliminate *Salmonella* infections due to a higher proportion of its serovars exhibiting antibiotic resistance (Thung et al., 2016). Both the typhoidal and non-typhoidal serovars are of importance for human health and are expanding their drug resistance profile.

Many outbreaks of antibiotic-resistant *Salmonella* are being registered in many countries. In 2017, the non-typhoidal *Salmonella* serovar, Urbana, caused disease outbreaks through contamination of papaya, which showed resistance against tetracycline and streptomycin (Hassan et al., 2019). Resistance against nalidixic acid and ciprofloxacin has also been reported (Barry et al., 1984). Multidrug-resistant *Salmonella* have also been observed as part of food contamination in pork which resulted in an outbreak in 2015 (Carstens et al., 2019; Doyle, 2015; Laufer et al., 2015). These isolates were resistant to ampicillin, streptomycin, sulfisoxazole and tetracycline. Antibiotic resistance is also a result of genetic adaption of some species of *Salmonella* within multiple hosts (Ahmed et al., 2009). Antibiotics being added into the food chain e.g. used in rearing of poultry, beef and pork, are a likely cause of the antibiotic resistance among *Salmonella* species that can affect human health.

1.2. The importance of metal ions in biology

All living organisms are composed of a complex mixture of organic and inorganic compounds, such as carbohydrates, proteins and lipids, and metal ion complexes. Inorganic species cannot be biosynthesised like the organic compounds and must instead be acquired from the extracellular growth environment. A limited subset of metal ions are fundamental in biology (magnesium, calcium, sodium, potassium, manganese, iron, copper and zinc), which have very specific biological roles including as charge carriers, electrolytes, and as enzymatic cofactors. However, many of these metal ions can poison cells if their concentration becomes elevated, so their concentrations within living systems must be strictly controlled via homeostatic regulation. Each organism has a set of homeostatic proteins for each metal, that controls acquisition, detoxification,

and intracellular distribution of that specific metal ion, ensuring a satisfactory supply of the required metal for the cell's essential metal-dependent functions while simultaneously controlling the potential for damage that would be caused by an excess of the metal ion. Once inside the host, a pathogenic bacterium must obtain all of its necessary nutrients, including a supply of essential metal cofactors, directly from the host. This creates an opportunity for the host immune system to try to limit the growth of an invading pathogen through limiting the availability of these essential metal ions to the bacterium, a process that has been termed 'nutritional immunity' (Hood and Skaar, 2012).

1.2.1. The roles of copper in biology and importance of bacterial copper homeostasis

The medical and commercial exploitation of copper, including solid copper and inorganic salts of copper, include being used as astringents, sanitizers and antifungals to treat wounds and in agriculture and also to purify drinking water or to control contamination of water during storage, and in contraceptive intrauterine devices (Borkow and Gabbay, 2009). Indeed, for over a century copper has been used as a fungicidal agent in agriculture, particularly on vineyards, and as a growth promoter in animal farming. Organic and inorganic copper compounds have also been used for the treatment of various skin diseases like syphilis, TB and anemia amongst other sicknesses (Grass et al., 2011).

The mechanisms of cellular toxicity of copper have been investigated intensely in recent years, In many systems it has been assumed that toxicity is primarily caused by copper-dependent redox-cycling reactions leading to the *in vivo* generation of reactive oxygen species (ROS) (Fu et al., 2014; Knauert and Knauer, 2008; Gómez-Mendikute and Cajaraville, 2003). But recent studies have instead identified a different mechanism, where toxicity appears to be driven by the ability of copper to bind tightly at the active sites of metalloenzymes, specifically those that contain iron-sulfur (Fe-S) clusters (Macomber and Imlay, 2009). This mechanism not only prevents the catalytic activity of the mis-metallated Fe-S cluster-containing enzymes, but also releases the displaced iron from the clusters into the bacterial cytosol, that can then catalyse production of ROS (Kiley and Beinert, 2003). Because of this toxicity of excess copper, studies have demonstrated that 'free' copper ions, i.e. copper associated with no ligands other than water, do not exist inside either eukaryotic (Gerber et al., 2004) or prokaryotic cells (Cornelis et al., 2011; Changela et al.,

2003). Instead, copper (and other metals) can be considered to form ‘pools’, each bound to specific biological macromolecules that ‘buffer’ their availability (Cobine et al., 2004; Cotruvo Jr et al., 2015; Schlief and Gitlin, 2006). Copper availability inside cells is repressed through the action of copper efflux and sequestration proteins, which have extraordinarily tight affinities for copper (Solioz and Stoyanov, 2003; Wang and Guo, 2006; Arredondo and Núñez, 2005; Burkhead et al., 2009).

Cells use many mechanisms for copper handling, resulting in copper homeostasis. These comprise copper sensors, transporters, metallochaperones, and copper delivery and insertion proteins, each with high affinity and specificity for copper (Burkhead et al., 2009; Cornelis et al., 2011; Schlief and Gitlin, 2006; Solioz and Stoyanov, 2003).

Copper ions are removed from the cytosol by the ATP-dependent activity of a class of copper-transporting P-type ATPases, that belong to a highly conserved family of copper homeostasis proteins (Solioz and Stoyanov, 2003; Lutsenko et al., 2007; Lutsenko and Petris, 2003; Horn and Tümer, 1999). In eukaryotes, these copper efflux pumps (called ATP7A and ATP7B in humans and Ccc2 in yeast) work in conjunction with a cytosolic copper metallochaperone (ATOX1 in humans and Atx1 in yeast) to transport copper from the cytosol into the trans-Golgi network (TGN) to supply this essential cofactor to newly-synthesised secreted copper enzymes (Bleves et al., 2010; Balamurugan and Schaffner, 2006; Festa and Thiele, 2011; Banci et al., 2009; Howell et al., 2010). In bacteria, this P-type ATPase transporter is usually named CopA, and effluxes copper from the cytosol into the periplasm of Gram-negative bacteria or into the extracellular environment in Gram-positive bacteria. These membrane pumps are the primary mechanism of detoxifying the bacterial cytosol of excess copper ions (Rensing et al., 2000; Petersen and Møller, 2000). CopA is closely related to eukaryotic ATP7A and ATP7B (Yu et al., 2017). Bacterial CopA can function either alone or in concert with the bacterial ATOX1/Atx1 homologue, CopZ, for the removal of cytosolic copper (Dennison et al., 2018; Solioz, 2018b; Puig and Thiele, 2002). Indeed, a recent discovery has identified a CopZ homologue in an organism that was not previously thought to have this copper metallochaperone, *Escherichia coli*. In *E. coli*, a form of CopZ can be created from the

copA gene by the process of programmed ribosomal frameshifting, where both full length and truncated transcripts are synthesised from a single gene (Drees et al., 2017; Drees et al., 2015).

Several types of bacterial metal-dependent transcriptional regulators, termed metal sensors, work to control the production of the copper efflux pump CopA (Waldron and Robinson, 2009; Porcheron et al., 2013), ensuring that it is only synthesised during conditions of copper excess. For instance, in *E. coli* the expression of the *copA* gene is controlled by the copper sensor CueR (Stoyanov et al., 2001), whereas in Gram positive bacteria like *Mycobacterium tuberculosis*, *Staphylococcus aureus*, and *Bacillus subtilis*, the expression of the *copA* gene is controlled by a different metal sensor, CsoR (Liu et al., 2007; Baker et al., 2011).

Copper is an important component of the antimicrobial defence of the mammalian immune system that is used as a weapon to fight against invading pathogens (Festa and Thiele, 2012). Innate immune cells such as macrophages use copper as an antimicrobial weapon, leveraging the antimicrobial activity of copper ions (Samanovic et al., 2012). The killing potential of the intracellular compartment that detects and deactivates the invading microbes, called the phagosome, is enhanced by the accumulation of significant concentrations of copper ions (Dennison et al., 2018; White et al., 2009b; Ladomersky et al., 2017). In activated macrophages, protein levels of both the copper importer CTR1 in the cytoplasmic membrane and the intracellular copper transporter ATP7A are increased, and the ATP7A protein relocates from the secretory pathway (where it transports copper into the TGN for supply to secreted cuproenzymes) to the phagosomal membrane, (Lutsenko et al., 2007) where there are increasing in phagosomal copper levels (Wagner et al., 2006; Wagner et al., 2005). These data demonstrate that ATP7A that is responsible for the increased phagosomal copper concentrations during infection (Lutsenko and Petris, 2003). This increased copper toxicity in the lumen of the phagosome affects attacking pathogens that are enclosed within this compartment of macrophages.

It has been revealed in a number of different pathogenic bacteria that mutant strains that do not have the ability to express their copper detoxification systems such as CopA show reduced survival

inside macrophages, and often also decreased virulence in animal models of infection (Wang and Guo, 2006; Howell et al., 2010; Festa and Thiele, 2012; Lenz and Dillard, 2018; Baker et al., 2011; Shafeeq et al., 2011; Alquethamy et al., 2019; Shi et al., 2014; Francis and Thomas, 1997; Schwan et al., 2005; Osman et al., 2010; Purves et al., 2018; Zapotoczna et al., 2018). For some bacterial pathogens, during the infection cells up-regulate the expression of their copper export ATPases in a manner dependent on their copper sensing transcription factors (Heithoff et al., 1997), which together work as a protection mechanism by enhancing their capacity to export copper when they experience these high copper levels inside macrophages. For instance, two separate copper-responsive transcription factors that monitor the copper levels induce two *Mycobacterium tuberculosis* copper resistance operons under elevated copper conditions, suggesting the importance of copper resistance mechanisms for a productive infection by *Mycobacterium tuberculosis* (Liu et al., 2007).

1.2.2. **Copper toxicity in bacteria**

How does copper become toxic to cells? What are the mechanisms by which copper causes toxicity? The ability of copper ions to participate in a redox cycle between Cu(I)/Cu(II) is well-established *in vitro*, generating the reactive oxygen species (ROS) superoxide, hydrogen peroxide and the hydroxyl radical. Many studies have been conducted to suggest that this was the likely mechanism by which copper causes cytotoxicity. Reaction oxygen species are produced by copper from a Fenton-like reaction,. Under aerobic conditions, copper participates in the Fenton and Haber Weiss reactions, which ultimately lead to the production of highly damaging hydroxyl radicals (Fu et al., 2014):

$$Cu^{+} + H_2O_2 \rightarrow HO^{-} + HO^{-} + Cu^{2+}$$
$$O_2^{-} + Cu^{2+} \rightarrow Cu^{+} + O_2$$

These extremely reactive oxygen intermediates have opposite effects on macromolecules such as lipid peroxidation, oxidation of proteins and nucleic acid damage (Bandyopadhyay et al., 1999; Misba and Khan, 2019; Sharma et al., 2018). Sulfhydryl groups such as cysteine sidechains within

proteins or the cellular redox buffer glutathione can be oxidized by free copper ions (Ulrich and Jakob, 2019). Iron-based Fenton chemistry is well-established, *in vitro* and *in vivo*, and oxidative damage can be caused by high levels of ROS generated by free iron (Dai et al., 2018). Oxidative damage is suggested during copper toxicity, primarily due to induction of oxidative stress-induced genes during exposure to high concentrations of copper, but it appears to be produced only indirectly through the high amount of copper (Macomber and Imlay, 2009; Macomber et al., 2007). Indeed, the growth of *E. coli* was even more inhibited by copper ions under anaerobic conditions than under aerobic conditions (Bandyopadhyay et al., 1999; Macomber and Imlay, 2009). More remarkably, in *E. coli* the level of oxidative DNA damage caused by the addition of copper was actually reduced in cells also exposed to hydrogen peroxide (Sharma et al., 2019). Together, these observations suggest the toxicity of copper can be independent of oxygen and preclude ROS as being the key mechanistic component.

More recently, iron sulfur clusters have been shown to be a critical target of copper toxicity. Under conditions in which cells accumulate a high amount of copper, these clusters can be disrupted because of the high affinity of Cu(I), which is the predominant form of copper under the reducing conditions of the cytosol, for thiolate-containing species. Consequently, cytosolic copper ions can attack the cysteine (Cys) sidechains that bind the Fe-S clusters, resulting in separating of the cluster from the enzyme and subsequent inactivation of the Fe-S-dependent enzyme (Macomber and Imlay, 2009). In *E. coli* and *B. subtilis* iron acquisition and sulfur assimilation was increased because excess copper (Banci et al., 2001; Meydan et al., 2017), consistent with copper causing damage to Fe-S clusters central to iron and sulfur metabolism. The Fe-S clusters can be displaced in a direct way from Fe-S-containing enzymes, resulting in their inactivation, or the biogenesis of these clusters can be interrupted during their synthesis by the Fe-S cluster biogenesis machinery, or during the mechanism of their transfer from this machinery to target metalloenzymes. Enzymes having iron sulfur clusters in *Bacillus subtilis* that can be damaged by high levels of copper include biotin synthase (BioB), molybdopterin molybdenumtransferase (MoaA), as well as enzymes in the pyrimidine and branched chain amino acids biosynthesis pathways. In *E. coli*, copper ions can also disrupt other pathways, for instance by inhibiting dihydroxyacid dehydratase, that is present in the mutual branched chain amino acid synthesis pathway, isopropylmalate dehydratase (LeuC) found in the leucine branch of that pathway, fumarase-A (FumA) found in the tricarboxylic acid cycle

(TCA), and 6-phosphogluconate dehydratase in the pentose phosphate (PP) pathway; consequently, these enzymes create an obvious mechanism y which copper can cause deadly damage to cells (Banci et al., 2001).

It is very important to keep the level of 'free' copper (i.e. ions that are bound to no species other than water molecules) at very low concentrations in the cytoplasm. The copper efflux P-type ATPase, CopA, in bacteria ensures very low concentrations of free copper in cell by effluxing excess copper ions (Lutsenko and Petris, 2003). Based on Cu(I) affinity measurements of the bacterial copper sensors, there is essentially no free copper in cells (Changela et al., 2003). This is crucial to avoid the degradation of iron sulfur cluster cofactors of vital enzymes (Meydan et al., 2017). Increasing concentrations of bioavailable copper stop bacterial growth. Most bacteria solve this problem by having copper enzymes that can be found only in the periplasm or facing out from the cytoplasmic membrane, with the result that copper can simply be eliminated from the cytosol where it is not needed, thereby preventing toxicity. In certain bacteria, such as photosynthetic bacteria (cyanobacteria) or methanotrophic bacteria, copper is required by cytoplasmic copper-dependent enzymes, so in these organisms copper must be transported to intracellular compartments through the cytosol.

1.2.3. Bacterial copper homeostasis

Many of the details of what is known about copper homeostasis in prokaryotes are derived from the study of the key bacterial model organism *E. coli*. It is assumed that copper dependent proteins are exclusively situated in the periplasm or within the cytoplasmic membrane of *E. coli* (Rensing and Grass, 2003), with this enterobacterium not known to have any need for cytoplasmic copper. Indeed, few copper import systems have been identified in bacterial genomes (Wu et al., 2016; Leitzinger, 2017).

In both Gram-negative and Gram-positive bacteria, the primary protection mechanism against high levels of copper is conserved. The P-type ATPase, generally called CopA, pumps Cu(I) across the cytoplasmic membrane, detoxifying the excess copper from the cytoplasm (Odermatt et al., 1993; Rensing et al., 2000). The expression of the *copA* gene in *E. coli* is regulated in a copper-dependent

manner by the action of the copper sensor, CueR, located in the cytosol (Rensing et al., 2000). Other families of metal sensors perform this function in other bacteria.

An additional efflux pump is present in *E. coli*, the CusCBA transporter, that is a multi-protein complex found in the *E. coli* periplasm involved in the elimination of periplasmic copper (Franke et al., 2003). The proton motive force is used by the CusA protein, a member of the RND (resistance/nodulation/cell division) family, which complexes with both CusB and CusC to form a transporter with the ability to transfer copper from the periplasm to the extracellular space. Mechanically, CusCBA work as a kind of peristaltic pump with 3 alternating enzyme conformations, as was shown for a related system (Ridge et al., 2008; Seeger et al., 2006). The CusA protein has three methionine residues which are located in the periplasmic space that are responsible for specific binding and releasing of Cu(I) (Ridge et al., 2008). The CusCBA complex can detect periplasmic copper concentrations through three conserved N terminal residues to regulate transport efficiency (Kim et al., 2011). The Cus efflux pump is also transcriptionally controlled in a copper-dependent manner, like the gene encoding CopA. The two-component system, CusRS, senses the copper concentration inside the periplasm and then transfers this information through a phosphorylation/dephosphorylation relay to the cytosol to be able to transcriptionally control the genes encoding the Cus efflux pump.

A third common constituent of copper homeostasis are multi-copper oxidases (MCO). In *E. coli* Cu(I) is thought to convert sporadically to Cu(II) in the periplasm aerobically, but this oxidation reaction can be accelerated by the periplasmic MCO CueO. This can protect the periplasmic proteins from Cu(I), which can be potentially toxic due to its avidity for sulfur ligands (Singh et al., 2004). In addition, CueO might also be able to oxidize the siderophore enterobactin, resulting in a copper binding oxidation product that may also reduce the rate of copper entry into the cytoplasm from the periplasm (Grass et al., 2004).

Salmonella enterica is a close relative of *E. coli* so shares several of the same elements of copper homeostasis as *E. coli*, however there are also some important differences. Whereas CopA and CueO (called CuiD) are present in *Salmonella*, the Cus system is not. An alternative protein, CueP, which is absent from *E. coli* genomes, has been identified as an additional periplasmic copper

protection protein in *Salmonella* (Pontel and Soncini, 2009; Osman et al., 2010). CueP proteins are not only limited to *Salmonella* but can also be found in other bacterial genomes, including frequently in those of pathogenic bacteria. In the periplasm of *Salmonella*, CueP is present under growth conditions containing copper but does not transport copper. Instead, the role of CueP in copper tolerance is thought to be connected to its copper sequestration, especially under anaerobiosis, and also potentially in supplying of copper to the periplasmic Cu,Zn-superoxide dismutase enzymes localized to the *Salmonella* periplasm under aerobic conditions. CueP represents a major cellular copper pool (Osman et al., 2010). Under anaerobic growth situations, the Cus system and CueP seem to play the same role in conferring copper tolerance, despite very different molecular functions. Despite the lack of the RND-type Cus system in genomes of *Salmonella*, it is interesting that an extra tripartite RND efflux pump, Ges, is present in the *Salmonella* genome. This Ges system was identified and characterized as a gold responsive operon (Pontel et al., 2007). Copper is seemingly not transported by Ges (Checa et al., 2007).

The small metallochaperone GolB is present in *Salmonella*, that is proposed to be this organism's homologue of CopZ. Importantly, most *Salmonella* species possess a genetic duplication of CopA: in addition to the classical CopA, a second copper efflux P-type ATPase, named GolT, is also present. Expression of CopA is controlled by CueR, like in *E. coli*, whereas the GolT transporter is regulated by a second duplicated copy of CueR called GolS (Checa et al., 2007). The Gol system was originally recognised as a gold resistance operon, but later studies showed these components to be a partially redundant second copper detoxification system in *Salmonella* (Osman et al., 2010). Studies of *Salmonella* present the opportunity to observe the function of the genes and proteins of copper homeostasis within an intracellular pathogen. Reporter constructs, designed to measure the copper-dependent expression of *copA*, waere established for this. Expression of *copA* is dependent only on copper ions, and no other significant stress factors potentially present within macrophage phagosomes, altered *copA* levels. Increased activities of this reporter, led to the conclusion that the infection of macrophages by *Salmonella* resulted in expression of the *copA* transporter gene (Osman et al., 2010). This suggested that, within host phagocytic cells after engulfment, bacteria detect high levels of copper ions, which are thought to be an immune protection mechanism against infection. Moreover, deletion of both CopA and GolT led to significantly decreased ability of *Salmonella* cells to survive inside macrophages than the wild type control (Ladomersky et al.,

2017), indicating copper resistance is a necessity for persistence of infecting *Salmonella* in a macrophage model.

Crucially copper-transporting P-type ATPases from both host and pathogen perform remarkable opposing roles during infection (White et al., 2009a). The host Golgi copper transporter relocates to the phagosome to pump copper across the phagosomal membrane in order to increase the lumen copper concentration, whereas the bacterial transporter effluxes copper from the bacterial cytosol across its cytoplasmic membrane to transport excess copper from the cell back into the phagosome lumen. When the mammalian exporter ATP7A was repressed, that caused decreased the killing of invading *E. coli* (White et al., 2009a). On the other hand, *E. coli* cells were more sensitive to macrophage-mediated killing when CopA was deleted. However, in a murine model of infection, no fundamental differences were seen between wild type *Salmonella* and the CopA/GolT double mutant (Osman et al., 2010). This might be a significance of the specific animal model used in these experiments, or a reflection of very subtle differences between the two strains during the development of infection. For example, the CueO protein was still present in these mutant *Salmonella* cells, which may have a dominant effect. It would be interesting to study the role of CueO in such experiments, and to test a triple mutant lacking *cueO* as well as the genes encoding the two transporters, in these models of infection. One study has identified a phenotype of *cueO* in a murine model of infection by *Salmonella* (Achard et al., 2010). A mucoid phenotype and a cluster behavior was seen for *E. coli* and *Salmonella* because of the disruption of CueO in cells, that was also seen under conditions of copper stress (Grass and Rensing, 2001).

Related studies have been performed in various pathogenic bacteria, including in *Legionella pneumophila* (Rankin et al., 2002), *Pseudomonas aeruginosa* (Schwan et al., 2005) or *Mycobacterium tuberculosis* (Ward et al., 2010). For example, *M. tuberculosis* harbors eleven metal-translocating P_{IB}-type ATPases. Only one, CtpV, can be directly linked to copper homeostasis in this organism (Ward et al., 2010; Darwin, 2015). Copper stress was increased in strains lacking CtpV. However, infected animals showed less lung injury, weaker immune responses and improved survival of the host after infection with CtpV-deficient strains compared to infection with wild type *M. tuberculosis*. Remarkably, *M. tuberculosis* has a unique copper homeostasis factor that is essential for virulence in this organism. This MctB (mycobacterial

copper transport protein B) is found in the outer membrane, interacting with the mycobacterial cell wall (Wolschendorf et al., 2011). However, MctB appears to be involved in copper efflux because the loss of MctB made cells more liable to copper toxicity and mutant cells contained approximately one hundred times more copper as compared to the wild type cells. A novel dipartite copper efflux system was observed through interaction of MctB and the copper ATPase CtpV (Wolschendorf et al., 2011). If the nature of this interaction is physical or functional is still unresolved. Deficiency of MctB in *M. tuberculosis* results in a severe copper dependent phenotype, both in growth experiments *in vitro* and in animal models. It was observed that the infection with *M. tuberculosis* decreased one hundred times in guinea pig lymph nodes and one thousand times in lungs due to the deletion of MctB (Wolschendorf et al., 2011). This consequence suggests an important role of CtpV and MctB in *M. tuberculosis*.

1.2.3.1. P-type ATPases

In 1957, Jens Skou observed the effect of many cations on a homogenate of crab's leg nerves that were caught on the beach of Denmark. On the basis of that observation, he suggested the idea of 'membrane potential' which is made by a K^+ transporting ATPase, now acknowledged as a Na^+/K^+ ATPase that can transport Na^+ and K^+ ions across the axonal membrane using energy obtained from the hydrolysis of ATP (Robinson, 1997). In later years, several tissues and organisms showed more ion pumps with comparable properties. They include the sarcoplasmic reticulum (SR) Ca^{2+} ATPase, which work as a regulator for the contraction of skeletal muscle (Hasselbach, 1961), the gastric H^+/K^+ ATPase that provide the acidity of the stomach, and the H^+ ATPase, which creates the membrane potential in fungal and plant cells (Slayman et al., 1970).

P-type pumps are a large, universal and varied family of membrane proteins that are fundamental to several transport processes in all living organisms. Generally, P-type ATPase genes are more common in eukaryotes compared to bacteria and archaea. In *E. coli*, just four types of P-type ATPase have been identified (Axelsen and Palmgren, 1998). Only one P-type ATPase is found in thermophilic archaean *Methanococcus jannaschii* (Bult et al., 1996), whereas some parasites have no such ATPases (Axelsen and Palmgren, 1998). Forty five P-type ATPases have been recognized in the *Arabidopsis thaliana* genome (Axelsen and Palmgren, 2001) compared to the *Saccharomyces cerevisiae* genome which contain 16 P-type ATPases.

All P-type ATPases are multiple-domain membrane proteins with molecular wight of 70–150 kDa. On the basis of sequence homology, the P type ATPase family can be divided into 5 branches, which are indicated as: Type I, Type II, Type III, Type IV and Type V ATPases. A total of 10 subtypes or classes can be noted from these branches (Axelsen and Palmgren, 1998; Palmgren and Axelsen, 1998). Each subtype is thought to be specific based on a certain substrate ion.

P-type ATPase are important in translocating copper ions across biological membranes, exclusively as Cu(I). They transport copper between the cytosol and different organelles, along with efflux of high levels of copper concentration out of cells through efflux. A subfamily of the P-type ATPases are considered to be heavy metal-transporting ATPase (P_{1B}-ATPases) including the copper ATPases (López-Marqués et al., 2010). Members of this huge family can be found in the genomes of bacteria, archaea and eukaryotes, where they use ATP as the energy source for the active transport of copper ions across biological membranes (López-Marqués et al., 2010; Axelsen and Palmgren, 1998). In the cytoplasmic area of the of these polytopic membrane proteins, important sequence motifs common to all P-type ATPases are conserved, including the ATP nucleotide binding (N domain) domains, phosphorylation (P) and catalytic activation domain.

Copper ATPases transport copper across cellular membranes consuming ATP. This occurs via a series of mechanistic steps in a process comprising the specific binding and delivery of copper to the transmembrane region of the copper ATPase, followed by moving the metal to the other side of the membrane, which is linked to the binding and hydrolysis of ATP, and finally the release of the substrate on the other side of the membrane (Lutsenko et al., 2007). The N terminal domain of many copper-transporting ATPases have an additional copper binding domain, which is localised within the cytosol. These share similar coordination to either CopZ- or cupredoxin family of copper metallochaperone proteins, and contain copper binding Cys residues, often in a CXXC motif (Braymer and Giedroc, 2014; López-Marqués et al., 2010; Lutsenko et al., 2007). Copper-transporting ATPase activity is thought to be in some way manipulated by binding of copper and/or the copper-binding partner metallochaperone protein to this domain.

1.2.3.2. Copper metallochaperones

The cytosolic bioavailable copper level is kept low by metallochaperones, which are high affinity soluble copper binding proteins. Their function if to avoid copper binding and copper-dependent damage to non-specific proteins, i.e. proteins that do not usually bind copper. Additionally, copper metallochaperones can also direct and carry copper to specific target proteins, either copper-requiring enzymes or the P-type ATPase transporter clients. That indicates that, in addition to a preserved metal binding motif, metallochaperones must have conserved structural arrangements to recognize and deliver copper to specific copper-binding sites of their associated client proteins. Cox11, Cox17 and Sco1 proteins are known chaperones in yeast, which transport copper to the Cu_A and Cu_B of cytochrome *c* oxidase (CcO), whereas Cu,Zn-superoxide dismutase acquires copper through interaction with CCS, and Atx1 transports copper to the yeast P-type ATPase N terminal (Robinson and Winge, 2010).

Bacterial copper metallochaperones, generally called CopZ, are most closely analogous to eukaryotic Atx1. This protein has 73 amino acids, including a coppere-coordinating CXXC motif, in both eukaryotes and prokaryotes. Copper can be delivered through Atx1 to the sites of P type ATPases N-terminus (NMBD) in yeast, and also in bacteria (Robinson and Winge, 2010). Alternatively, it is thought that the metallochaperones can directly deliver copper to the ATPase transmembrane binding site (TMBS) that is centrally involved in copper translocation (Robinson and Winge, 2010).

1.2.3.3. Copper storage proteins

It has been known for decades that small, cysteine-rich cytosolic proteins called metallothioneins (MTs) can store excess cytosolic copper in eukaryotes (Pountney et al., 1994; Calderone et al., 2005; Banci et al., 2010). In certain types of pathogenic mycobacteria and some environmental bacteria, metallothionein proteins have also been characterised (Gold et al., 2008), but most bacteria lack metallothionein genes. In 2015, a new family of bacterial copper storage proteins (Csps) were discovered in the methane-oxidizing bacterium (methanotroph) *Methylosinus trichosporium* OB3b (Vita et al., 2015). Genes encoding Csps appear to be more common in bacterial genomes than those encodeing metallothioneins (Vita et al., 2016).

The discovery of a new family of copper storage protein in these Gram-negative, environmentally important organisms that metabolise methane was not surprising. In all methanotrophs, the conversion of methane to methanol is performed in a copper-dependent catalytic step through the membrane-bound particulate methane monooxygenase (pMMO), (DiSpirito et al., 2016). Recent observations demonstrated that pMMO has a mono-nuclear copper active site, however, it was earlier suggested that it had a di-nuclear active site (Cao et al., 2018). The alternative, soluble MMO (sMMO) has a di-nuclear iron active site, however only a few methanotrophs used this sMMO when copper levels become limiting (Rosenzweig et al., 1993).

Understanding the way methanotrophs accomplish their conversion of methane to methanol and use copper for methane oxidation has environmental importance because of methane being a strong greenhouse gas, and is also important for forthcoming applications of biotechnology of these organisms and their MMOs (Jiang et al., 2010; Haynes and Gonzalez, 2014; Kalyuzhnaya et al., 2015). Methanotrophs need very high levels of copper for methane oxidation, and for that reason they likely have novel copper handling systems. For example, these organisms were identified to produce methanobactin (Mbn) (Kim et al., 2004; Krentz et al., 2010), which works in copper acquisition and is considered analogous to certain iron binding siderophores (Ward et al., 2010) and therefore called a chalkophore (Kim et al., 2004). This very peculiar copper uptake system utilizes Mbn, a modified peptide secreted to sequester environmental extracellular copper for subsequent uptake (DiSpirito et al., 2016; Kim et al., 2004). The *mbnA* gene was recognized in an operon along with proteins that code for enzymes that are thought to be involved in methanobactin maturation and modification reactions, in apo-Mbn export and in the re-import of Cu(I)-Mbn (DiSpirito et al., 2016; Krentz et al., 2010; Semrau et al., 2013; Gu and Semrau, 2017; Dassama et al., 2016). Few genomes of non-methanotrophic bacteria possess an obvious Mbn operon (Krentz et al., 2010). The current model suggests that an oxidation process releases the Mbn-bound metal ion once the complex has been imported inside the cells (El Ghazouani et al., 2011), with a conformational variation at the N-terminal of the peptide seeming to be significant in this process (Baslé et al., 2018).

In an effort to isolate intracellular Cu(I)-Mbn by chromatography, a 12k Da protein was identified that purified with copper from cell extracts of *M. trichosporium* OB3b. *In vitro* this protein, named Csp1, can bind up to 12-14 Cu(I) ions per monomer, with an average Cu(I) binding affinity ~ 1×10^{17} M^{-1} (Vita et al., 2015). In the crystal structure (Vita et al., 2015), each monomer was found bound to 13 copper ions in a remarkable manner along the core of a four helix bundle (Vita et al., 2015; Lombardi, 2015). Some copper sites are in CXXXC motifs, with 4 Cu(I) ions are bound by two thiolates on the same alpha helix, whereas many other copper ions are bound by 2 Cys residues on different helices. The solvent-accessible sites at the beginning of the bundle (the opposite side has a number of hydrophobic side chains), through which Cu(I) ions are likely to enter and leave, have different properties (Vita et al., 2015). In total, the Csp1 protein can bind 52 solvent-protected Cu(I) ions inside a tetrameric quaternary structure, suggesting a role in storage, so the name of this novel family of copper proteins (the Csps) was invented (Vita et al., 2015). Interestingly, three Csp homologues were found in the genome of *M. trichosporium* OB3b. Csp1 was the first discovered, as mentioned above was called Csp1 (MtCsp1 indicates that it originates from M. trichosporium OB3b), whereas the two others are known as MtCsp2 and MtCsp3.

Three Csps are present in this model methanotroph; two (*Mt*Csp1 and *Mt*Csp2) possess predicted twin arginine translocate (Tat) targeting signal peptides and are thereby exported from the cytosol. *Mt*Csp1 has been characterized and is a tetramer that can bind up to 52 Cu(I) ions, mainly via Cys residues (Vita et al., 2015), but *Mt*Csp2 has not yet been characterised (although it shows significant homology to *Mt*Csp1). Given its Tat pre-sequence and high homology (58% sequence identity) with Csp1 it is presumed to be performing a redundant, or at least overlapping, role to Csp1. Importantly, deletion of both the genes encoding for *Mt*Csp1 and *Mt*Csp2 increases the rate of switchover from pMMO to sMMO in *M. trichosporium* OB3b, when cells are transitioned from copper-sufficient to copper-deficient growth conditions, implicating these proteins in the storage of copper for methane oxidation (Vita, et al., 2015). Crucially, the genome of *M. trichosporium* OB3b also encodes a third Csp homologue, denoted Csp3, that shares only 19% sequence identity with Csp1. Csp3 lacks a signal peptide and must therefore be cytosolic (Vita et al., 2016). Homologues of this cytosolic protein are present in the genomes of a wider range of bacteria than those of the non-cytoplasmic forms, Csp1 and Csp2, suggesting cytosolic Csps may play a broadly conserved role in copper homeostasis in bacteria.

The twin-arginine translocation (Tat) pathway is one of a number of bacterial protein secretion systems (Figure 1.2) which serves the role of transporting folded proteins across the bacterial cytoplasmic membrane from the cytosol to the periplasm (Wickner and Schekman, 2005). The Tat system has been suggested to be commonly employed for the secretion of proteins that require a cofactor for function, and can influence metal selectivity (Tottey et al., 2008). It is widespread within the microbial world, with homologues of the genes that encode the Tat transport apparatus found in genomes of archaea, bacteria, chloroplasts, and plant mitochondria (Yen et al., 2002) The Tat pathway acts separately from the general secretory (Sec) pathway (Figure 1.2), which transports proteins across these same membranes in an unfolded state (Stephenson, 2005).

The Tat pathway exports numerous proteins that are involved in virulence. For example, in the opportunistic human pathogen *Pseudomonas aeruginosa*, two secreted virulence factors (both phospholipases) are mis-localized in *tat* mutants (Voulhoux et al., 2001). The Tat pathway of *P. aeruginosa* is also involved in the transport of further virulence factors (Ma et al., 2003; Bleves et al., 2010). Disruption of the Tat pathway abolishes virulence of pathogenic pseudomonads including *P. aeruginosa* and the plant pathogens *Pseudomonas syringae* pv. Tomato (Caldelari et al., 2006; Zhurina, 2009). In *Salmonella*, the infection and survival of pathogen also requires two type III secretion systems, T3SS1 and T3SS2 (Ibarra and Steele-Mortimer, 2009; Jajere, 2019; Palmer et al., 2005; Berks et al., 2000), although there has been no links discovered between these secretion systems and metal homeostasis.

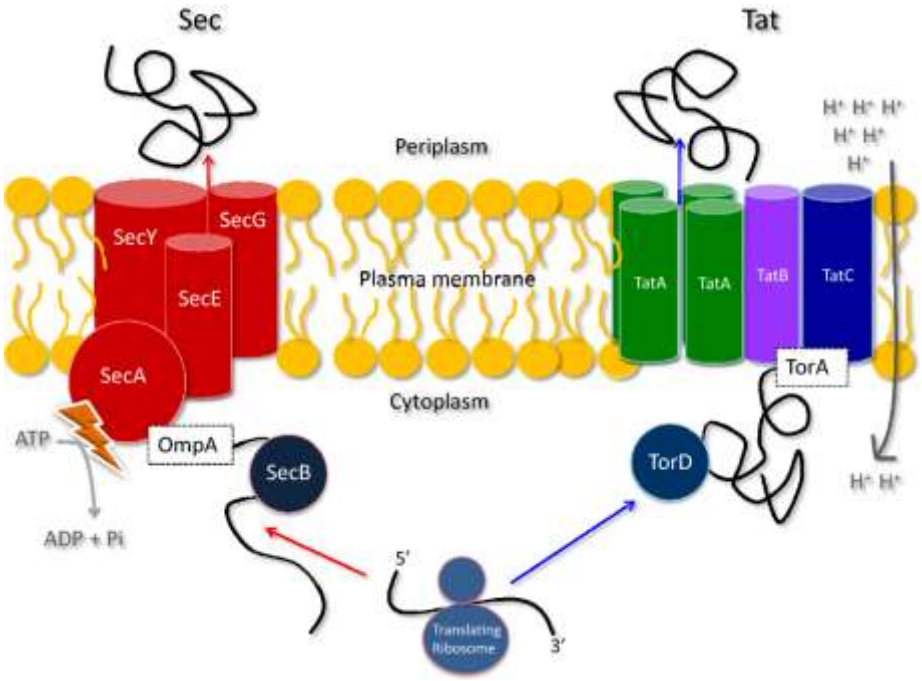

Figure 1.2. Schematic overview of the Sec- and Tat-dependent pathways for protein translocation in bacteria.

Proteins are exported from the cytoplasm by the Sec pathway primarily in bacteria. Sec translocates unfolded or partially folded proteins across the plasma membrane. On the other hand, folded proteins are translocated across the plasma membrane by the Tat pathway. In our case, Csp1 from *N. gonorrhoeae* is expected to be exported by Tat pathway. Figure taken from (Frain et al., 2019).

In most bacteria, the Sec translocase consists of SecB (a secretion specific chaperone), SecY, SecE and SecG, and a peripheral associated ATPase, SecA. SecY, SecE and SecG make up the protein-conducting channel. SecA is responsible for translocation of secretory proteins across the membrane and works as motor protein (Wickner et al., 1991; De Keyzer et al., 2003; Osborne et al., 2005). Tat translocases are composed of either two or three subunits , i.e. TatA and TatC or TatA, TatB and TatC. These collectively work as the Tat translocase, and translocate folded proteins across the cellular membranes by largely unknown mechanisms (Müller and Bernd Klösgen, 2005; Robinson and Bolhuis, 2004).

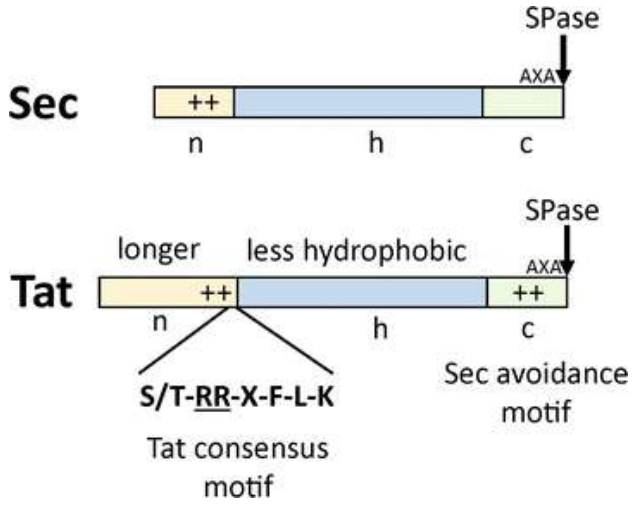

Figure 1.3. Schematic overview of the pre-sequences recognised by the Sec- and Tat-dependent pathways for protein translocation in bacteria.

Proteins are secreted from the bacterial cytosol via two independent mechanisms, designated Sec (top) and Tat (bottom). Each class of secreted proteins is recognised by the respective protein translocation machinery by specific N-terminal pre-sequences that have conserved properties. Sec signals are shorter, and contain an N-terminal sequence (n) including positive charges, followed by a hydrophobic region (h), and finally a C-terminal sequence generally including an AXA motif that marks the position of post-translocation cleavage by signal peptidases (SP). Tat pre-sequences are generally longer, contain a recognisable consensus motif in their n region, a less hydrophobic h region, and positive charges in the c region that act as a 'Sec avoidance' motif. Figure is taken from (Freudl, 2018).

The precise function and physiological role of copper storage proteins (both of Csp1 and Csp3 types) is not yet clear. It is clear that they have the ability to bind a high number of copper ions with significant affinity. A role as a copper store has been postulated based on evidence rfom *M. trichosporium* OB3b, but they may play a role in also preventing cellular copper toxicity. Copper storage proteins could also play a role in dealing with the high copper levels experienced during infection by invading pathogens.

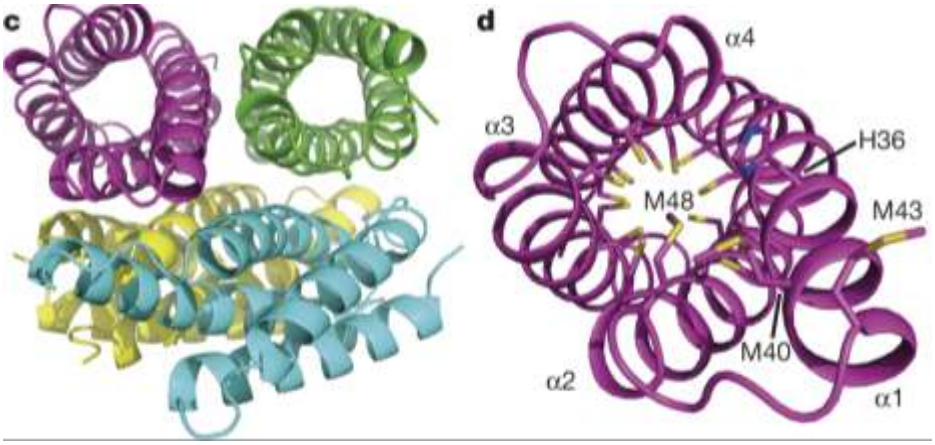

Figure 1.4. The structure of apo-Csp1 from *M .trichosporium* OB3b.

The tetrameric form of Csp1 was observed in the asymmetric unit of the crystal structure of apo-Csp1, with all of the Cys oriented to point their thiolate-containing sidechains into the core of the four-helix bundle. Cys residues are shown as sticks for one monomer in the right panel. The solvent-exposed 'opening' into the centre of the four helix bundle is facing outwards (Vita et al., 2015)

Crystal structures of a Csp3 loaded with a high ratio of Cu(I) gives important information about the atomic-level architecture of these proteins (Vita et al., 2016) and has been suggested to explain the mechanism of loading of a Csp with the metal ions. When excess Cu(I) equivalents were added, a large number of metal binding sites are occupied, including the 12 dominant central sites that are common to Csp1 and Csp3. These central sites have potential to form intermediates of a $[Cu_4(S\text{-}Cys)_4]$ type, which could ultimately resolve for the formation of the clusters of $[Cu_4(S\text{-}Cys)_5(O\text{-}Asn)]^-$, $[Cu_4(S\text{-}Cys)_6]^{2-}$ as well as $[Cu_4(S\text{-}Cys)_5]^-$. Five Cu(I) sites assemble at the opening of the tube that is formed by the four-helix bundle, and the main core sites are buried behind these. Formation of Cu(I) clusters, similar to those that form in inorganic complexes with organothiolate ligands, is used by proteins that transport copper in the eukaryotic and prokaryotic cytosols (Robinson and Winge, 2010).

Crystal structures of a partially loaded (2 mole equivalents) copper storage protein is indicative of an unusual loading mechanism (Baslé et al., 2017). One such structure contains four partially occupied sites, categorised as Cu11, Cu12, Cu13 and Cu14, which display differential loading with

copper in the crystal. Site Cu11 shows occupancy of about 0.25 equivalents, and the remaining three show occupancy of about 0.35. It is thought that this structure shows a glimpse of the creation of a symmetrical tetra nuclear cluster. It was observed that both Cu12 and Cu14 are bound with the cytosolic residues of CXXXC motifs ultimately to the same α-helix while on the other side both Cu11 and Cu13 are held by Cys residues located on different helices.

1.2.3.4. Gene expression and regulation of Csp1 in *Neisseria gonorrhoeae* or *Salmonella* Csp3.

Very little is known about the function copper storage protein 1 (Csp1) or with respect to its regulation and expression in any bacterial system. In many bacteria e.g. *E. coli* and *Bacillus*, there are specific sensors that respond to the concentration of Cu ions in either the cytosol or periplasmic space (Waldron and Robinson, 2009). For example, CueR in *E. coli* (Changela et al., 2003), the pair of cytosolic sensors CueR and GolS in *Salmonella* (Pontel and Soncini, 2009) and CsoR in many other bacteria such as *Geobacillus thermodenitrificans* (Corbett et al., 2011; Chang et al., 2014). Each of these sensory proteins have the ability to sense the level of Cu in cytosol, and then they bind to/release from the promoters upstream of copper-responsive genes to turn on and off the expression of genes of effectors such as CopA, and this regulation plays a vital role in copper toxicity tolerance (Pontel and Soncini, 2009; Volpicella et al., 2017; Solioz, 2018a; Andrei et al., 2020). However, genes encoding Csp proteins have not been reported to be under the regulatory control of any known copper-sensing transcriptional regulators (e.g. CueR or CsoR) in any bacterium.

It has been reported that CopA expression is not regulated by Cu concentration in *N. gonorrhoeae*, as it is expressed equally under all Cu concentrations tested. We may conclude that *N. gonorrhoeae* apparently has no copper sensors for the regulation of CopA (Djoko et al., 2012) and therefore it is unlikely that Csp1 is directly Cu-regulated in *N. gonorrhoeae*. Conversely, the level of CopA expression is regulated by reactive nitrogen species, as these species interact with copper and act as antimicrobial agents within the innate immunity response (Djoko et al., 2012). No specific research is available that has interrogated the potential copper-dependent regulation of Csp1 in *N. gonorrhoeae,* and this is a huge gap for future research.

It has been reported that *Salmonella* do have copper sensory proteins, CueR and GolS (Osman et al., 2010), which respond to the level of Cu ions. As a result of elevated copper, CueR turns on the expression of CopA and GolS turns on the expression of GolT (Fu et al., 2014). Both of these proteins are homologous to conserved copper efflux transporters. We may assume that if the cell is going to turn on expression of CopA in response to copper using this highly specific mechanism, it might also turn on expression of Csp3 under the same conditions and using the same mechanism as Csp3 would be anticipated to function at high concentrations of copper. However, no evidence has yet been presented that either of these known copper-dependent regulators in *Salmonella* regulate expression of the *csp3* gene (Osman et al., 2010). Indeed, no evidence has been presented in any bacterial system, as yet, that any *csp* gene is regulated in a copper-dependent manner, which might suggest that the role of Csp proteins in bacteria is not directly related to defending the cell against toxicity caused by a build-up of elevated copper concentrations in either the cytosol or periplasm.

1.3 Aims and objectives of the thesis

Research hypothesis

The overall goal of this study was to interrogate the copper binding properties and to characterise the structure of two uncharacterised members of the copper storage protein family from pathogenic bacteria, namely *Neisseria gonorrhoea* Csp1 and *Salmonella enterica* Csp3.

Project aims

1. Develop a reliable protocol to express and purify recombinant *Neisseria gonorrhoeae* Csp1 and *Salmonella enterica* Csp3 proteins from *Escherichia coli* host cells in high yield for subsequent characterisation.

2. Develop methods to accurately measure the protein concentration of each Csp protein.

3. Determine the structure of one or more of these Csp proteins.

4. Measure copper binding to Csp proteins.

6. Determine whether the competitor metals zinc and silver also bind to Csp1/Csp3.

Chapter 2: Materials and Methods

2.1. Bacterial strains

Bacterial strains (*Escherichia coli* BL21, BL21 Rosetta and DH5α) were cultured in Luria-Bertani (LB) growth medium. Samples in a rich growth medium were stored long-term at -80°C containing 25% (v/v) sterile glycerol, in 2 ml cryotubes. LB-agar plates containing the appropriate antibiotics were inoculated using samples from the frozen glycerol stock. Plates were incubated overnight at 37°C.

2.1.1. Preparation of competent *E. coli* cells

An overnight culture of the relevant strain of *E. coli* was prepared for the next working day in LB medium by inoculation from a plate, followed by incubation at 37°C with 180 rpm orbital shaking. On the following day, 100 ml of fresh growth media was inoculated (1:1000) with the host strain from the overnight culture. This culture was incubated with shaking at 37°C for approximately three hours until OD_{600nm} reached ~0.4. The cell suspension was immediately placed for 15 minutes on ice, and was then centrifuged at 4000 *g* for 10 minutes. The supernatant was discarded, and the cell pellet was resuspended in 30 ml of ice cold buffer TFB1 (100 mM $RbCl_2$, 50 mM $MnCl_2$, 30 mM potassium acetate, 10 mM $CaCl_2$, 15 % v/v glycerol, pH 5.8) and incubated on ice for 2 hours. The suspension was subsequently centrifuged at 4000 *g* for 10 minutes at 4°C, the supernatant was discarded, and the pellet was resuspended in 8 ml of ice cold buffer TFB2 (10 mM MOPS, 10 mM $RbCl_2$, 75 mM $CaCl_2$, 15 % v/v glycerol, pH 6.8) and incubated on ice for 15 minutes. Aliquots (100 ml) of cells were flash-frozen in liquid nitrogen then stored at -80°C until required.

2.2. Transformations of bacterial cells with plasmid DNA

Chemically competent *E. coli* cells were kept at -80°C and thawed on ice immediately before use. Plasmid DNA solution (2 µl) was added, followed by incubation on ice for 20 minutes. After incubation, the thermoblock was used to heat shock the mixture at 42°C for 45 seconds, followed by another incubation on ice for 2 minutes. After that, 900 µl of LB was added to the mixture of transformed cells to start the cell recovery process. The sample was incubated at 37°C with 185

rpm orbital shaking for one hour. Bacterial cells (200 µl) were plated out onto LB agar plates which contained the appropriate antibiotics and incubated overnight at 37°C.

2.3. Growth media and antibiotic

Bacterial medium was sterilised by autoclaving at 120°C for 30 minutes at 1 atmosphere pressure. All supplements, e.g. antibiotic, was made by dissolving in Milli-Q water, and then sterilized using disposable filter with a 0.22 µm pore at room temperature and under aseptic conditions (i.e. in the presence of a Bunsen burner). Two kinds of bacterial media were used in the project, one of these media was Lysogeny broth (LB) and the second one was minimal medium (M9). Before culturing the bacterial cells, an appropriate antibiotic was added at the following concentration 50 µg ml^{-1} kanamycin.

- (M9) MINIMAL MEDIUM (500 mL

-Make 5X M9 salt containing:

-Na2HPO4 · H2O 21.25 g

- KH_2PO_4 7.5 g

- NaCl 1.25 g

- NH_4Cl 2.5 g

- Adjust PH 7.4

Prepare the following mix in sterilised conical flasks :

1. Add 5X M9 Salt 100mL
2. Add 0.5ml $CaCl_2$

- Then mix them by shaking incubator for 5-10 minutes

3. Add 2mM 10ml MgSO4 (depends on your available stock)

- Add Autoclaved ddH2O and top up until 500m

- Then mix them again by shaking incubator for 5-10 minutes

4. Add 10mL 20% Glucose
5. Add 100µl of 0.5% Thiamine and mix it in the shaking incubator.

-Lysogeny broth medium (LB) in (500 ml)

1. Add 5 g/L^{-1} NaCl
2. Add 5 g/L^{-1} Tryptophan
3. Add 2.5 g/L^{-1} Yeast extract

- Mix them by magnetic stirrer for 5 to 10 minutes in conical flask

- Then Sterilise the mix by using autoclave system

Table 2.1.3. The recipe of making the two chemical media that have used in the study.

2.4. Overexpression of *Neisseria gonorrhoeae* Csp1 and *Salmonella enterica* sv. Typhi Csp3 in LB medium

For large-scale expression, a single colony of *E. coli* BL21 cells, previously transformed with the expression plasmid pET29a-Csp1/3, was inoculated into 10 ml of LB containing 50 µg ml^{-1} kanamycin and incubated at 37°C with 185 rpm orbital shaking. The overnight culture (1000 µl) was used to inoculate 500ml of fresh LB containing kanamycin and incubated for approximately 4 hours until the OD_{600nm} reached to 0.4. Then 1 mM of the protein synthesis inducer, which was isopropyl β-D-1-thiogalactopyranoside (IPTG), was added, followed by 14 hours incubation at 37°C with 185 rpm orbital shaking. Cells were harvested by centrifugation (4000 *g*, 30 min, 4ºC), washed in 20 mM Tris pH 8.5, and frozen at -20°C.

2.5.1. Small scale overexpression of *Neisseria* Csp1 and *Salmonella* Csp3 in minimal medium.

In order to determine the optimal conditions for protein over-expression in minimal medium, small-scale expression testing was initiated. Firstly, 10 ml of LB containing 50 µg ml^{-1} kanamycin was inoculated with a single colony of *E. coli* cells transformed with the expression vector to start an overnight culture and incubated at 37°C with 185 rpm orbital shaking. On the following day, the overnight culture (10 ml) was used to inoculate 200 ml of fresh M9 medium containing 50 µg ml^{-1} kanamycin and incubated for approximately 7 hours until the OD_{600nm} reached 0.4. Then 1 mM of the inducer IPTG was added. At several time points, aliquots were collected. These pellets were resuspended in PBS buffer and lysed by sonication to determine the optimum the time of protein expression. By resolving aliquots of these extracts on SDS-PAGE it was found that 17 after addition of the inducer resulted in maximal expression of the protein.

2.5.2. Large scale overexpression of *Neisseria* Csp1 and *Salmonella* Csp3 in minimal medium.

A large volume of M9 medium (500 ml) was prepared to begin protein overexpression. As previously, a single colony of *E. coli* transformed with the expression plasmid was inoculated into 10 ml of LB containing 50 µg ml^{-1} kanamycin and incubated at 37°C with 185 rpm orbital shaking overnight. The following day, a volume of 1000 µl was used to inoculate 500 ml of fresh M9 containing kanamycin, and incubated for approximately 7 hours until the OD_{600nm} reached ~0.4. Then 1 mM of inducer IPTG was added and the bacterial culture was incubated at 37°C, with 185

rpm orbital shaking. Cells were harvested by centrifugation (4000 *g*, 30 min, 4°C), washed in 20 mM Tris pH 7.5, 10 mM EDTA, and frozen at -20ºC.

2.6. Protein extraction from *E. coli* cells.

Frozen cell pellets of *E. coli* after expression of the target recombinant proteins were thawed on ice and resuspended in 20 ml of 20 mM Tris buffer, pH 8.5. Then, the resuspended cells were lysed by sonication on ice (cycling: 6 times for 6 seconds sonication, one minute between each cycle on the ice). The resulting cell lysate was transferred to 50 ml centrifuge tubes and spun down by centrifugation in a JA25.5 rotor at (19.000 *g*, 30 min, 4°C). The supernatant was transferred to a fresh 50 ml falcon tube and kept on ice. The sample was filtered using a syringe filter (0.45 µm) prior to chromatography.

2.6.1. Gradient anion exchange chromatography of crude cell lysate (AEC)

Liquid chromatography purification of proteins was applied by using the ÄKTA start system (GE Healthcare). The cleared cell lysate was loaded onto a 5 ml HiTrap Q HP anion exchange column (GE Healthcare), which had already been pre-equilibrated with 10 ml of 20 mM Tris buffer, pH 8.5, then 10 ml of 1 M NaCl in 20 mM Tris, pH 8.5, and followed by 10 ml of 20 mM Tris buffer, pH 8.5. After washing in the binding buffer, protein elution was completed using a 9 column volumes (CV) linear (0-1 M) NaCl gradient, collecting 2 ml fractions. Eluted fractions were analysed by SDS-PAGE (19% acrylamide w/v).

2.6.2. Size exclusion chromatography (SEC) (preparative SEC)

Size exclusion chromatography (SEC) columns were stored in 20% ethanol and maintained based on manufacturer's instructions (GE Healthcare). Fractions of protein purified by AEC, that were found to contain recombinant Csp1/Csp3 proteins by SDS-PAGE analysis, were further purified by using preparative SEC on a Superdex 200 16/600 PG. The column was previously equilibrated with 1.5 column volumes (CV) of SEC buffer (20 mM Tris, 150 mM NaCl, pH 8.5). An AEC fraction (2 ml) was loaded onto the column at room temperature and resolved in SEC buffer, with 2 ml fractions collected and analysed on SDS-PAGE to evaluate the purity.

2.7. Sodium dodecyl sulphate-polyacrylamide gel electrophoresis (SDS-PAGE)

The expression and purity of proteins were evaluated by using SDS-PAGE. All SDS-PAGE gels were prepared using the Mini-PROTEAN Handcast system (Bio-Rad) containing upper layer of stacking gel and bottom layer of resolving gel (Table 2.7.1). Gels were prepared and resolved according to the manufacturer's instructions, and stained with Expedeon InstantPAGE Coomassie Brilliant Blue protein stain.

Resolving gel	Stacking gel
1. H_2o (1.5 ml)	1. H_2o (3.4ml)
1. 30% acrylamide (10.13 ml)	2- 30% acrylamide (830 µl)
2. 1.5M Tris PH 8.8 (4 ml)	3-1.0M Tris PH6.8 (630 µl)
1. 10% SDS (160 µl)	4-10% SDS (50 µl)
1. 10% ammonium persulfate (160 µl)	5-10% ammonium persulfate (50 µl)
1. TEMED (16µl)	6-TEMED (5 µl)

Table 2.7.1. Composition of 19% gel solutions for SDS- PAGE

2.8. Inductivity coupled plasma mass-spectroscopy (ICP-MS)

Inductively coupled plasma mass spectrometry (ICP-MS) is used to measure the elemental content of solutions. ICP-MS is a technology that enables the simultaneous measurement of concentrations of multiple elements/isotopes with outstanding sensitivity and resolution. An alternative approach was considered, utilising atomic absorption spectroscopy (AAS), but was not utilised as it is (a) less sensitive and (b) requires consumption of multiple aliquots of purified protein to measure multiple elements. The ability to measure multiple elements was crucial for my experiments. For instance, the presence or absence of contaminating metals in purified 'apo' samples was more effectively checked by ICP-MS, whereas the results of a Cu/ Zn/Ag binding experiment required that we measured copper, silver and zinc in the same sample. Use of atomic absorption would have

consumed three of each sample, and would have been more time-consuming due to having to change the bulb and set up the instrument differently for each metal measurement.

The samples were diluted (30-fold) in high purity nitric acid (Merck) containing a known concentration of internal metal standards (HNO_3 + 20 μg/L Ag and Pt or HNO_3 + 20 μg/L Co and Pt). The same solution was used to prepare elemental standards containing the target metals at varying concentrations (0, 1, 5, 10, 50, 100 μg/L) for construction of a standard curve. The ICP-MS detected target ions (^{55}Mn, ^{56}Fe, ^{59}Co, ^{65}Cu, ^{66}Zn, ^{107}Ag, ^{195}Pt) using the same technical conditions used in (Vita et al., 2015). The analysis of each sample was prepared in triplicate and unknown values calculated using a standard curve.

2.9. Determination of protein concentration

2.9.1. Bradford assay

The principle of this classical method for measuring protein concentrations is that the binding of protein molecules to Coomassie dye under acidic conditions results in a colour change from brown to blue that correlates with protein concentration. This is based on measuring the relative abundance in samples of the basic amino acid residues; arginine, lysine and histidine, which react with the dye**.**

The protein sample was measured by using the Bradford method (as per instructions from the Coomassie Plus protein assay kit, ThermoFisher Scientific) by comparing absorbance at 595 nm. The unknown protein concentration was calculated by comparison with a standard curve of known concentrations of bovine serum albumin (BSA).

2.9.2. A280 measurements

The concentrations of proteins were measured by monitoring absorbance at 280 nm. The principle of such measurements rests on the absorbance in this region of aromatic residues, particularly that of tryptophan residues.

A UV/visible spectrum was obtained in the wavelength range between 200 nm and 800 nm, with the sample placed inside a quartz cuvette (1 cm pathlength) in the UV-Vis Spectrometer, a Lambda 35 model (Perkin Elmer). Protein concentrations were calculated by using the theoretical extinction coefficients, ε_{280nm}, that were calculated using the ProtParam online software, and using the Beer Lambert Law ($A=\varepsilon cl$).

2.9.3. DTNB

Ellman's reagent, also known as 5,5'-dithiobis-(2-nitrobenzoic acid) or DTNB, is a chemical used to quantify the concentration of thiol groups in a sample. A solution of this compound produces a measurable yellow coloured product when it reacts with sulfhydryl groups.

The process was applied inside an anaerobic chamber (Belle Technologies) to quantitate free sulfhydryl groups in solution. Required buffers in this assay were: reaction buffer (RB), 930µl, 1 M Na_2HPO_4; 70 µl 1 M NaH_2PO_4; 9 ml 6 M guanidine HCL or 8 M Urea, and reaction solution (RS) containing 0.02 g DTNB per 5.0 ml RB. Samples were mixed with a fresh solution of DTNB reaction buffer and with either 6 M Guanidine or 8 M Urea buffer to unfold the protein in order to expose the Cys residues to the reagent, and the resulting absorbance was measured at wavelength 412 nm. Concentration of thiols was determined using the ε_{412nm} of DTNB = 14.150.

Reaction buffer (RB)	Reaction Solution (RS)
930µl Na_2HPO_4(1M)+70 µl NaH_2PO_4+9ml 6M Guanidine or 8M Urea	0.02g DTNB /5.0ml RB

Table 2.9.3. A recipe of required solutions and buffer of DTNB test

2.9 4. Amino acid analysis

Samples of purified Csp1/Csp3 proteins were sent to Alta Biosciences Ltd, after previously determining the protein concentration using the other methods described above, for quantitative analysis of the amino acid content. Results were obtained for 16 out of 20 amino acids that could be quantified, from which an average was taken and used to calculate the protein concentration from the amino acid analysis.

2.10. Monitoring copper binding to Csps using UV/visible spectroscopy

Purified samples and required copper dilution solution (CuDs), as well as the SEC buffer (20mM Tris, 150mM NaCl pH 8.5), were all prepared under anaerobic conditions. The amount of copper needed for a titration was calculated based on measured protein concentration. This was determined by Bradford Assay after applying a correction factor based on correcting the Bradford data according to the relative result from quantitative amino acid analysis. Several tubes of Csp1 were prepared in the anaerobic chamber in order to yield identical protein concentrations for incubation. The final compositions of each solution (of protein plus copper) required to monitor copper binding to Csp1 (Table 2.10.1) and Csp3 (Table 2.10.2) are shown in the tables. Those tubes were incubated overnight inside the anaerobic chamber at room temperature, and the following day were measured using UV/visible spectroscopy (200-800 nm).

Equivalence	Cu(0)	Cu(10)	Cu(20)	Cu(30)	Cu(50)
Protein	900µl	900µl	900µl	900µl	900µl
(CuDs) buffer	100 µl	90 µl	80 µl	70 µl	50 µl
(10mM Cu)	0	10 µl	20 µl	30 µl	50 µl

Table 2.10.1. Purified Csp1 protein (10 µM) was incubated with different copper concentration for measuring copper stoichiometry by UV/visible spectroscopy followed by analytical SEC.

Equivalence	Cu(0)	Cu(10)	Cu(20)	Cu(25)	Cu(30)	Cu(50)	Cu(75)	Cu(100)
Protein	147 µl	147 µl	147 µl	147 µl	147 µl	147 µl	147 µl	147µl
(CuDs) buffer	853 µl	843 µl	833 µl	828 µl	823 µl	803 µl	778 µl	753 µl
(10mM Cu)	0	10 µl	20 µl	25 µl	30 µl	50 µl	75 µl	100 µl

Table 2.10.2. Purified Csp3 protein (10 µM) was incubated with different copper concentrations for measuring copper stoichiometry by UV/visible spectroscopy followed by analytical SEC.

2.10.1. Analytical size exclusion chromatography

Each of the samples prepared and incubated with copper for UV/visible spectroscopy were subsequently injected onto a size exclusion column (Superdex S200 10/300, GE Healthcare) to resolve bound and unbound metal. The column was previously equilibrated in SEC buffer, 10 mM Hepes, 50 mM NaCl pH 7.0, and was resolved in this same buffer, collecting 1.5 ml fractions. These size exclusion fractions were then prepared for elemental analysis by diluting them into nitric acid solution followed by ICP-MS analysis (see section 2.8).

2.11. Test of Zn/Ag binding to Csp1/Csp3

We built the experimental design based on adding different metals in a specific order with a subsequent incubation period, in order to determine whether binding of one metal could prevent the binding of a subsequent metal. Silver and zinc were added to purified protein Csp1/Csp3 to investigate the effect of their putative binding on subsequent copper binding the structure of those proteins.

The experimental steps were performed under anaerobic conditions and sealed cuvette tubes were used to prepare the solutions for spectroscopy. Metal concentrations were calculated and then were added to achieve fixed numbers of mole equivalents relative to the protein concentration. Protein concentration was determined by Bradford assay based on a correction factor derived from the quantitative amino acid analysis. The first three tubes contained each metal on its own (either 10 equivalents of copper, 1 equivalent of silver or 1 equivalent of zinc), and two further contained one metal (silver or zinc) that would subsequently receive copper after incubation. The result for those samples was that one equivalent of silver or zinc had been added to the protein sample followed by an hour incubation, then ten equivalent of copper were added, followed by a further one hour incubation. The remaining volume was composed of buffer as is shown in Table 2.11. Protein was added last to these metal solutions, then each of those tubes was left for an hour of incubation at room temperature in the anaerobic chamber, followed addition of Cu(I) to those that required a second metal addition and then a further incubation period.

Samples were subsequently resolved to separate bound and unbound metals by injecting onto an analytical size exclusion column. This utilised a Superdex S200 10/300 column which was previously equilibrated in the SEC buffer of 10 mM Hepes, 50 mM NaCl pH 7.0. Following size exclusion, fractions were diluted in nitric acid to analyse metal composition by ICP-MS (see section 2.8).

Metals	10 equ. Cu	1 equ. $AgNo_3$	1 equ. $ZnCl_2$	1 equ. $AgNo_3$+ 10 equ. Cu	1 equ. $ZnCl_2$+10 equ. Cu
(SE) Buffer	140.5 µl	140.5 µl	140.5 µl	138 µl	138 µl
Protein	357µl	357 µl	357 µl	357 µl	357 µl
$ZnCl_2$ (1mM)	-	-	2.5 µl	-	2.5 µl
$AgNo_3$ (1 mM)	-	2.5 µl	-	2.5 µl	-
Cu (10 mM)	2.5 µl	-	-	2.5 µl	2.5 µl

Table 2.11. experimental design of Effect of Zn/Ag binding to Csp1/Csp3

2.12. Determination of crystal structure

2.12.1. Initial screening and optimisation

The protein purification for crystallography were as described above (see sections 2.6.1 and 2.6.2). Subsequently, purified samples of Csp proteins were concentrated using Amicon Ultra-concentrators (10 kDa molecular weight cut-off) to the target concentration of ~20 mg ml^{-1}. Initial crystallisation screening was performed under supervision of Dr Arnaud Basle, using the screen JCSG in 96 wells crystallization plates. A mosquito robot was used to prepare trials with the method of sitting-drop of vapour diffusion at 20°C. Each condition was tested in two sitting drops (100 nl crystallisation liquor + 100 nl protein solution, and 200 nl crystallisation liquor + 100 nl protein) against 800 µl reservoir solution. The diffraction data collection and protein crystal structure solvution was performed by Dr. Arnaud Basle using methods equivalent to (Vita et al., 2015) and the Pymol program was used to produce images of the protein structures.

Chapter 3: Investigating Cu(I), Ag(I) and Zn(II) binding to Csp1 from *Neisseria gonorrhoeae*

3.1. Introduction

The etiological agent of the human disease called gonorrhoea is the Gram negative bacterium *Neisseria gonorrhoeae*, which is an obligate human pathogen. It is the second most common bacterial infection that causes sexually transmitted infections (STIs) after *Chlamydia tracomatis* in North America (Leone et al., 2013; Control and Prevention, 2012). Globally, gonorrhoea has gained more attention of scientists in recent years because of the rapid spread of antibiotic resistance genes among isolates of gonococcus, improving its ability to tolerate multiple antibiotic classes, including tetracyclines, penicillins, sulphonamides, fluoroquinolones and many others.

Gonorrhoea is found to be common in young adults in North America and Canada. It is often asymptomatic in women, but sometimes women experience severe pelvic pain, pelvic inflammation and tubal infertility syndrome, while men develop prostatitis, epididymitis and urethral swelling. Newborns may also develop ocular infection due to exposure to infected secretion (Ng and Martin, 2005).

The genome of *Neisseria gonorrhoeae* encodes a homologue of a new family of copper storage protein, Csp1, that is a putative periplasmic protein. A previous study characterised the first member of this protein family in methanotrophic bacteria (Vita et al., 2015). This family, the copper storage proteins (Csp), are a new family of Cys-rich proteins that function as copper storage proteins in bacteria for safe copper handling.

Djoko and colleagues in 2012 characterized one mechanism that *N. gonorrhoeae* uses to avoid copper toxicity. They identified the gonococcus homologue of CopA, the P-type ATPase that effluxes copper from the bacterial cytosol. The authors showed that a mutant strain that lacked *copA* was more sensitive to high levels of copper concentration compared to the wild type strain, indicating a potential role of CopA in defending against copper toxicity. The *N. gonorrhoeae* strain with a deleted *copA* gene also showed a reduced ability to survive within human cervical epithelial

cells, presumably due to high concentrations of copper inside the host cells. So the experimental work evaluated that CopA is key to the copper defence system of *N. gonorrhoeae*.

The *N. gonorrhoeae* Csp homologue is, almost uniquely amongst bacterial pathogens, predicted to be targeted to the periplasmic compartment as it contains a pre-peptide leader sequence predicted to target it for secretion by the Tat system. Most bacterial Csp homologues lack a signal peptide and are therefore suggested to be cytosolic. Recent studies have revealed crystal structure of copper storage proteins, showing that both cytosolic and periplasmic Csps are highly similar in structure.

A single periplasmic Csp homologue has been characterised. Csp1 from *Methylosinus trichosporium* OB3b is a tetrameric protein, with each monomer consisting of four helix bundles. This protein has a capacity to bind up to maximum of 52 Cu(I) ions per tetramer primarily via its 13 Cys residues per monomer, which show high affinity with these metal ions (Vita et al., 2015). So this protein was suggested as major copper chelating agent in the periplasm (or perhaps internal compartments) of *M. trichosporium* OB3b cells. Indeed, Vita and colleagues in 2015 confirmed that Csp1 is major Cu ion containing protein in extracts from *M. trichosporium* cells. On the other hand , many metalloproteins can bind to more than one metal ion *in vitro*, with metal ions interacting with various amino acids that possess electronegative atoms that possess a lone pair of electrons that can form coordinate bonds, such as Cys, His, Asp and Glu (Sharma et al., 2018). To date, no published studies have investigated the metal selectivity of a Csp family protein to determine whether the are selective for Cu(I), or if instead they are capable of coordinating multiple different ions from the *d*-block metals.

The signal peptide of Csp1 and Csp2 target the Tat (Twin Arginine Translocation) machinery to move out of the cytosol, while Csp3 is presumably cytosolic due to absence of signal peptides. Tat transport could be a mechanism by which cells relocate the large number of copper ions that can associate with Csp1 from the cytosol, as Tat substrates are transported in a folded state, or alternatively the Tat system may be engaged to ensure the protein is folded inside the cell prior to translocation, perhaps to avoid formation of disulphide bonds between the key Cys residues during post-translaocation folding in the oxidising periplasm (Palmer and Berks, 2003).

Csp1 is likely translocated out of the cytosol via the Tat system in *Methylosinus trichosporium*. Although its close homologue, Csp2, has not been characterised, it shows high sequence homology with Csp1 and also possesses a similar signal peptide (Vita et al., 2015). The signal peptides of both Csp1 and Csp2 of *Methylosinus trichosporium* OB3b are predicted to target the Tat machinery to translocate out of the cytosol, as is the predicted signal peptide in Csp1 from *Neisseria gonorrhoea*. Thus Csp1 from *Methylosinus trichosporium* OB3b and from *N. gonorrhoeae* are both predicted to be localised to the periplasm, target Tat, and they share significant sequence similarity as shown in (Figure 3.1)

Figure 3.1. Sequence comparison of Csp1 in *Neisseria gonorrhoeae* and *M. trichosporium* OB3b.

Sequence alignment of the Csp1 proteins present in *M. trichosporium* OB3b (denoted OB3bCsp1) and in *Neisseria gonorrhoeae* were created in Clustal Omega. The conserved Cys residues are highlighted in yellow. This pair of Csp1 proteins have 32.2% sequence homology overall. The [.], [:], and [*] symbols show strong and weak similar sequence positions, respectively.

The range of essential micronutrients required by living organisms, for instance copper and zinc, are the same for bacterial pathogens and for the human host. Recent studies have demonstrated an important role for these metal ions in the immune system's protection against pathogens. This new concept, termed nutritional immunity, is one in which the immune system uses a strategy of inducing either starvation or excess of the essential *d*-block metal ions to protect the host against

infectious bacteria. For example, it has long been established that the inflammatory response leads to reduced bodily availability of iron, a mechanism that functions to inhibit growth of bacteria by depriving them of access to this essential micronutrient (Ong et al., 2006). Conversely, macrophages seem to use high concentrations of copper as a toxic weapon to kill bacteria engulfed within the phagosomal compartment (Ladomersky and Petris, 2015; White et al., 2009). In mammals, copper is also an essential factor involved in the differentiation and maturation of leukocytes that participate in adaptive immunity by engulfing pathogens. A lack of Cu in the body leads to neutropenia, suggesting its essential role in the innate immune defence mechanisms against bacterial pathogens (Djoko et al., 2015). It is also reported that most of metalloproteins are relatively specific and function with only one type of metal ion. This chapter describes my study of the copper-binding properties of the Csp1 copper storage protein from *N. gonorrhoeae*.

3.2. Result

3.2.1. Cloning, Expression and Production of Csp1 Recombinant Protein

Prokaryotic expression systems are widely used for overproduction of recombinant protein in various field of biochemistry, structural biology and biotechnology. A prokaryotic system is mostly selected among various other systems because of the advantage of very fast growth rate of bacteria under aerobic conditions, ease of culture, having a relatively simple and easily modifiable genome, and enabling very high-level expression of the target protein, both on laboratory and industrial production scales. This enables bacterial systems to yield large amounts of protein product in a very short period of time, at low cost, and using a well understood set of tools for the genetic manipulation of transcription and translation. *E. coli* bacteria represent the most commonly used model for genetic manipulation as a prokaryotic cloning and expression system. Recently, *Bacillus* species have been used increasingly in different biotechnological projects after *E. coli*. The *E. coli* prokaryotic system is also preferable for mutational studies and for investigating the mechanisms of enzymes, drugs and chemical production (Porowińska et al., 2013).

For the expression of recombinant protein, the amplified *csp1* gene from *Neisseria gonorrhoeae* was ligated into the commercial pET29a expression vector, which is routinely used in the Waldron lab because it effectively produces large quantities of heterologous proteins inside *E. coli* while

allowing robust growth under diverse culture conditions. The expression construct was previously prepared by undergraduate project student, Rebecca McCamley through a ligase-dependent cloning approach. The pET series of plasmids contain all necessary genetic elements for heterologous expression purposes, including a highly expressed promoter and effective terminator, selectable antibiotic resistance marker, and a low copy bacterial origin of replication.

Competent cells of strain *E. coli* BL21 Rosetta (which carry additional tRNA components to enhance expression of heterologous proteins) were transformed with the pET29a-NgCsp1 plasmid. A single positive clone, containing the plasmid for expression of the *csp1* gene for large-scale expression, was selected from a plate screened on the basis of kanamycin resistance conferred by the pET plasmid.

Cells transformed with pET-NgCsp1 for the production of Csp1 protein were cultured. An overnight culture was used to inoculate large volumes (1-6 L) of fresh growth medium (either LB medium or M9, depending on the required protocol), which was then incubated until they reached OD_{600nm} ~ 0.4, and recombinant protein production was induced with addition of a isopropyl β-D-1-thiogalactopyranoside (IPTG). The cultures were subsequently incubated for 16 h at 37 °C. Sample aliquots acquired from before and after this induction period enabled the presence of the target protein to be determined via SDS-PAGE. For purification, cells were harvested and washed in buffer, and the pellet was stored at 20°C.

3.2.2. Purification of recombinant Csp1 protein

The second essential step of studying proteins biochemically *in vitro* is to purify the overexpressed protein from crude *E. coli* extract by designing a suitable purification strategy. The aim of this strategy is to achieve a high level of purification to reach a purity close to homogeneity, while minimising the amount of time required for the purification to ensure that the sample of protein purified is as fresh as possible for subsequent biochemical characterisation. We developed a two-step purification strategy for Csp1 based on anion exchange chromatography (separating proteins in the crude extract on the basis of charge) followed by size exclusion chromatography (separating

proteins in the anion exchange eluant on the basis of size) as a rapid and effective purification that could be carried out over the course of two days or less.

The calculated pI (using the online tool Expasy) for NgCsp1 was 6.27, therefore we decided to use an anion exchange chromatography (AEC) matrix and with buffers at a pH above 7. This should result in a net negative charge on the target protein that would in turn create an affinity of the protein for the positively charged (quaternary ammonium) chromatography matrix. This would ensure binding of the target protein to the matrix, allowing a lot of contaminating proteins that are unable to bind to the matrix to be washed away, thereby achieving purification Furthermore, a gradient elution was selected, using salt as competitor of this ionic interaction between protein and matrix, to further enable selective elution to increase this purification step's effectiveness. AEC was thereby used to separate Csp1 from many of the contaminating protein species according to their charge.

The pellet of *E. coli* cells that were expressing the recombinant protein was thawed on ice, resuspended in buffer and lysed by sonication. The cell lysate was centrifuged and the clarified lysate filtered in preparation for chromatography. Two steps of ÄKTA protein purification were performed to purify the target recombinant protein Csp1 from crude soluble extract of the *E. coli* expression cells. The first purification step used anion exchange chromatography (AEC) (Figure 3.2), which selectively binds and releases species based on their anionic nature. The protein was therefore purified from the complex extract by separating the components according to the extent to which they are acidic. The clarified supernatant was first loaded onto an anion exchange chromatography column under low salt conditions at pH 8.5. Under these conditions, acidic groups on Csp1 (predicted pI = 6.27) would be net deprotonated and consequently negatively charged, and it should therefore show a binding affinity of negatively charged protein for the positively charged ammonium moieties associated with the anion exchange chromatography column.

After a pre-equilibration period (this is the period labelled 'binding buffer' in (Figure 3.2), of the soluble crude extract was loaded onto the column and then washed to remove any low affinity-

bound proteins using low salt buffer (the period labelled 'flow through' in figure 3.2). Finally, the proteins bound to the column were eluted using a linear [NaCl] gradient (from 0-1 M NaCl, shown as a dashed line in the figure), again at pH 8.5 (labelled 'eluted target' in figure 3.2). The charges in the salt solution act to compete for binding to the matrix against the bound protein, and therefore increasing salt concentrations will progressively lead to elution of more negatively charged protein species. Protein eluting from the column was tracked by constantly measuring A280nm, which is a wavelength where protein (especially aromatic residues) absorb light. The chromatogram showed the elution of a number of protein peaks from the AEC column between 110 and 180 ml.

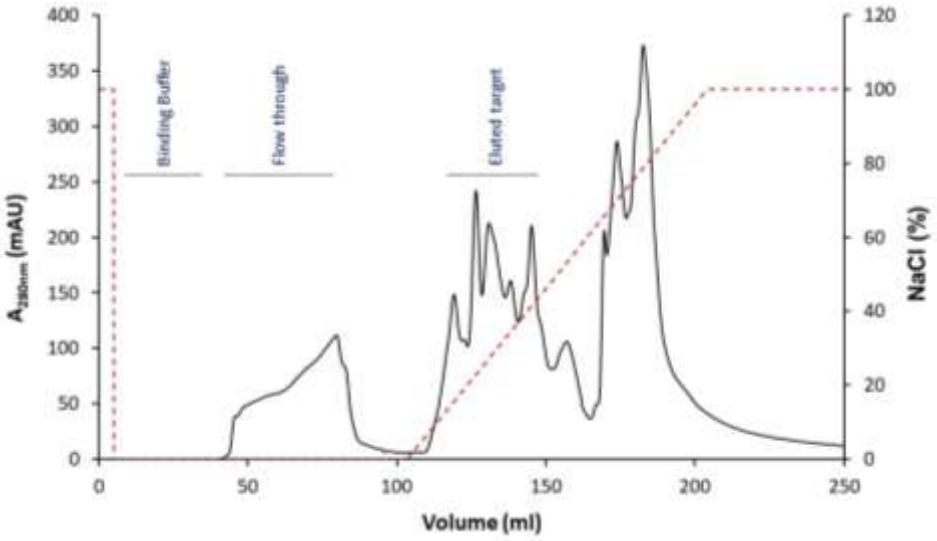

Figure.3.2. Chromatogram from anion exchange chromatography (AEC) purification of recombinant protein Csp1 from crude *E. coli* lysate.

AEC chromatogram of Csp1 purification from crude *E. coli* lysate, showing a linear NaCl gradient elution (dashed red line) of proteins (detected using A_{280nm}, black line). The purification was done using a 5 ml HiTrap Q HP anion exchange column connected to an AKTA Start system. Low salt buffer (20 mM Tris, pH 8.5) and high salt buffer (20 mM Tris, pH 8.5, 1M NaCl) were mixed to generate the gradient. This pH was selected to ensure acidic groups on Csp1 (predicted pI = 6.27). The column was washed after loading to remove any low affinity-bound proteins from the *E. coli* crude extract using low salt buffer (Flow through). Protein elution stage used a linear [NaCl] gradient from 0-1 M NaCl (Eluted target). This is a representative

chromatogram taken from a single purification, but this AEC was performed numerous times (>10 occasions) to purify Csp1.

An aliquot (10 µl) of each of the fractions from AEC with significant A280nm absorbance was loaded on SDS-PAGE gels, which were subsequently stained with Coomassie Brilliant Blue (Figure 3.3), to evaluate the purity of the target protein in the eluted fractions from anion exchange chromatography (Figure 3.2). The gel showed that Csp1 had been partially purified from the crude extract (Figure 3.3), but as expected after a single purification step there remained a number of protein contaminants of varying masses, which led to the conclusion that the fractions needed at least one further step of purification.

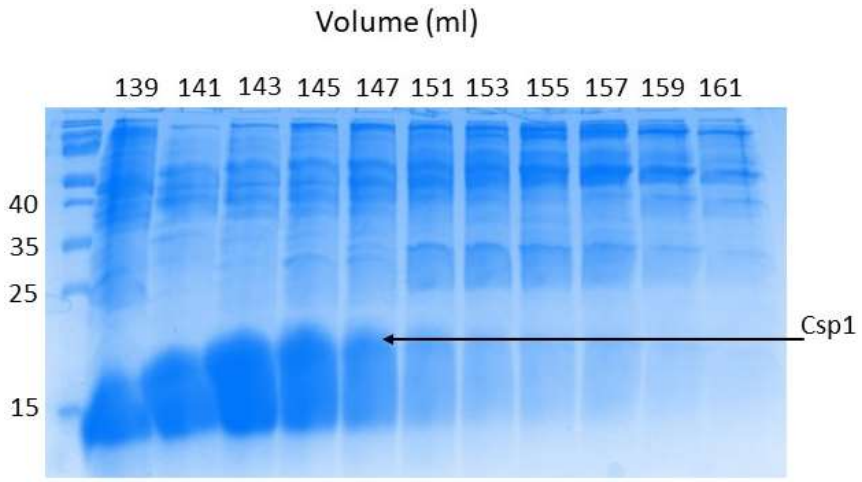

Figure 3.3. SDS-PAGE of eluted fractions from AEC purification of recombinant protein Csp1 from crude *E. coli* lysate.

Eluted fractions from AEC purification of Csp1 from *E. coli* lysate were collected (2 ml) at the start of the salt gradient (see region labelled 'Eluted target' in figure 3.2). An aliquot (10 µl) of each of these eluted fractions was boiled in the presence of 1% SDS and 10 mM DTT, then resolved on an SDS-PAGE gel (19% acrylamide w/v), stained with Coomassie Brilliant Blue and visualised with Image Lab software. The elution volume of the fractions from AEC are indicated (above). Molecular markers (left) indicate molecular weight of standard proteins. The arrow (right) indicates the target Csp1. Note that the predicted mass of Csp1 is 13,675 Da (Expasy). This is a

representative gel taken from a single purification, but this AEC/SDS-PAGE analysis was performed numerous times (>10 occasions) to purify Csp1.

In order to increase the purity of the preparation of the Csp1 protein, a further protein purification step was combined into the purification strategy. The Csp1 protein is quite small in size (expected molecular weight according to calculation using online bioinformatics tools Expasy ~13,675 Da for a monomer), but previously characterized homologues have been shown to form tightly bound homotetramer structures, and therefore the expected size of the Csp1 protein in its homotetrameric form was ~54 kDa. Based on that predicted molecular weight, we therefore decided to select size exclusion chromatography (SEC) as a suitable second purification step. This looked to be especially viable as a purification strategy because the contaminants detected in the Csp1 preparation after anion exchange chromatography were of relatively large masses compared to the target protein (Figure 3.3). Due to this large tetrameric mass, we selected Superdex 200 as the most suitable size exclusion chromatography matrix, based on its anticipated resolving range according to the manufacturer's information. Fractions containing Csp1 that had been eluted from the anion exchange column (Figure 3.3) were pooled together and injected onto a preparative column of Superdex 200 16/600. The column was previously equilibrated overnight in size exclusion buffer (20 mM Tris, 150 mM NaCl, pH 8.5), and then the sample was resolved in the same buffer. The purification process was performed at room temperature, with protein absorbance again measured by monitoring A280nm as before, and 2 mL fractions were collected throughout the run as shown in chromatogram (Figure 3.4).

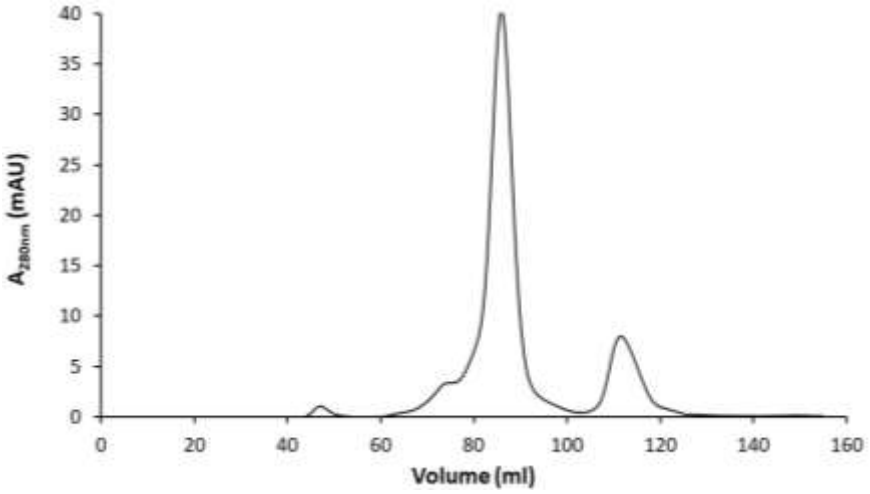

Figure 3.4. Size exclusion chromatography (SEC) chromatogram of recombinant protein Csp1 after initial AEC.

Size exclusion chromatography purification of Csp1 from a combined sample prepared from some of the fractions eluted previously from anion exchange chromatography (Figure 3.2). The fractions labelled as 139-141-143-145-147 in (Figure 3.3) were pooled and resolved in 20 mM Tris, 150 mM NaCl pH 8.5 using a Superdex S200 16/600 preparative column on an AKTA Pure FPLC system at room temperature. To collect eluted samples, 2 ml fractionation was used over 1.5 column volume. This is a representative chromatogram taken from a single purification, but this AEC was performed numerous times (>10 occasions) to purify Csp1.

To determine the fractions in which the Csp1 protein had eluted from SEC, aliquots of each of the fractions that exhibited a significant absorbance at 280 nm (Figure 3.4), and thus contained some protein content (across the region: 78-80-82-84 ml), were resolved by SDS-PAGE (Figure 3.5). This allowed us to evaluate the fractions' purity, by staining for protein using Instant Blue (Expedeon) Coomassie Brilliant Blue, and visualised with Image Lab™ software. The Csp protein was found to elute across volume 76-84 ml, however fractions 82-84 contained one primary contaminant with a mass larger than 15 kDa whereas fractions 76-78 contained higher mass protein in the region of 40 to 55 kDa. Nonetheless, these contaminants represented only a minor contribution to the total protein in each of these fractions, which was dominated by the presence

of the target band representing the Csp protein. SDS-PAGE analysis therefore proved that the purification had worked well, and that the Csp1 protein was very abundant in fractions 76 to 84. However, none of those fractions showed that the protein was completely pure. The ratio of the target protein to the contaminants differed in different fractions, for instance in fraction 78, Csp1 was predominantly contaminated with high molecular weight proteins whereas in fraction 84 I have similar amount of protein with quite little of the high molecular weight proteins.

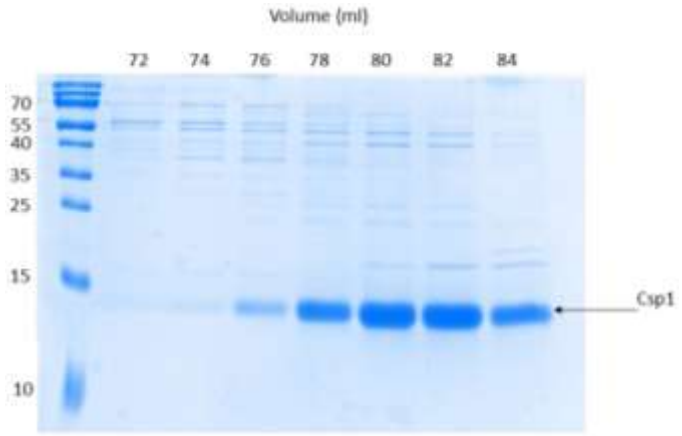

Figure 3.5. SDS-PAGE showing protein content of eluted fractions of size exclusion after purification of recombinant protein Csp1.

An aliquot (10 µl) of each fraction (2 ml) across the main elution peak across the protein-containing region (78-84ml in Figure 3.4) were analysed by SDS-PAGE. Samples were boiled for ten minutes in the presence of SDS and DTT, and resolved on 19% (w/v) gel and stained for protein using Instant Blue (Expedeon) Coomassie and visualised with Image Lab™ software to investigate the sample purity. The numbers on the left relate to molecular weight of protein standards (Promega). In addition to this, the arrow on the right indicates the band that represents Csp1, which has a predicted mass of 13,675 Da. This is a representative gel taken from a single purification, but this SEC/SDS-PAGE analysis was performed numerous times (>10 occasions) to purify Csp1.

3.2.3. Protein quantitation of Csp1

The next step, after the purification of Csp1, was quantifying the recombinant protein in order to design the next experimental stages in an effort to estimate copper stoichiometry. In any biochemistry research situation, it is important to be able to accurately determine the concentration of protein in solution. Nonetheless, protein concentration measurement is still a challenge, with the availability of several distinct methods of protein measurement, but with each method having different advantages and disadvantages. The chosen method will depend on specific factors, for instance, the speed and cost of each analysis, the sensitivity of detection, the availability of specialist reagents or equipment needed for the analyses, and the different composition of amino acids in the proteins to be measured.

For my experiments, based on the accuracy of the protein concentration measurement step it will be possible to prepare the desired amount of each metal solution to perform a titration, and as a result determination of metal stoichiometry. The result measured after adding one molar equivalent of metal to a protein would be greatly affected by, for example, a two-fold error in protein measurement. Very few Csp proteins have been tested experimentally, and the authors of a prior study noted that quantitation of *Mt*Csp1 was challenging (Vita et al., 2015).

Several methods were used to try to measure the concentration of the purified Csp1 recombinant protein. First, it was measured following the Bradford method (using the Coomassie Plus Protein Assay reagent, ThermoFisher Scientific). This method works by measuring the absorbance, A595nm, of a reaction of the protein solution to be measured with this Bradford reagent and then comparing this intensity of the reaction with an unknown concentration of protein with that of the reaction of the same reagent with standard solutions of bovine serum albumin (BSA). These standard solutions are used to construct a ‘standard curve’, which enables us to calculate the estimated protein concentration of the unknown sample. The principle of this Bradford assay is that the binding of protein molecules to Coomassie dye under acidic conditions results in a colour change, from brown to blue, so that the intensity of blue colour indicates the concentration of protein in the sample. This method is specifically measuring the abundance of basic amino acid

residues, i.e. arginine, lysine and to a lesser extent histidine, which are the amino acids that react with the colorimetric reagent in the Bradford reaction. This leads to a limitation in the accuracy of the Bradford assay for measuring protein concentrations – that the ratio of these amino acids within the target protein is very unlikely to be equal to the ratio of these amino acids within the protein standard, BSA, thereby giving rise to a potential systematic error in the assay. The absorbance was measured at 595 nm, the peak absorbance of the blue colour after the Bradford reaction. Dilutions of the purified Csp1 protein were prepared, and then mixed with a fixed volume of the Bradford assay reagent. Simultaneously, suitable serial dilutions of the protein standard, BSA, were also prepared in the same microtitre plate, in the same buffer, and mixed with the same fixed volume of Bradford reagent. All samples were prepared in triplicate and mean values taken. After a brief incubation time, the absorbance was measured at 595 nm and a standard curve was created using the absorbance observed plotted against the protein concentration for each of the BSA standards. This standard curve was then used to mathematically calculate the estimated protein content of 'unknown' samples containing purified Csp1 protein, which was then converted into a molarity (Figure 3.6).

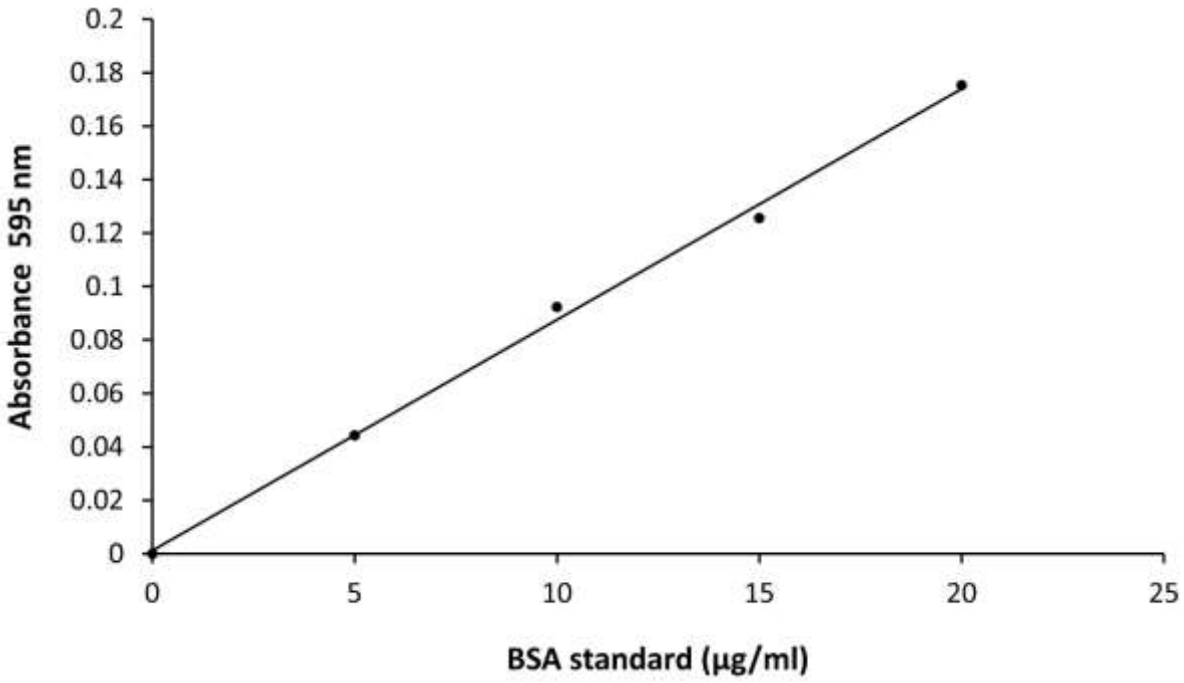

Figure 3.6. The standard curve of BSA from a Bradford assay.

In order to estimate the quantity of Csp1 present in purified recombinant protein fractions, a Bradford assay was used. Suitable serial dilutions were prepared of an aliquot of the protein standard, BSA (2 mg/ml, Pierce), were prepared to achieve concentrations between 0 and 20 μg/ml. These dilutions used the same buffer that the Csp1 protein sample was prepared in (generally SEC buffer, 20 mM Tris, 150 mM NaCl pH 8.5). These were pipetted into a microtitre plate. The unknown protein sample, in this case diluted samples of Csp1, were prepared in the same way in technical triplicate, and added to other wells of the plate. Each sample and standard was mixed with the same fixed volume of Bradford reagent. (200 μl) After a brief incubation (~5 minutes), the absorbance was measured at 595 nm on a plate reader. A Bradford standard curve was created by plotting the absorbance of the different dilutions of the BSA standards of known concentrations. The unknown concentration of Csp1 was then estimated from this standard curve, which was then mathematically converted into a molarity. A representative standard curve is shown, but this assay was performed on numerous occasions (>20) to quantify Csp1.

The second method utilised for estimating the concentration of Csp1 was UV-visible absorption spectroscopy (Figure 3.7). This method exploits the fact that certain aromatic amino acids (particularly tryptophan, but also to a lesser extent phenylalanine and tyrosine) exhibit a significant absorbance of light in the UV region of the spectrum, specifically at 280 nm wavelength. Samples of purified protein were transferred into a quartz cuvette (1 cm pathlength) and a UV/visible region absorption spectrum obtained between 200-800 nm wavelength, blanked against the same buffer as the protein was dissolved in. An estimated extinction coefficient (ε_{280nm}) for the Csp1 protein was calculated using the ProtParam online tool, $\varepsilon = 4{,}470\ M^{-1}\ cm^{-1}$, which was subsequently used to calculate the Csp1 concentration from the absorbance at 280 nm by using a special equation, the Beer-Lambert Law ($A = \varepsilon cL$, where A=absorbance at 280 nm, ε= the extinction coefficient for the protein at 280nm, c=concentration, and L=pathlength).

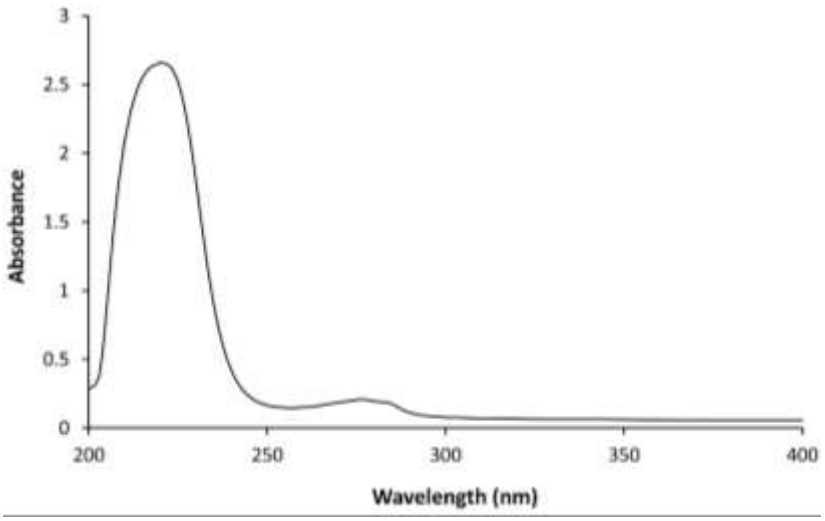

Figure 3.7. Using UV-visible spectroscopy to estimate Csp1 concentration.

The concentration of Csp1 was determined by measuring absorbance at 280 nm. A UV/visible spectrum was obtained in the range between 200 nm and 800 nm. A solution of Csp1 was placed in a quartz cuvette (1 cm pathlength) in the UV-Vis Spectrometer Lambda 35 (Perkin Elmer), which was blanked against buffer (20mM Tris/150mM NaCl PH 8.5). The concentration of Csp1 protein in the sample was calculated using the Beer Lambert Law (A=εcl) (A = εcL, where A=absorbance at 280 nm, ε= the extinction coefficient for the protein at 280nm, c=concentration, and L=pathlength). An estimated extinction coefficient for the Csp1 protein was calculated using the ProtParam online tool, ε = 4,470 M^{-1} cm^{-1}. A representative spectrum is shown, but this assay was performed in triplicate.

The third method usind to estimate Csp1 concentration used the reagent 5,5'-dithiobis-(2-nitrobenzoic acid) (DTNB, also known as Ellman's reagent), which reacts with sulfhydryl groups so that a coloured product may be produced at the end of the reaction. Hence a potentially reliable method is provided that makes use of measuring reduced cysteines and other free sulfhydryl in the solution. When Ellman's reagent is used it estimates sulfhydryl groups, either by comparing to a standard curve using standard solutions containing known concentrations of a sulfhydryl compound (e.g. reduced glutathione, Sigma), or through direct spectroscopic determination using the known extinction coefficient of the resulting complex of sulfhydryls with DTNB (14,150 M^{-1}

cm^{-1} at 412 nm). The DTNB reagent is used for simple quantification of Cys-containing proteins, but requires that the protein is in the unfolded state and must be performed under anaerobic conditions to avoid oxidation reactions from removing sulfhydryl groups through formation of disulfide bonds. The experimental process was therefore performed inside an anaerobic chamber, using buffer that has high concentration of chaotropic reagents like 8 M urea or 6 M guanidine hydrochloride (Figure 3.8).

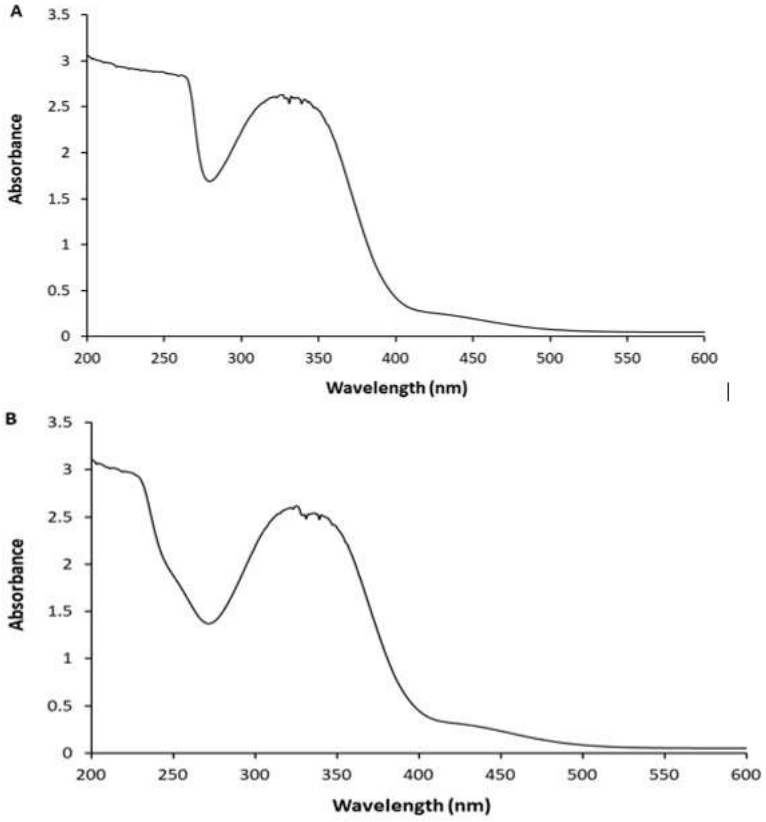

Figure 3.8. Using DTNB reagent for quantification of thiols in the unfolded protein in the presence of 8 M urea and 6 M guanidine hydrochloride.

Ellman's reagent reacts with sulfhydryl groups and produces a measurable yellow colour, which enables it to be used to measure protein concentrations of proteins that contain Cys residues. The experimental process was performed under anaerobic conditions inside an anaerobic chamber to minimise oxidation of Cys residues. The protein solution was diluted with a chaotropic reagent (A: 8 M urea; B: 6 M guanidine hydrochloride) to unfold the protein and expose the Cys residues. This solution was then mixed with a solution of 5 mM DTNB, incubated for 30 minutes in the chamber,

then this solution was measured in the UV/visible spectrophotometer. Csp1 concentration was estimated by measuring the absorbance at the wavelength of 412nm, and using extinction coefficient 14,150 M^{-1} cm^{-1}. This method was performed as a single experiment but in technical triplicate, with a mean value reported.

Unfortunately, during analysis of multiple preparations of Csp1 protein, it was observed that the calculated values of the Csp1 protein concentrations that were obtained using these three approaches was inconsistent. It was therefore difficult to continue experiments which aimed to estimate the Cu(I) binding stoichiometry of the Csp1 protein until this problem of Csp1 protein quantitation was resolved.

In an effort to resolve this conflict between multiple assays of protein measurement concentration, a sample of recombinant Csp1 was sent for quantitative amino acid analysis by Alta Biosciences Ltd. This type of analysis remains the 'gold standard' for protein quantitation, but without the required specialist equipment it is expensive and time-consuming, relying on external contractors. The sample was processed by Alta to allow them to measure the concentration of each of the individual amino acids present in the sample (Table 3.1.3A). If we assume that Csp1 was the only protein present (i.e. we ignore the presence of low-levels of unknown protein contaminants from *E.* coli), we can interpret these data as representing the concentration of Csp1 in the sample, assuming we know the amnio acid composition of the protein from its sequence.

The results shown in the table demonstrate the abundance of each of the individual amino acids measured by Alta, along with the respective amino acid content in the known sequence of Csp1 that was expressed from the pET construct. This is followed by a calculation of the estimated concentration of Csp1 in the sample, based solely on that amino acid. The actual concentration of the protein can therefore be estimated by taking an average of these values, as a measure of concentration on the basis of all of the amino acids. Based on the report which was received from Alta Biosciences Ltd, giving quantities of 16 out of the 20 amino acids (the other four - Phe, Trp, Lys and Arg - cannot be measured due to technical issues during the hydrolysis process), this

allowed us to calculate the average measured protein concentration from the amino acid analysis to determine what we believed the most accurate concentration of Csp1 protein.

Amin acid		nmole/ml	µg/ml	mg/ml	AA content Csp1	[Estimated Csp1 in µM]
Cysteic acid						
Hydroxyproline						
Aspartic acid	D	188	21.7	0.0217	9	20.88889
Threonine	T	148	15	0.015	6	24.66667
Serine	S	150	13.1	0.0131	7	21.42857
Glutamic acid	E	330	42.6	0.0426	13	25.38462
Proline	P	43	4.18	0.00418	2	21.5
Glycine	G	92.7	5.29	0.00529	4	23.175
Alanine	A	558	39.7	0.0397	25	22.32
Cystine	C	27.2	6.04	0.00604	14	1.942857
Valine	V	147	14.6	0.0146	6	24.5
Methionine	M	72.5	9.51	0.00951	4	18.125
Isoleucine	I	32.9	3.72	0.00372	1	32.9
Leucine	L	293	33.2	0.0332	12	24.41667
Tyrosine	Y	52.8	8.62	0.00862	3	17.6
Phenylalanine	F	9.19	1.35	0.00135	0	-
Histidine	H	148	20.3	0.0203	12	12.33333
Tryptophan	W		-	-	0	-
Lysine	K	168	21.5	0.0215	7	24
Arginine	R	75.4	11.8	0.0118	3	25.13333
Totals		2540	272	0.272		21.44987

Table 3.1.3.A. Amino acid analysis yield of Csp1.

An aliquot (1 ml, estimated to be 20 µM from DTNB assay) of a sample of purified Csp1, which had been previously quantified by A280, Bradford, and DTNB, was analysed for amino acid compositions by Alta Biosciences Ltd. The values in this table represent the measured concentration of amino acids and the relative amino acids compositions (AA content Csp1) of purified Csp1, with the exception of Phe, Trp, Arg and Lys which could not be measured. This enabled the calculation of the concentration of protein based on the measured concentration, and number in the Csp1 sequence, of each amino acid (last column). An average of these values was used as a measure of the absolute concentration. This value, in run, was used to generate correction factors for measurements by Bradford, A280nm and DTNB assay (Table 3.1.3B). This experiment was performed once, with Alta performing the analysis in technical triplicate and reporting here a mean value.

This analysis was performed on a batch of Csp1 protein which had previously been quantified using the three methods described above (Bradford, UV/visible spectroscopy and Ellman's reagent). We then used this amino acid analysis value to generate correction factors from this analysis relative to the other three methods employed. This correction factor was linked to the other concentrations, which were measured by Bradford Assay, DTNB assay and A280, allowing us to correct those values (Table 3.1.3.B). For example, it is clear that the amino acid analysis and the DTNB assay gave the most similar results (correction factor 0.825).

Protein measurement method	Protein concentration in (µM)
1- Bradford assay	57 µM
2-Uv/vis spectroscopy	44 µM
3-DTNB	26 µM
4-Amino acid analysis	21.45 µM

Table 3.1.3B. Protein measurement outcomes using different assays

The data presented in this table came from a single biological sample (n=1) and using the three protein quantitation assays: Bradford assay, UV/visible spectroscopy, DTNB assay, and quantitative amino acid analysis. The ratios between these values were used as correction factors to allow rapid quantitation of protein concentration by each in-lab assay, corrected for the discrepancy observed between that method and the quantitative amino acid analysis 'gold standard'.

Four different methods of protein measurement were used in an effort to minimise the error in the determination of the concentration of purified Csp1. However, it is clear that there were significant discrepancies between the measured Csp1 protein concentration as determined with each of these methods (Table 3.1.3B). The final method was quantitative amino acid analysis, which is assumed to be most accurate. Generally, this method is a gold standard for protein concentration

measurement. Being a direct measure based on up to 20 amino acids (16 in this case), it is anticipated to have relatively low error as an average is taken across all the amino acids measured. Crucially, it is clear from the data in Table 3.1.3.A that at least 14 of the amino acids (excluding the four that could not be measured, plus Cys which is also problematic for chemical reasons) gave broadly similar results, at least within an order of magnitude. This gives additional confidence that the average measurement of ~21.5 µM was accurate, as it is hard to imaging that all of these amino acids could have generated a similar systematic error in their determination.

On the other hand, the other methods that have been used in my project have obvious sources of error. Protein concentration measurement by A280 is highly dependent on the presence of Try residues, which absorb strongly in this range of the spectrum. However, Csp1 contains no Trp residues (Table 3.1.3A). A smaller amount of absorbance in this spectral region arises from Phe and Tyr residues, which are present. This resulted in a small extinction coefficient for Csp1, which may have resulted in significant error, especially if one or more contaminating proteins contained a number of Trp residues.

The Bradford Assay measures primarily Arg and Lys residues, and compares their reaction with the Bradford reagent in comparison to a 'standard' protein, BSA. However, there is no reason for BSA to contain the same proportion of these residues as Csp1 (Table 3.1.3A). If there are disproportionately more of these residues in Csp1 than there are in BSA, this would explain why our Bradford assay quantified the concentration of Csp1 as significantly higher than that measured by amino acid analysis (Table 3.1.3B).

Conversely, the DTNB reaction showed a relatively good correlation with the quantitative amino acid analysis. This suggested that DTNB would be the most accurate method for measuring the concentration of Csp1, with only a small correction factor needed to adjust results from the DTNB assay. However, this assay relies on rigorously anaerobic conditions to avoid complications by oxygen as it only measures thiol groups. During this study, we were experiencing problems with our anaerobic chamber, and therefore this method was not always available.

Table 3.1.3B demonstrates that all of these methods produce significant errors - including amino acid analysis. Unfortunately, due to a lack of the specialist equipment in-house, it was impractical to do amino acid analysis every time. Therefore, the only routinely applicable choice at that time was Bradford assay, which had been previously used in a previous study (Vita et al., 2015). In addition to this, it is cheap and quick and does not rely on particular conditions such as the anaerobic conditions inside the chamber like DTNB. In subsequent experiments, we utilised Bradford assay with a correction factor (0.376) for determining Csp1 concentration, at the unfortunate risk of potential systematic errors in protein concentration determination.

3.2.4. Determination of metal stoichiometry

Stoichiometry of metal binding means the number of metal ions that can bind to a molecule of protein. Measuring this stoichiometry can be important for understanding the structure and function of many metalloproteins and metalloenzymes. But it is especially important here, when trying to understand the function of this family of Csp proteins that are hypothesised to bind and sequester a large number of copper ions, whether this function solely in sequestration of copper under toxic conditions or for storage in order to release copper later when it becomes limiting.

Determining stoichiometry requires techniques for precise and accurate determinations of both protein and metal concentrations. The only way to avoid this need would be to use mass spectrometry to directly measure the mass of metal added to a protein, such as electrospray ionization mass spectrometry (Cole, 1997) (ESI-MS). This has shown effective results by overcoming this obstacle, showing a high sensitivity, and by providing the precise and accurate mass data of various complexes of metal-protein complexes. Protein binding to metal ions, and the stoichiometry of binding, is more routinely determined with the help of UV/visible absorption spectrophotometry.

At this step, we aimed to calculate the copper binding stoichiometry of *N. gonorrhoeae* Csp1, which means knowing the number of copper ions that can bind to Csp1. So this step relied on the accuracy of protein measurement which was discussed in the previous section. In order to improve the accuracy of stoichiometry calculation, the recombinant protein was purified from *E. coli* cells that were cultured in M9 minimal medium to avoid copper binding to the protein within the *E. coli* cell and subsequently co-purifying with the target recombinant protein and thereby interfering with the result accuracy. Data initially using protein purified from *E. coli* cells that were cultured in rich LB medium was found by ICP-MS elemental analysis to be contaminated with copper (>3 mole equivalents, based on Bradford assay of protein concentration), and it was found to be very hard to acquire a pure apo-protein by extracting copper from this form.

We aimed to estimate the copper binding stoichiometry of Csp1 *in vitro*. Utilising the methods described for estimating Csp1 protein quantitation, we used two methods for determining how much copper it was capable to bind. One method used UV/visible spectroscopy to monitor binding of Cu(I) to the cysteine residues of Csp1 through measurement of ligand-to-metal charge transfer absorptions. The other method involved direct detection of the amount of copper bound to Csp1 after resolution of a mixture of protein and excess copper through a size exclusion chromatography column.

In order to assess the binding of copper with Csp1 protein via UV-visible spectroscopy, which can copper binding to cysteine residue thiol-containing sidechains by monitoring ligand-to-metal charge transfer bands at different wavelengths (200-350 nm), the recombinant protein was incubated overnight with various concentrations (0, 10, 20, 30 and 50 equivalence, in triplicate) of Cu(I) in an anaerobic chamber for equilibration purposes (section 2.10). Then, the absorbance of each sample was determined at 210–350 nm using the UV/visible spectrophotometer after the overnight incubation period.

The results (Figure 3.9) showed a significant increase in absorbance from the Csp1 samples in this region of the spectrum in the presence of Cu(I) ions, indicating binding of Cu(I) to Cys residues in the Csp1 protein. However, unexpectedly it was observed that the absorbance kept increasing, even after addition of what was intended to be 50 mole equivalents of copper. Therefore, there was no evidence of copper saturation of Csp1 in this experiment. In addition, to try to improve the stoichiometry determination, we designed an experiment with higher copper concentrations added to Csp1, however the protein precipitated badly at these high concentrations resulting in poor spectra that could not be interpreted (data not shown).

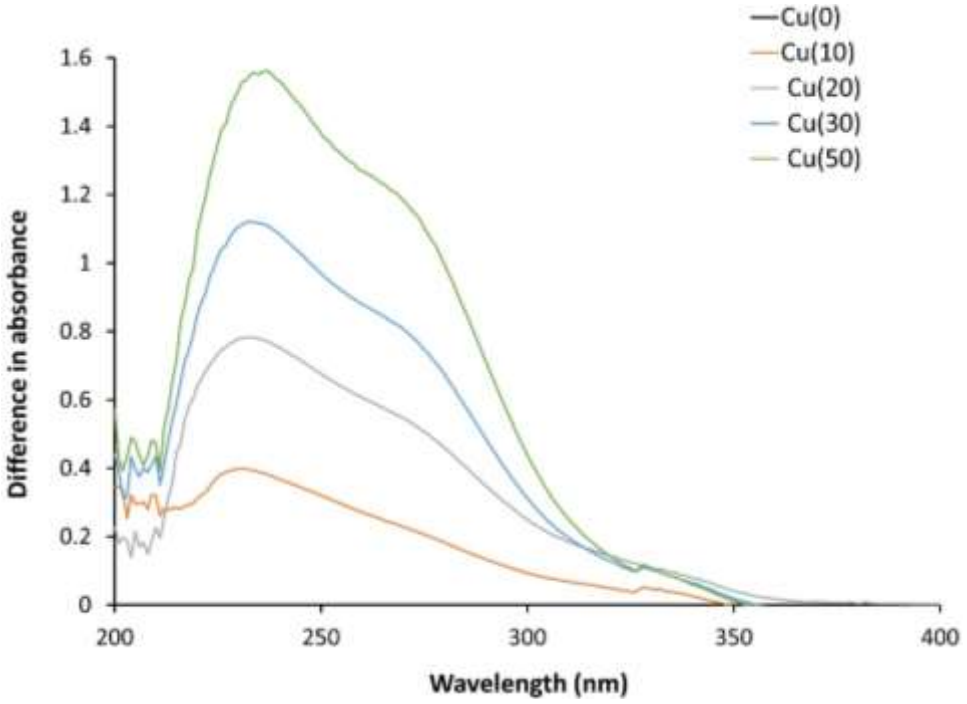

Figure 3.9. The binding of Cu(I) to *N. gonorrhoeae* Csp1 monitored by UV/visible spectroscopy.

In order to evaluate the binding of Cu(I) ions with Csp1 protein via UV-visible spectroscopy, various copper concentrations were used (0, 10, 20, 30 and 50 molar equivalents). The starting concentration of Csp1 that used was 10 µM, as determined by Bradford assay using a correction factor derived from quantitative amino acid analysis. Each sample was incubated overnight in the presence of a specific concentration of copper inside an anaerobic chamber for equilibration purposes in

20mM Tris, 150mM NaCl pH 8.5. The next day, the UV/visible spectrum of each sample was collected. The difference spectra are shown, which were calculated by subtracting the absorbance of the apo sample (i.e. with no added copper) from each of the copper-loaded samples (hence why the zero copper spectrum is a flat line at 0). The spectra showed a significant increase in absorbance in the presence of Cu(I) ions, consistent with binding of Cu(I) ions to Cys residues. However, the figure showed that the absorbance kept increasing, even after addition of what was intended to be 50 mole equivalents of copper, consequently there was no evidence of copper saturation of Csp1 in this experiment. The data presented in this figure is derived from a single biological replicate. This experiment was repeated two further times and, on both occasions, there was evidence of protein precipitation at high copper concentration but consistently all three replicates suggested copper stoichiometry substantially greater than 20.

These data nonetheless confirmed that copper binds to sulfur, indicating the coordination of metal ions by Cys residues within recombinant Csp1. These results are also found to be in agreement with the data in Vita et al., 2015, which also detected the high absorbance value due to characteristic ligand-to-metal charge transfer transition from Cys to Cu(I). The stoichiometry data were in contrast to our expectations, because we expected it to saturate at these levels if the protein concentration was correct. Based on homology to other Csp proteins, we expected the stoichiometry to be somewhere around 20. For this reason, I selected levels of copper that I expected would saturate the protein by 20 equivalents, with higher copper concentrations giving no further increase in absorbance. There are really only two possible conclusions: either the stoichiometry is a lot higher than we thought, meaning this protein has a capacity greater than 20 copper ions, or we there is a substantial error in the determination of the protein concentration.

injected onto size exclusion chromatography using Superdex S200 10/300, which was previously equilibrated in the buffer of 10 mM Hepes, 50 mM NaCl, pH 7.0, collecting 0.5 ml fractions (Figure 3.10). It was observed according to the chromatogram that Csp1 (Figure 3.10) in all

samples was eluted at the same volume with a single peak at 15ml, including the sample of as-purified Csp1 with no copper added. This is consistent with it being a single protein species in all cases, estimated to be a tetramer as demonstrated for other Csps. No other significant, discrete A280 bamds were observed in the chromatogram, except for (i) a broad absorbance of high mass in the highest copper concentration, anticipated to reflect protein precipitation, and (ii) an absorbance at the column's total volume, likely reflecting unbound metal. This is consistent with Figure 3.3.and also consistent with previous publications (Vita et al., 2016; Vita et al., 2015) that showed that the mass of the protein did not change on binding of copper and the position of the absorbance peak did not change, consistent with all molecules being tetrameric with or without copper ions. and indicated that copper did not change the form. Also, the absorbance at 280nm in the peak at 15 ml increased with increasing copper relative to the control (with the exception of the sample incubated with 30 equivalents of copper, in which the absorbance at 280 on size exclusion chromatogram went down, which possibly occurred because of the precipitation). This is expected, given that binding of Cu(I) to Cys residues clearly results in increased absorbance of Csp1 at 280 nm (Figure 3.9).

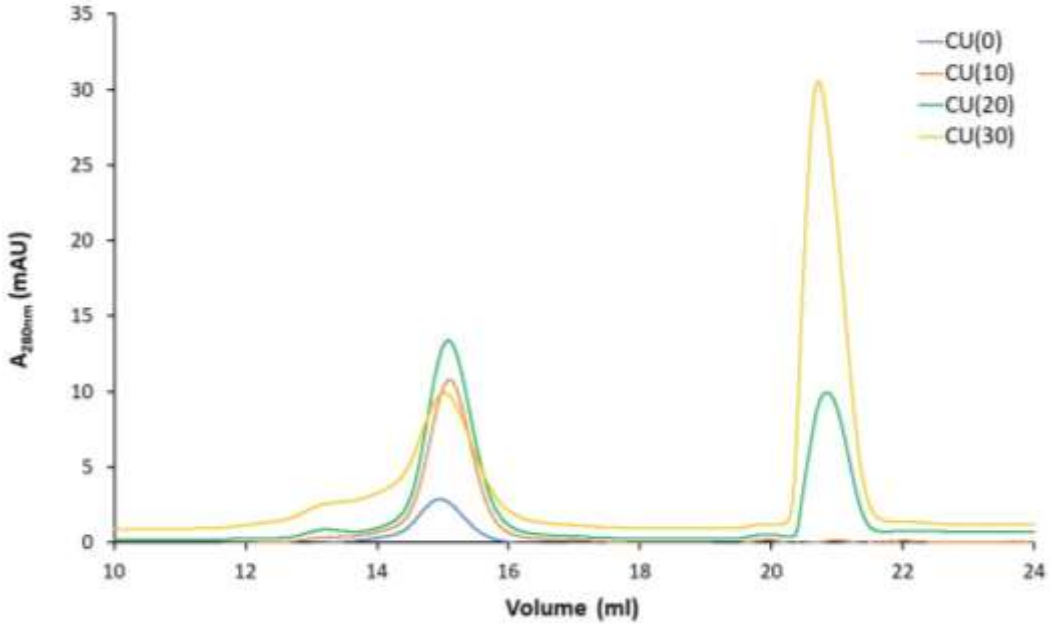

Figure 3.10. Analytical SEC to resolve copper-treated samples of Csp1.

Samples of recombinant Csp1 protein (10 μM, as determined by Bradford assay) were incubated in the presence of 0, 10, 20, 30 equivalent of Cu(I) in an anaerobic chamber overnight and used for UV/visible spectroscopy (Figure 3.9). Each sample was subsequently injected (1.5 ml) onto a size exclusion column, Superdex S200 10/300, which was equilibrated and resolved in 10 mM Hepes, 50 mM NaCl pH 7.0 on an ÄKTA pure purification system at room temperature. Each trace shows the absorbance at 280nm, reflecting protein eluting from the column, which is moderated by binding of Cu(I) (Figure 3.9), increasing intensity. Note that no SDS-PAGE analysis of these fractions is available as the gel was not scanned, but this can be compared with the gel in Figure 4.10. This experiment was performed on three biological replicates, but only a representative set of chromatograms are shown.

When taking the absorbance of each sample by using UV/visible spectroscopy it was noticed that the samples of 30, and especially the 50 copper equivalent sample, showed a lot of precipitation. The 50 equivalent sample was so obviously precipitated that it was eliminated to avoid damaging the SEC column. After injection of the sample with 30 equivalents of copper onto the column, it was observed in the chromatogram that the precipitation had led to the presence of a broad peak of high mass and a decreased in the absorbance at the peak at 15 ml, suggesting protein was significantly aggregated.

The last step in the determination of the copper stoichiometry was metal analysis of the SEC fractions using inductively coupled plasma mass-spectroscopy (Figure 3.11). Each of the eluted fractions from the size exclusion chromatography step were prepared by dilution into nitric acid to measure metal content by ICP-MS (see Section 2.8). I also attempted to measure the protein concentration in those fractions by Bradford assay. Unfortunately, however, I did not detect any significant concentration of protein in the peak fractions. After elemental analysis by ICP-MS, we therefore were unable to accurately measure a stoichiometry (by dividing the copper concentrations in the peak fractions by protein concentration in the same fractions). Nonetheless, despite these limitations, I calculated an estimated stoichiometry from these data. The result of the

stoichiometry by ICP-MS, when 30 equivalents of Cu(I) were added, was 23. In two further replicates, where 15 equivalents of copper were added (data not shown), the stoichiometry measured by ICP-MS was 21.7 and 30 respectively. It is tempting to draw a conclusion from these numbers, as they are in a similar range to the stoichiometries determined previously for others Csps, but, as noted, these numbers have clear errors associated with them due to the inability to detect significant amounts of Csp1 protein in the eluted fractions and must therefore be interpreted with extreme caution.

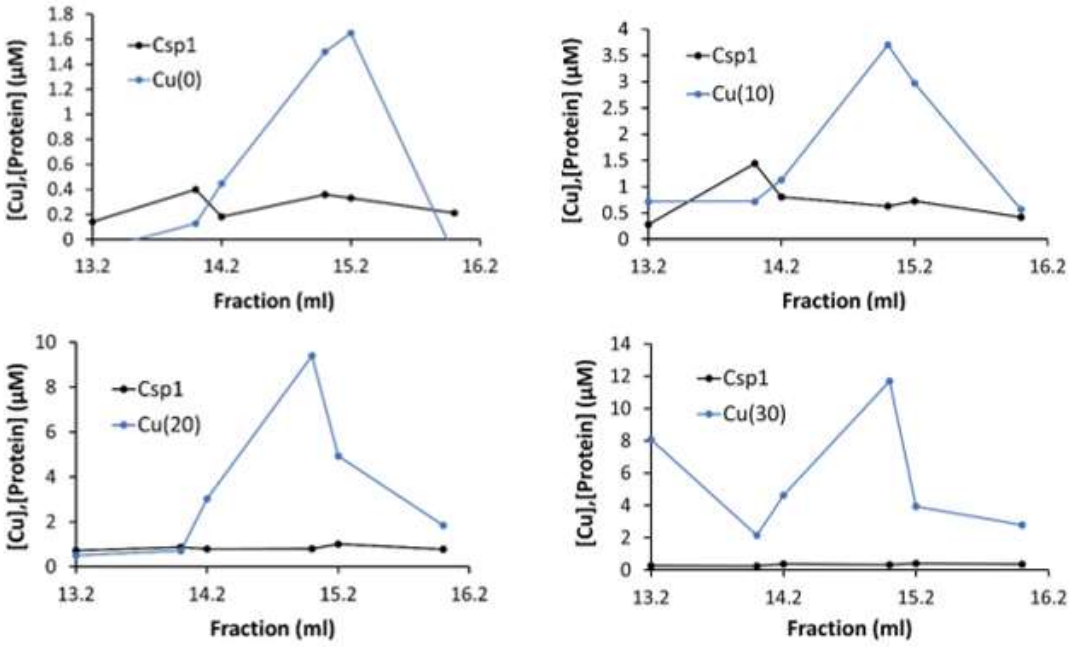

Figure 3.11. A representative set of chromatographs of copper measured by ICP-MS in SEC fractions of copper treated samples of Csp1.

Samples of Csp1 (10μM) were incubated with varying molar equivalents of Cu(I) (0.10.20.30) and resolved by analytical SEC (Figure 3.10). The resulting fractions (0.5 ml) were analysed to measure copper content by using ICP-MS and by Bradford assay to estimate protein concentration. The data presented here are from a single biological replicate, which was the same sample as was used for the experiment in Figure 3.9. A similar experiment was performed two further times and a similar result

was obtained on each occasion. Fractions numbers were converted to ml as per AKTA software.

In conclusion, although the data demonstrate copper binding in high stoichiometry, the precise stoichiometry could not accurately be calculated using either UV/visible spectroscopy or SEC/ICP-MS. The main problem we had was a limited yield of protein, which precipitated when left in the fridge over a few days. As a result, I had to use a relatively small amount of protein in each experiment and therefore we observed that A280 detected the presence of protein in the key fractions, but this could not be accurately measured by Bradford. In addition, the protein was vulnerable to precipitation when high concentrations of copper were added to it, further limiting the scope of the experiments I could perform to measure the Csp1 copper binding stoichiometry. Nonetheless, I did collect evidence of copper binding to sulfur, consistent with the expected binding of Cu(I) ions to Cys residues, and I observed binding through multiple additions of copper by uv/visible, size exclusion and ICP-MS.

Previous studies (Vita et al., 2016; Vita et al., 2015) have estimated the approximate Cu(I)-binding stoichiometry using similar methods. Those studies estimated stoichiometries of 15 to 20 copper ions per monomer for MtCsp3 and of 17 to 21 copper ions per monomer for BsCsp3, and a lower stoichiometry of 12-14 copper ions per monomer for the periplasmic Csp1. Crystal structures of copper-loaded samples of two of these homologues demonstrated binding of 19 copper ions bound at the core of the MtCsp3 monomer, and 13 copper ions bound at the core of the MtCsp1 monomer (Vita et al., 2016; Vita et al., 2015).

3.2.5. Effect of Cu/Zn/Ag binding

Neisseria gonorrhoeae Csp1 belongs to the family of copper storage protein and can bind many copper atoms. However, no experiments have been published to study whether these proteins are also able to bind other essential metal ions, or whether they're entirely selective for Cu(I). The

purpose of this part of the study was to investigate the binding of metals other than copper ions, such as zinc and silver, to this Csp1 protein.

Silver was chosen as a non physiological metal, i.e. it is not essential in biology, but which has properties similar to that of the target metal ion, Cu(I). For example silver binds to similar binding sites as copper, and is below copper in periodic table resulting in similar chemical properties. Silver has a preference for sulfur coordination, like Cu(I), and prefers to be coordinated in a digonal or trigonal coordination geometry (Gudipaty and McEvoy, 2014).

Bacterial cells contain many more zinc-proteins than copper-proteins. Zinc is located next to copper in periodic table and has similar properties, but unlike silver, zinc is a physiological metal. For these reasons, copper and zinc can often bind to similar binding sites. In addition to this, cells have both copper and zinc present, so zinc binding to copper proteins such as Csps could interfere with copper-protein function.

Purified Csp1 protein was prepared and measured by amino acid analysis and based on that value we determined the amount of metals for the experiment., as with the copper binding experiments (section 3.3.1). First, three samples of protein were incubated overnight with either ten equivalents of Cu(I), one equivalent of Ag(I) or Zn(II). Each of the tubes containing these samples were incubated overnight inside an anaerobic chamber (Table 2.11). Next, I prepared samples that would be exposed to two different metals. First, I added one equivalent of silver to one protein sample and one equivalent of zinc to another sample, and these two tubes were incubated for one hour. Next, ten equivalents of copper was added to each of these tubes.

The second step was using size exclusion chromatography on these samples, similar to the experiments with copper alone. Again we used Superdex S200 10/300 which was previously equilibrated and then was resolved in the buffer of 10 mM Hepes /50 mM NaCl pH 7.0.

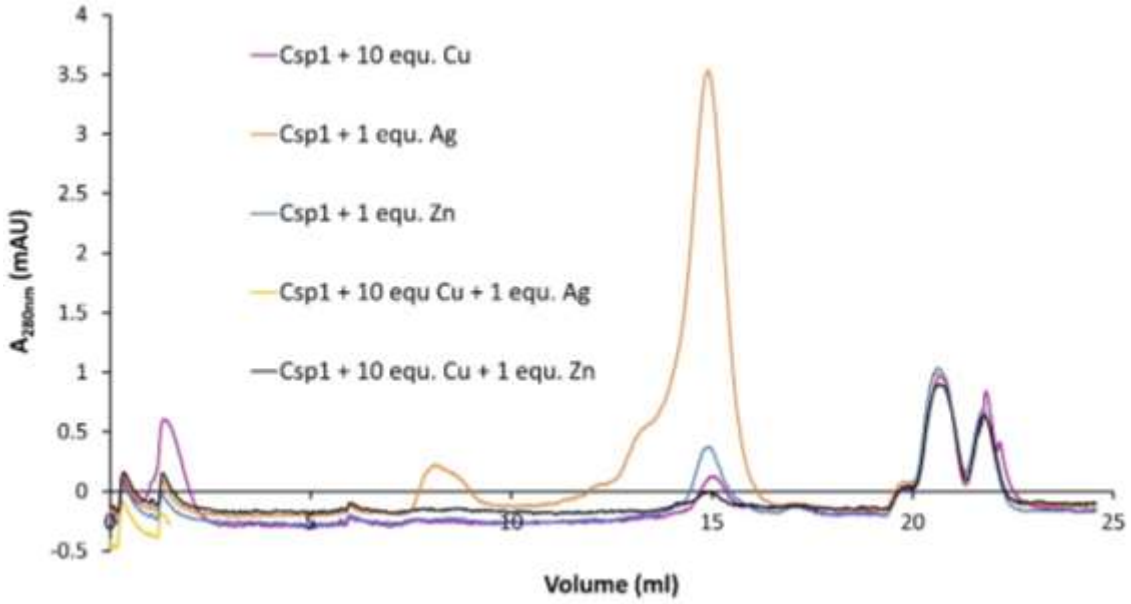

Figure 3.12. SEC chromatogram of Csp1 treated with Cu/$AgNO_3$/$ZnCl_2$.

Samples of purified Csp1 (5µM) were mixed with either ten equivalents of Cu(I), or with one equivalent of Ag(I) or Zn(II). Two further samples were treated first with Ag(I) or with Zn(II), incubated for one hour, and then challenged with ten equivalents Cu(I). All of the samples were incubated overnight inside an anaerobic chamber, followed by injecting and resolving by analytical size exclusion chromatography on Superdex S200 10/300 in 10 mM Hepes,50 mM NaCl PH7.0. The absorbance traces, A280nm, are shown. The data presented here are from a single biological replicate n=1.

Inductively coupled plasma mass-spectroscopy (ICP-MS) was the used to analyse metal content (Section 2.8), and determined the concentration of copper, silver and zinc ions in the elution fractions. Likewise, Bradford assay was used to measure the protein concentration in these fractions, but as previously, the results from the Bradford assay showed very low concentration of protein.

As previously, the main protein peak eluted around 15 ml from size exclusion chromatography, consistent with all forms remaining as tetramers in solution regardless of the metals they were incubated with. In addition, the A280 trace from the size exclusion showed a significantly elevated absorbance in the silver treated sample compared to the other traces, for unknown reasons. All metals that have been used in this experiment were incubated with the same concentration of Csp1 inside the chamber, making it unclear why this single fraction showed such an elevated absorbance. Interestingly, this increase was not observed in the fraction that was exposed to Ag(I) first and then challenged with Cu(I), which indicates that, if this increased absorbance is caused by binding of silver ions, then the silver must have been subsequently displaced by addition of copper ions.

The same fractions were analysed for protein content by Bradford assay and for metal by ICP-MS (Figure 3.13). Unfortunately, the 'control' sample, the copper-treated sample, did not contain protein or copper at the peak fractions. This is likely due to the low protein concentrations used.

The Bradford Assay did show some protein content in the peak fractions of the silver treated samples that were consistent with SEC (Figure 3.13). The ICP-MS analysis also detected silver in these fractions, indicating that silver was bound to Csp1, roughly half of one equivalent. However, the problem in this experiment was that we did not detect copper binding in the positive control experiment , so we must be very careful in interpreting these data.

After adding 1 equivalent zinc chloride, no zinc was detected in the fractiosn that showed peak A280nm absorbance, indicating that zinc ions did not bind to Csp1 (Figure 3.13).

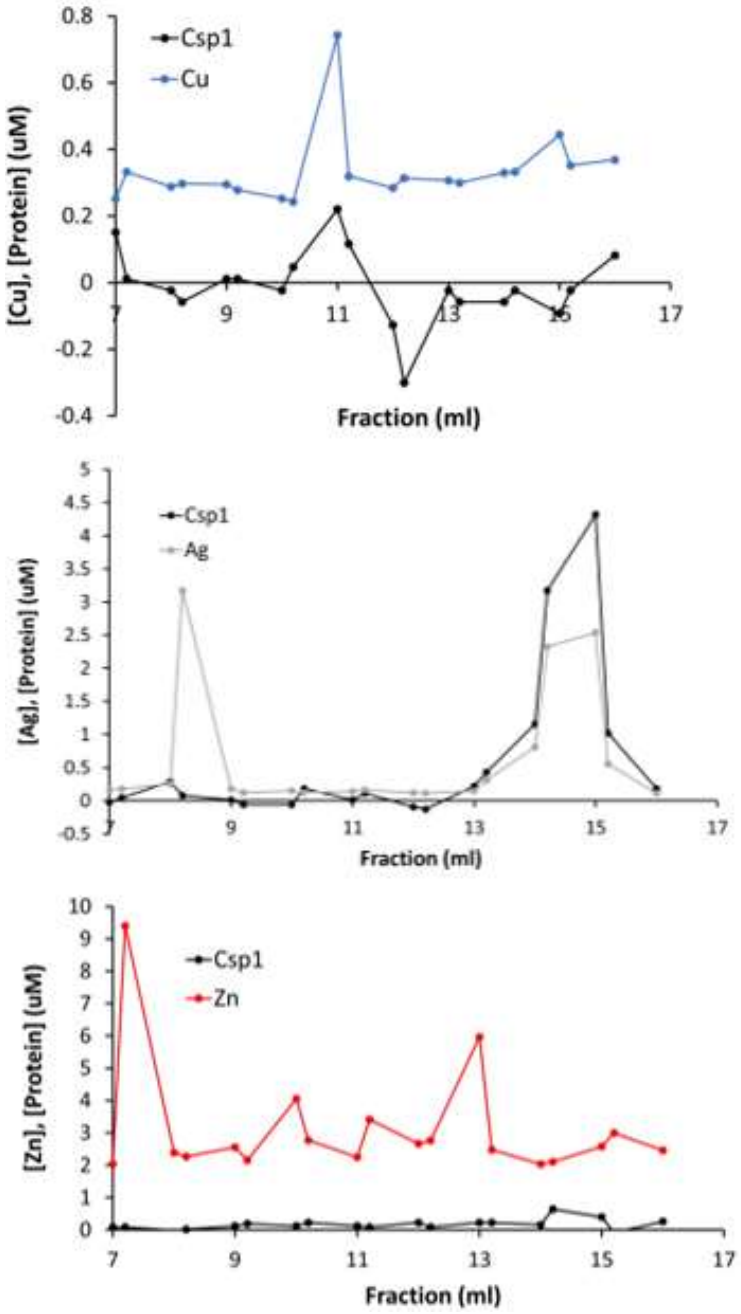

Figure 3.13. Binding of Cu, Ag and Zn to recombinant Csp1 using ICP-MS.

Protein samples of Csp1, incubated with either ten equivalents of Cu(I), or one equivalent of either Ag(I) or Zn(II), were resolved by analytical SEC on a Superdex S200 10/300 column in 10 mM Hepes, 150 mM NaCl, pH 7.0. The resulting fractions of SEC (Figure 3.12) were prepared for metal analysis by using ICP-MS (Section

2.8). Protein concentration in those fractions were measured with Bradford assay. This experiment was performed once, n=1.

Unfortunately, these are inconclusive results. We cannot indicate that any part of the experiment succeeded, to conclude that Csp1 showed diversity of bonding with other metal ions in addition to copper, because of it being a single experiment and because the positive control, in which only copper was added to Csp1, failed to give a positive result of copper binding. In addition, the protein concentrations used were necessarily low due to a shortage pf purified recombinant protein for these experiments.

The second part of this experiment was carried out using a combination of two metal ions incubated with the same sample of Csp1. In each case, the 'wrong' metal was added followed by a 1 hour incubation period before excess Cu(I) was subsequently added. In the case of initial incubation with silver nitrate, there was no longer the presence of silver in the protein containing fractions (Figure 3.14) as measured by ICP-MS. This is in contrast to when Ag(I) ions were added to Csp1 alone (Figure 3.13). Instead, we detected copper ions, as shown in Figure 3.14 in the Csp1-containing fractions, suggesting that copper was able to displace the Ag(I) ions that had initially bound to the protein. However, again this experiment was only done once, and the positive control makes it difficult to draw firm conclusions. In the zinc experiment, I detected no metal ions at all in the peak fractions at 14-15ml, and additionally the Bradford did not detect a protein yield in any fractions. As a result, no conclusion can be drawn from this experiment.

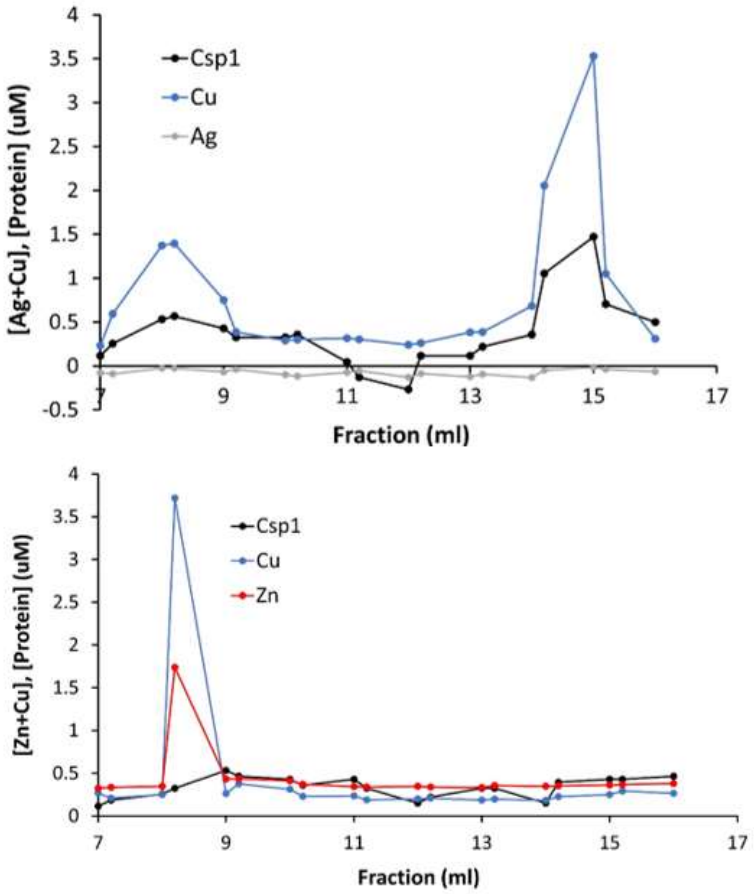

Figure 3.14. Binding of Cu, after incubation with Ag and Zn, to recombinant Csp1 using ICP-MS.

Protein samples of Csp1 were initially incubated with one equivalent of either Ag(I) or Zn(II) for one hour, and then were challenged by subsequent addition of ten equivalents of Cu(I), followed by incubation overnight in an anaerobic chamber. The samples were subsequently resolved by analytical SEC on a Superdex S200 10/300 column in 10 mM Hepes, 150 mM NaCl, pH 7.0. The resulting fractions of SEC (Figure 3.12) were prepared for metal analysis by using ICP-MS (Section 2.8). Protein concentration in those fractions were measured with Bradford assay. This experiment was performed once, n=1.

3.3. Discussion

The new family of copper storage proteins (Csps) were originally identified in methanotrophic bacterium using metalloproteomics approaches. Metalloproteomics is the analytical study and identification of metalloproteins in an organism, either prokaryote or eukaryote. Interest has developed for the recognition and characterization of novel metalloproteins. Knowledge of the mode of interaction of these metalloproteins with a number of metal ions relies on *in vitro* analysis. This part of my research work focused on the identification and quantification of metal ions were able to bind to the Csp1 protein from *Neisseria gonorrhoeae*, a homologue of that originally described in methanotrophic bacteria (Vita et al., 2015).

In this study recombinant Csp1 protein was expressed and produced at scale by using the simple and efficient *E. coli* prokaryotic system. The crude protein was purified via two stages of purification. First, the protein was purified by anion exchange chromatography, and the purity of the protein resulting was evaluated on SDS-PAGE. This indicated the presence of the ~13 Da Csp1 protein, along with other impurities in the Csp1-containing fraction. So, a second dimension of protein purification was employed to ensure these impurities were mostly removed. This second stage of purification was via size exclusion chromatography, and again, afterwards SDS-PAGE was utilized to confirm the purity of recombinant protein.

Although the purification was successful, experiments using this recombinant protein were significantly hampered throughout this study by issues with the stability of the protein. When stored in the refrigerator over the course of a few days, the protein yield reduced and particulates were observed in the samples, suggesting that the protein had a tendency to precipitate, even in the absence of metals. This precipitation became pronounced when the protein was subsequently exposed to copper, especially at high molar equivalents. As a result, several experiments that were performed had to use rather low concentrations of protein, which subsequently made it difficult to detect the protein, and its bound metal, at the end of the experiment. This in turn made it difficult to interpret the results to draw firm conclusions.

Csp1 protein from *Neisseria gonorrhoeae* is constituted of ~30% cysteine residues and this characteristic allows this family of protein to bind preferably with transition metal ion copper (Vita et al., 2015; Vita et al., 2016). This feature has suggested its role in metal storage, either in detoxification, to protect organism from harmful effects of toxic copper ions, and/or to accommodate copper ions for subsequent usage when copper availability later decreases. Tarasava and colleagues in 2016 also reported the metallothionein (MT) from *Triticum astevum* showed ability to associate with a large number of metal ions. Their results showed the high affinity of MT with copper and zinc metal ions.

Measuring the protein concentration in an accurate way was the cornerstone for addressing the project's central question, which was determination of the copper-binding stoichiometry, as well as which other metals can bind to Csp1 like silver and zinc. Measuring a protein's concentration accurately is still a challenging step in biochemistry. Finding an ideal method to calculate the concentration of the Csp1 protein was an important step to help us to answer these questions.

A number of quantitation methods were employed, and each method that was used has advantages and disadvantages For instance, A280 measures primarily Try residues, with a further small contribution of Phe and Tyr residues. But Csp1 does not contain tryptophan, which made this approach prone to significant potential error. DTNB was obviously a good way to measure the concentration of Csp1, given its number of cysteines. However, this assay adds an extra layer of complications in that relies on good anaerobic conditions which we had access to intermittently, but unfortunately our anaerobic chamber was not always functioning and working at the level we needed it to be. Indeed, the oxidation often appeared as a noise in the baseline using UV/visible spectroscopy, or alternatively the addition of this compound did not produce a measurable yellow colour during the assay even when added to cysteine which was the positive control. This led to several wasted preparations of protein.

In the end I decided the best approach was to use something a Bradford assay, which also was used in a previous study (Vita et al., 2015), combined with a correction factor that was derived from a quantitative amino acid analysis. Table 3.1.3B showed the different values of Csp1 concentration obtained using these different approaches and highlights the variation in the measured protein concentration. It also illustrates why we thought that the correction factor from amino acid analysis would be a good solution to correct the concentration value determined by Bradford assay to determine the actual number.

However, based on the huge numbers from the calculation of the copper stoichiometry from the UV/visible spectrophotometry assay, it indicates that the correction factor was not a good enough solution. Perhaps we were misled by table 3.1.3B into believing the correction factor would enable me to determine the stoichiometries. I conclude that there remained a significant error on the protein concentration determination, which in turn led to a significant error in the stoichiometry calculations.

Nonetheless, table 3.1.3B showed that the DTNB assay gave results that were the closest to those from the amino acids analysis. With hindsight, we should have accepted this method as the only one that could be used accurately. Alternatively, we could have produced a more accurate version of (Table 3.1.3B) by doing, for example, ten replicates of each protein determination, ideally using ten different biological replicates. For instance, by taking ten different preps and ensuring that each of those preps would have gone through amino acids analysis, Bradford, DTNB and A280, we could have reduced the error bars and increased the accuracy of the final measurements, and better selected the method that would give the best results.

.
The initial test of copper binding to Csp1 protein used UV/visible spectroscopy. Addition of copper to Csp1 protein resulted in detection of a broad spectral feature at 250-350 nm, consistent with the binding of Cu(I) ions to sulfur. This was anticipated as Csp1 is expected to bind copper via its cysteine residues. However, the titration showed that this feature continued increasing at a

stoichiometry vastly in excess of that anticipated (<25 mole equivalents), with no evidence of the feature saturating even after incubation with 50 mole equivalents of copper. That indicated that only one of two possibilities existed: either it has a much higher stoichiometry, or the protein concentration was not accurate. Given the homology between *N. gonorrhoeae* Csp1 and other proteins of this family that have already been characterised in vitro, I cannot believe that the protein binds more than 50 copper and that led me to believe that most likely explanation of these data is that the protein concentration was wrong.

The quantification of copper binding to Csp1 protein was also carried out through comparing the amount of copper that comigrated with the protein through ICP-MS analysis after samples were resolved by SEC. The Csp1 protein, incubated with individual or combinations of metal ions (Cu, Ag and Zn), were resolved as separate peaks with no difficulty.

In the case of copper incubation with Csp1, the UV absorbance signal was significantly increased in Csp1-containing fractions (Figure 3.10), which is consistent with the observed increase in absorbance of the Cu-bound form of the protein in this wavelength range (Figure 3.9). This increased absorbance was exhibited after incubation with 10 mole equivalents of copper but did not increase further after further additions of copper, which could indicate that the protein was precipitating at higher copper concentrations or that it was saturated. Some baseline lift was certainly seen at high copper concentration incubation in UV/Visible spectroscopy analysis. Figure 3.10 showed an absence of saturation even with 50 mole equivalents of copper added, so when we put those two together, we do not believe that the protein was saturated at 10 mole equivalents. Therefore this indicates that the problem was likely to be precipitation. Unfortunately, although copper could be detected in the resulting fractions, no significant concentration of protein could be detected by Bradford, which made any interpretation of these data in terms of metal stoichiometry unreliable. The conclusion is that this analysis was badly affected, primarily due to having to use very low protein concentrations for the assay leading to intense measurement difficulties after size exclusion chromatography. Nonetheless, taken at face value, the data indicate that overexpressed Csp1 can bind large numbers of copper ions. These results are also found in accordance with Vita et al. 2016 in the case of the BsCsp3 recombinant overexpressed protein.

Furthermore, Straw et al. also reported the same kind of results in the case of Csp3 from *S. lividans*, as well as the Csps from *M. trichosporium* from the previous studies of Vita et al. 2016 and Vita et al., 2015.

The cysteine residues could also have the capability to bind to a number of other d^{10} electronic configuration metal ions, such as Zn or Ag. No zinc ions were found in the fractions in which Csp1 protein eluted, suggesting Csp1 does not bind this metal ion. This observation is in contrast with metallothioneins that store zinc, with Tarasava et al. in 2016 reporting that metallothionein from *Triticum astivum* binds zinc to recombinant protein. Dainty et al., 2010 showed that Atx1, which is the cyanobacterial copper chaperone, interacts with zinc in addition to copper under *in vitro* conditions. Totty et al. in 2014 determined that CucA, identified as one of the most abundant Cu containing protein present in the periplasm of cyanobacterium, also showed affinity with zinc metal ion. Yet Csp1 apparently does not bind zinc.

In my experiment, two separate peaks of silver were observed, and Csp1 protein was found in these peaks, indicating the protein potentially bound to Ag(I) ions in vitro. Protein was detected in those fractions, and the analysis suggested a silver binding stoichiometry of approximately one metal per protein molecule (Figure 3.13). However, the data from this part of the investigation must be interpreted cautiously, due to the fact that the positive control in the experiment was unable to demonstrate conclusively that copper was bound to Csp1.

In conclusion, although my experiments were not able to conclusively show the copper-binding stoichiometry of the *N. gonorrhoeae* Csp1 protein, we nonetheless confirmed that it binds significant numbers of copper ions and that this binding occurs primarily via the conserved Cys residues. Furthermore, I have presented some preliminary evidence, the first acquired, that a Csp protein is also able to bind Ag(I) ions in vitro, yet it appears not to be capable to bind Zn(II). These preliminary observations will require additional experiments designed in future to confirm the diversity of metal ions that are able to be bound to Csp proteins, and whether they bind within the Csp tube or solely on the outside.

Chapter 4: Metal binding and the structure of Csp3 from *Salmonella enterica*

4.1. Introduction

The predicted periplasmic Csp homologue, designated Csp1, from *Methylosinus trichosporium* OB3b was the first member of this protein family to be identified and characterised (Vita et al., 2015). Some limited evidence was provided in that initial publication that Csp1, along with its close homologue from the same organism, Csp2, can act as a store of copper that can be used to supply this cofactor to that organism's crucial copper-dependent enzyme, particulate methane monooxygenase (pMMO). The pMMO present in the methanotrophs catalyse the conversion of methane to methanol, and requires a large amount of copper as cofactor to regulate this metabolic activity (Balasubramanian et al., 2010)**.** *Methylosinus trichosporium* OB3b, methanotrophs are able to switch to the use of a soluble iron enzyme (sMMO) in case of Cu deficiency. The *N. gonorrhoeae* Csp1 protein is predicted to be structurally and functionally analogous to the Csp1 from *M. trichosporium* (see Chapter 3).

However, three Csps were reported in this model methanotrophs. Two, *Mt*Csp1 and *Mt*Csp2, are suggested to be exported from the cytosol due to presence of a Tat-targeting signal peptide, while the third homologue, Csp3, lacks a predicted signal peptide entirely and so is suggested to be strictly cytosolic. In *M. trichosporium* OB3b, *Mt*Csp1 and *Mt*Csp2 gene deletion increases the switchover rate from pMMO to sMMO, indicating their role in copper storage (Vita et al., 2016).

Although a subsequent study characterised the structure and copper-binding properties of the cytosolic homologue, *Mt*Csp3, from *M. trichosporium* OB3b (Vita et al., 2016), its role in copper homeostasis remains to be clarified. This organism is very difficult to perform such studies, however, due to the lack of systems for easy genetical manipulation of their genomes. Such methods are necessary to study the *in vivo* function of a protein, because we would need to study the phenotype of a deletion mutant (and perhaps also strains that over-express the protein) to determine what role the protein plays in the cell. Furthermore, no studies have been performed to characterise the role or sub-cellular localisation of the homologues of other known copper homeostasis proteins encoded in the genome of *M. trichosporium* OB3b, such as CopA or CopZ. This organism also has internal membrane-bound compartments – unusually for bacteria – which

further complicates *in vivo* studies of this organism. Nonetheless, *Mt*Csp3 was shown to form four-helix bundles structures within the monomers, and these monomers in turn assemble into homotetramers, just like Csp1 (Vita et al., 2016). Each monomer binds a large number of copper ions at its core with high affinity.

The same study also characterised a cytosolic Csp homologue in the Gram-positive bacterium, *Bacillus subtilis* (Vita et al., 2016). This protein forms the same structure as *Mt*Csp3, and also binds a large number of copper ions at the core of the tube formed within its four-helix bundle structure. Some limited evidence was provided in this study for a different function *in vivo* in *B. subtilis*. In this case, the phenotype of a *B. subtilis csp3* strain, which showed increased vulnerability to copper toxicity in stationary phase, was interpreted as implying a role in sequestration of excess copper inside the cytosol when cells are cultured under high copper conditions (Vita et al., 2016). A similar phenotype was detected in a different study of the cytosolic Csp3 homologue from *Streptomyces lividans* (Straw et al., 2018). Notably, the copper homeostasis system of *Bacillus subtilis* has been more thoroughly characterised. This organism possesses a single CopA and CopZ, which efflux copper and confer copper tolerance, and a copper dependent transcriptional sensor (Baslé et al., 2017; Gaballa et al., 2003; Gaballa and Helmann, 2003). The deletion of these genes leads to increasing the sensitivity of high copper level (Radford et al., 2003)
.

We wanted to study the putative cytosolic Csp3 homologue from *Salmonella* for similar reasons to our study of Csp1 - because this protein not yet been studied as a member of the Csp family, but here as a member of the cytosolic subset of Csp proteins from another pathogenic bacterium. Additionally, Csp1 had proven to be very difficult to work with, with low expression and purification yields, poor protein stability when stored under refrigerated conditions, and inconsistent data from metal-binding assays, so we decided to try an alternative Csp protein from a pathogen to determine whether or not the difficulties we were having working with protein were specific to Gonorrheal Csp1 or were general properties of Csps. *Salmonella* Csp3 purification yields were slightly higher and the protein showed better stability, enabling determination of its crystal structure (Chapter 5).

Salmonella Csp3 is expressed in a different sub-cellular compartment, with Csp1 predicted to be localised to the periplasm in *Neisseria gonorrhoea* but Csp3 in *Salmonella, Bacillus* and *Methylosinus trichosporium* OB3b are predicted to be localised in the cytosol because they have no signal peptide unlike MtCsp1 and MtCsp2. Nonetheless, they share significant sequence similarity and they share the sequence positions of most of the cysteine residues, as shown in (Figure 4.1).

Figure 4.1. Sequence comparison of Csp3s from different bacteria.

Sequence alignments of (top) the Neisseria Csp1 and the Salmonella Csp3, and (bottom) the Csp3 proteins present in *Salmonella*, *M. trichosporium* and *Bacillus subtilis*, were created in Clustal Omega. The conserved Cys residues are highlighted in yellow. Csp3 in *Salmonella* has 21.48% sequence identity to Csp1 from *Neisseria gonorrhoeae*, whereas it shares 24.06% with *Mt*Csp3. The [.], [:], and [*] symbols reveal strong and weak similar sequence positions.

4.2. Results

4.2.1. Cloning, Expression and Production of Csp3 Recombinant Protein

As in the previous chapter, in order to study the Csp3 protein in vitro, it first needed to be expressed and purified. The selection of the right expression system is based on the level of production of target protein, the growth rate of the host cell and the required culture conditions for the host (Choi et al., 2006). In the case of our chosen bacterial expression system, *E. coli* BL21 cells were used, and as for *Ng*Csp1 (Chapter 3), we utilised the pET29a expression vector for recombinant protein expression.

The amplified *csp3* gene was ligated into pET29a vector and then transformed into *E. coli* DH5α cells (this was performed by former undergraduate student, Becca McCamley). Afterwards, competent cells of strain *E. coli* BL21 were transformed with this plasmid, and positive clones containing the *csp3* gene were selected for preparative scale expression. The positive transformed cells were screened on the basis of kanamycin resistance. The cells were cultured and were induced for the production of Csp3 protein with addition of a final concentration of 1 mM IPTG at OD_{600nm} ~ 0.4 for overexpression, then followed by an incubation period of up to 16 h at 37 °C. Samples were removed at various time points. The presence of target protein was analysed in crude extracts via SDS-PAGE (data not shown).

As with Csp1, for large scale production of Csp3 protein, a single transformed colony was inoculated into 10 mL of LB containing kanamycin (50 µg ml^{-1}) and grown overnight at 37°C with orbital shaking. The overnight culture was used to inoculate fresh LB media containing kanamycin (50 µg ml^{-1}) and cultured again approximately 4 hours until OD_{600nm} reached to 0.4 under the same culture conditions. Then the cells were induced with a final concentration of 1mM IPTG followed by the incubation period of 14 hours at 37 °C. The cells were harvested using centrifugation at 4 °C for 30 min. Then the supernatant was discarded and pellet was processed after washing with 20 mM Tris HCl, pH 8.5.

4.2.2 Purification of recombinant Csp3 protein

Based on similar arguments as for Csp1 (see section 3.1.2), a two step protein purification was adopted to purify and quantify the target recombinant protein Csp3 from soluble *E. coli* extracts using FPLC.

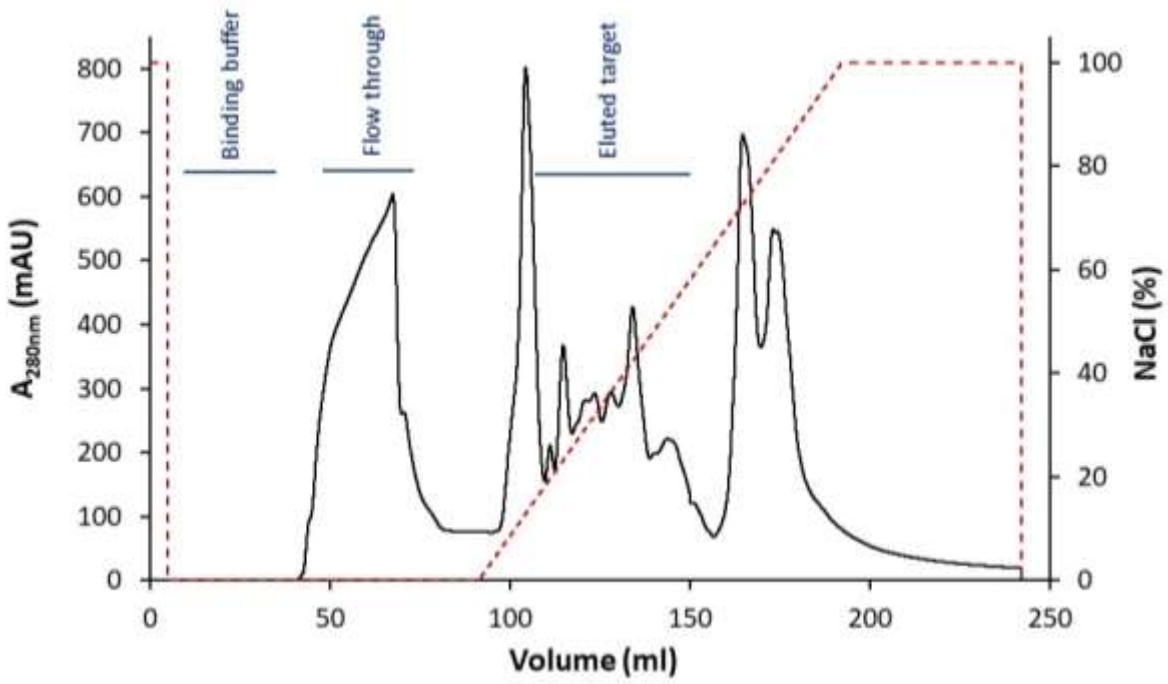

Figure 4.2. Anion exchange chromatogram of recombinant Csp3.

AEC chromatogram of *Salmonella* Csp3 purification from crude *E. coli* lysate, showing a linear NaCl gradient elution (dashed red line) of proteins (detected using A_{280nm}, black line). The purification was done using a 5 ml HiTrap Q HP anion exchange column connected to an AKTA Start system. Low salt buffer (20 mM Tris, pH 8.5) and high salt buffer (20 mM Tris, pH 8.5, 1M NaCl) were mixed to generate the gradient. This pH was selected to ensure acidic groups on Csp3 (predicted pI = 4.95). The column was washed after loading to remove any low affinity-bound proteins from the *E. coli* crude extract using low salt buffer (Flow through). Protein elution stage used a linear [NaCl] gradient from 0-1 M NaCl (Eluted target). This is a representative chromatogram taken from a single purification, but this AEC was performed numerous times (>10 occasions) to purify Csp3.

Again, the first purification step utilized AEC. We calculated the iso-electric point of Csp3 using expasy.org as pI = 4.95, which means that it should bind to a positively charged column at pH 8.5 through charge interactions. As before, *E. coli* cells were lysed by sonication and clarified supernatant was prepared and initially bound to an anion exchange chromatography column under low salt conditions. After loading of the soluble supernatant lysate (figure 4.2), the column was washed using low salt buffer (labelled 'flow through' in figure 4.2). A linear [NaCl] gradient (0-1 M) selectively eluted the proteins that remained bound to the anion exchange column (labelled 'eluted target' in figure 4.2). The chromatogram of Csp3 purification showed elution of a number of major proteins by the linear NaCl gradient elution (dashed line) (Figure 4.2). Aliquots of each fraction were resolved by SDS-PAGE (Figure 4.3), stained with Coomassie blue, to visually check the purity result of the target protein in the eluted fractions. Although SDS-PAGE showed that Csp3 had been partially purified from the crude extract, there were nonetheless a number of protein contaminants of varying masses still present after AEC, which suggested that the fractions needed at least one further step of purification.

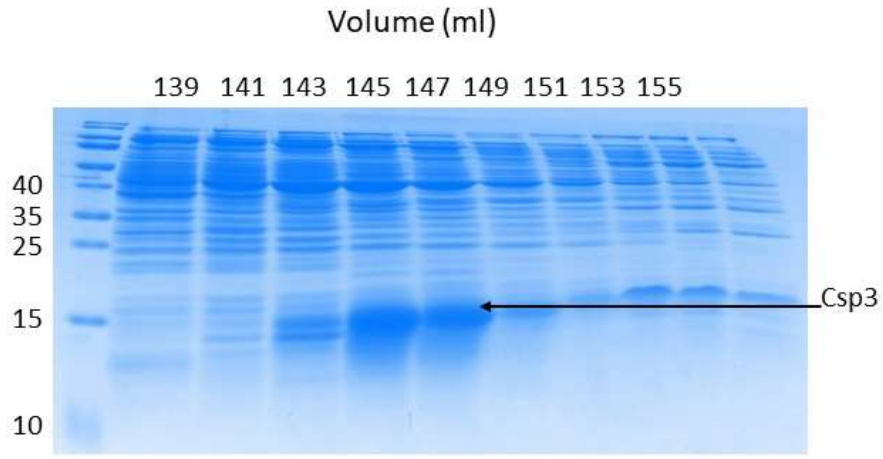

Figure 4.3. SDS-Page showing eluted fractions of AEC of recombinant Csp3.

Eluted fractions from AEC purification of *Salmonella* Csp3 from *E. coli* lysate were collected (2 ml) at the start of the salt gradient (see region labelled 'Eluted target' in figure 4.2). An aliquot (10 µl) of each of the eluted fractions from AEC was boiled for 10 minutes in the presence of 1% SDS and 10 mM DTT, and then loaded on an SDS-PAGE gel (19% acrylamide w/v), which was subsequently stained with Coomassie

Brilliant Blue stain and visualised with Image Lab software. The elution volume of the fractions from AEC are indicated (above). Molecular markers (left) indicate molecular weight of standard proteins. The arrow (right) indicates the target Csp3. Note that the predicted mass of Csp3 is 12,096 Da (Expasy). This is a representative gel taken from a single purification, but this AEC/SDS-PAGE was performed numerous times (>10 occasions) to purify Csp3.

The second step of Csp3 protein purification strategy was again size exclusion. Like Csp1, the Csp3 protein is small but homologues have been shown to form tightly bound homotetramers. Consequently, the expected size of the Csp3 protein in its homotetrameric form was ~53 kDa. Because of this tetrameric mass, we once more selected Superdex 200 as the most appropriate size exclusion chromatography matrix, based on its expected resolving range. Fractions containing Csp3 from the anion exchange chromatography (Figure 4.2) were pooled and resolved by size exclusion (Figure 4.4). Several significant protein peaks (i.e. peaks in 280nm absorbance) were observed to elute at different times during the chromatogram, demonstrating a purification effect. To identify the fractions in which the Csp3 protein had eluted, aliquots of each of the fractions that exhibited absorbance at 280 nm across the region 84-90ml, were resolved on SDS-PAGE (Figure 4.5) to evaluate the fractions' purity.

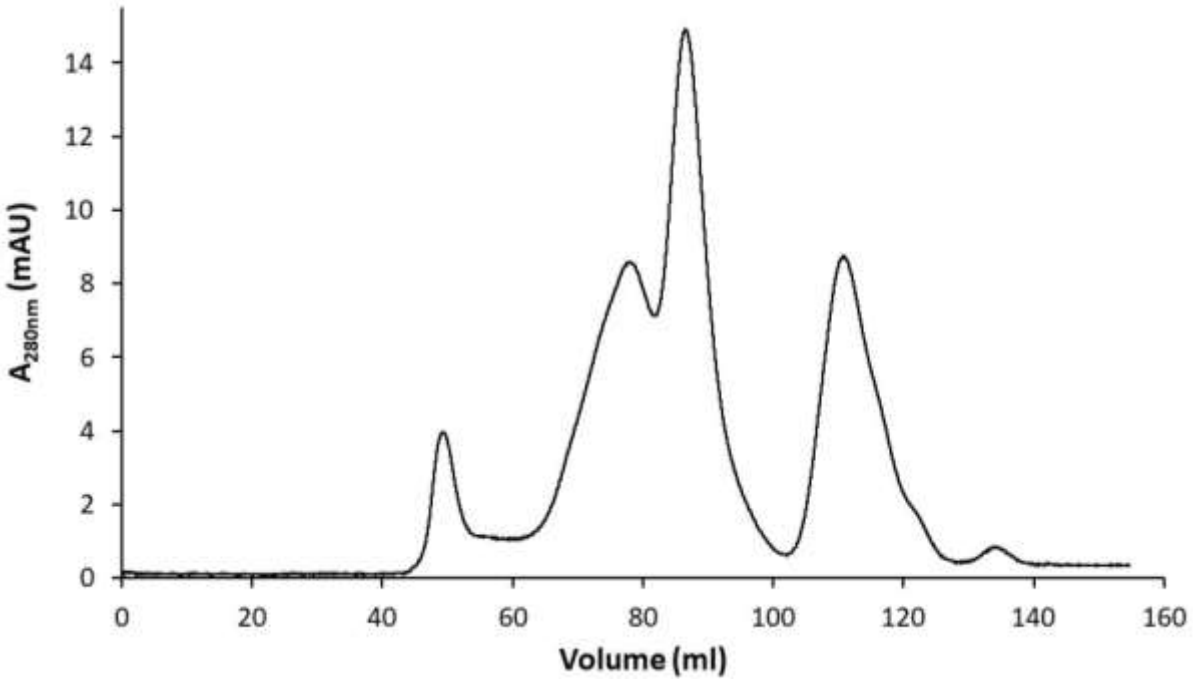

Figure 4.4. Size exclusion chromatography (SEC) chromatogram of recombinant Csp3.

Size exclusion chromatography purification of *Salmonella* Csp3 from the fractions eluted previously from anion exchange chromatography (figure 4.2) which were labelled as 143-145-147 (figure 4.3) were pooled and resolved in 20 mM Tris, 150 mM NaCl pH 8.5 using a Superdex 200 16/600 preparative column on AKTA Pure FPLC system at room temperature. A volume of 2 ml of the AEC-purified protein fraction was loaded onto the Superdex column and resolved in the same buffer with 2 ml fractionation over 1.5 column volume. This is a representative chromatogram taken from a single purification, but this SEC was performed numerous times (>10 occasions) to purify Csp3.

.

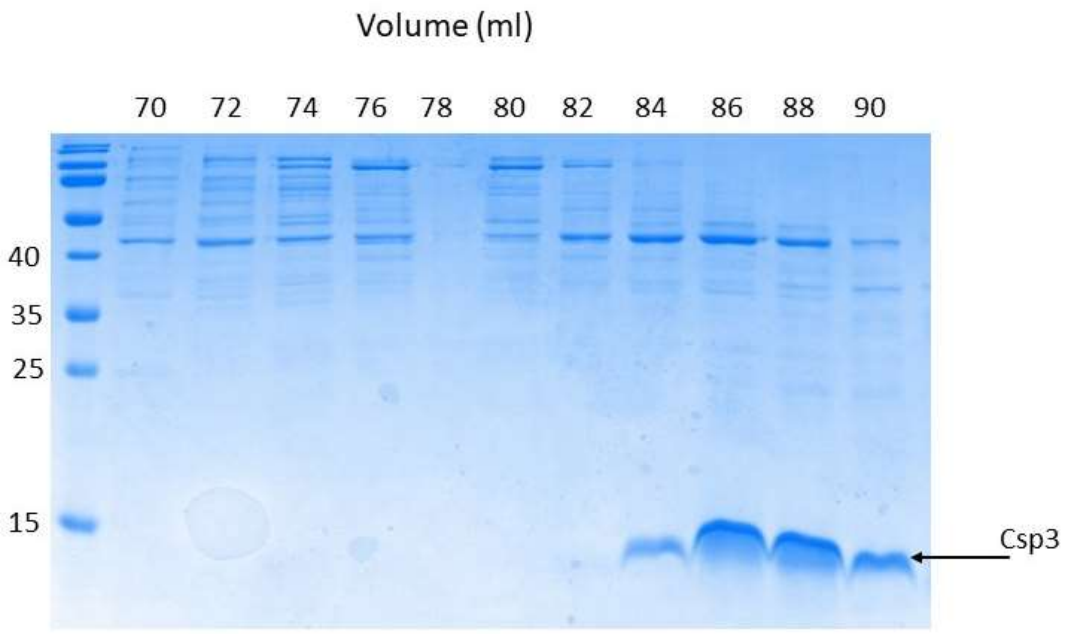

Figure 4.5. SDS-PAGE showing eluted fractions of SEC of recombinant Csp3.

An aliquot (10 µl) of each fraction (2 ml) across the main elution peak across the region (84-86-88-90 ml in figure 4.4) were boiled for ten minutes in the presence of SDS and DTT, and resolved on 19% (w/v) gel to investigate the protein's purity. Gels were stained for protein using Instant Blue Coomassie (Expedeon) and visualised with Image Lab™ software. The numbers on the left relate to molecular weight of commercial standards (Sigma). In addition to this, the arrow on the right indicates the band representing Csp3, which has a predicted mass of 12095.94 Da. This is a representative chromatogram taken from a single purification, but this SEC/SDS-PAGE was performed numerous times (>10 occasions) to purify Csp1.

4.2.3. Protein quantitation of Csp3

As with Neisseria Csp1, the next step after purifying the protein was protein quantitation to help us to build the next stages of the study based on the protein concentration. Accurate protein concentration measurement is obviously important in my project, as the aim was the determination of copper-binding stoichiometry. To measure this, we needed to calculat the required amount of copper to be added during the experiment, e.g. in mole equivalents, based on the value of the

protein concentration. As in Chapter 3, we used multiple ways to measure the protein concentration: spectrophotometrically using absorbance at 280 nm, using the Bradford assay and using a DTNB assay.

The concentration of purified Csp3 recombinant protein was first measured by following the Bradford method. This method uses a colorimetric reagent (Coomassie Plus protein assay; ThermoFisher Scientific) and compares the intensity of the colour developed in the presence of an unknown concentration of protein in the test samples with the intensities developed in the presence of a standard curve of known concentrations of bovine serum albumin (BSA). The method is primarily a means of measuring the presence of basic amino acid residues, arginine, lysine and histidine. The absorbance was measured at 595 nm.

Dilutions of the purified *Salmonella* Csp3 protein were prepared and mixed with a fixed volume of the Bradford assay reagent. Simultaneously, suitable dilutions of the protein standard, BSA, were prepared in the same microtitre plate, in the same buffer, and mixed with the same fixed volume of Bradford reagent. After a brief incubation (~5 minutes), the absorbance was measured at 595 nm, and a standard curve was constructed using the absorbance observed plotted against the absorbance observed for each of the BSA standards (Figure 4.6). This standard curve was then used to calculate the estimated protein content of the ‘unknown’ samples containing purified Csp3 protein, which was then mathematically converted into a molarity.

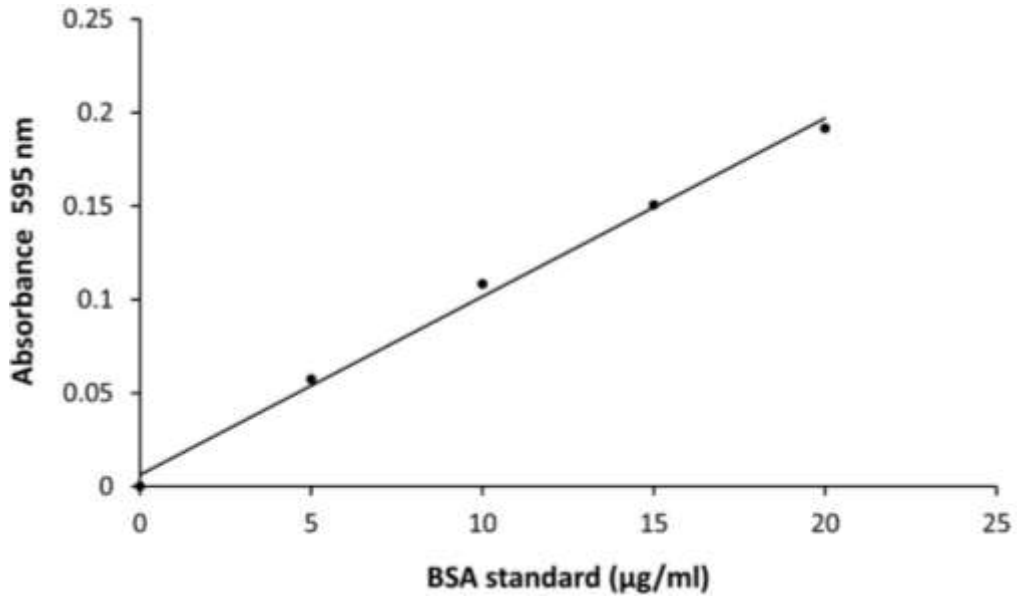

Figure 4.6. The Bradford assay standard curve of known concentrations of bovine serum albumin (BSA).

Dilutions of the purified *Salmonella* Csp3 protein were prepared and mixed with a fixed volume of the Bradford assay reagent. At the same time, suitable dilutions of the protein standard, BSA, were prepared in the same microtitre plate, in the same buffer, and mixed with the same fixed volume of Bradford reagent. After a brief incubation (~5 minutes), the absorbance was measured at 595 nm. Csp3 concentration was determined by calculation from this BSA standard curve, which was generated by plotting the absorbance of a different dilution of BSA standards of known concentrations.

As for Csp1, the second method utilised for estimating the concentration of Csp3 was UV-visible spectroscopy. Samples of purified Csp3 protein (1 ml) were transferred into a quartz cuvette (1 cm pathlength) and a spectrum obtained between 200-800 nm wavelength, blanked against the same buffer in which the sample was dissolved. An estimated extinction coefficient for the Csp3 protein was calculated using the ProtParam online tool, $\varepsilon = 2980\ M^{-1}\ cm^{-1}$, and this was used to calculate the Csp3 concentration from the absorbance at 280 nm (Figure 4.7**)**.

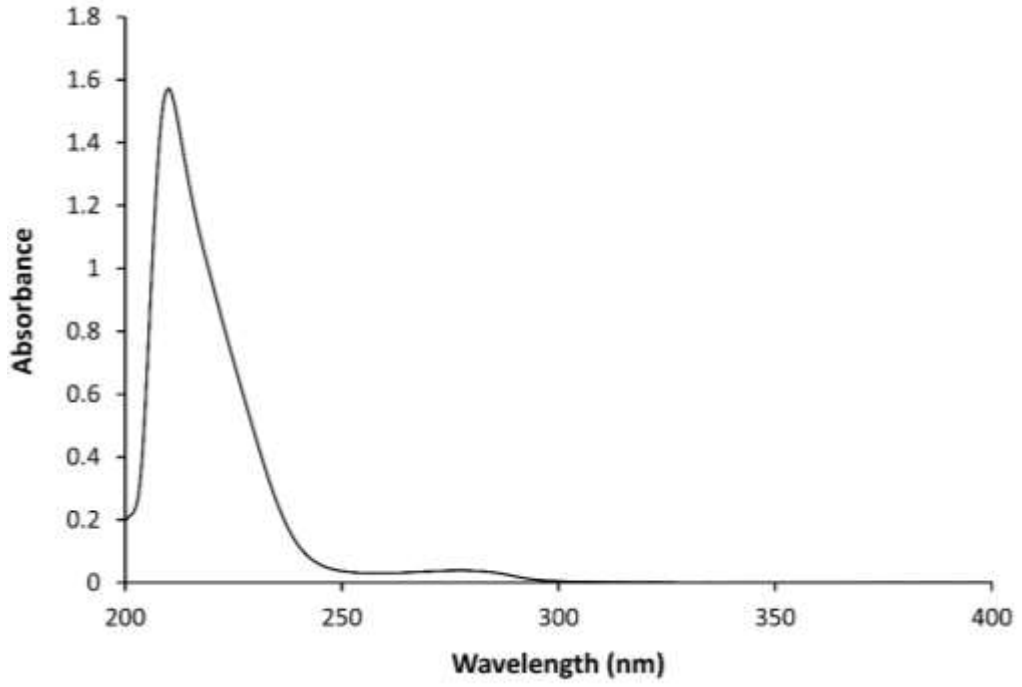

Figure 4.7. Using UV-visible spectroscopy to measure Csp3 concentration

The concentration of *Salmonella* Csp3 was calculated by monitoring absorbance at 280 nm. Csp3 was transferred to quartz cuvette (1 cm pathlength) and a UV/visible spectrum was obtained in the wavelength range between 200 nm and 800 nm, in the Lambda 35 UV-Vis Spectrometer (Perkin Elmer), blanked against buffer (20mM Tris, 150mM NaCl PH 8.5). The Csp3 protein concentration was calculated using a theoretical extinction coefficients, ε_{280nm}= 2980 M^{-1} cm^{-1} that was calculated using the ProtParam online software and using the Beer Lambert Law (A=εcl).

The third method again used the reaction between DTNB and sulfhydryl groups that yield a coloured product. Using Ellman's reagent protein concentration can be calculated through spectroscopic determination using the known extinction coefficient of the resulting complex of sulfhydryls with DTNB (14,150 M^{-1} cm^{-1} at 412 nm) where the number of Cys residues is known. The experimental process was performed again inside an anaerobic chamber for solutions of protein in the presence of chaotropic unfolding reagents such as 8 M urea and 6 M guanidine hydrochloride (Figure 4.8).

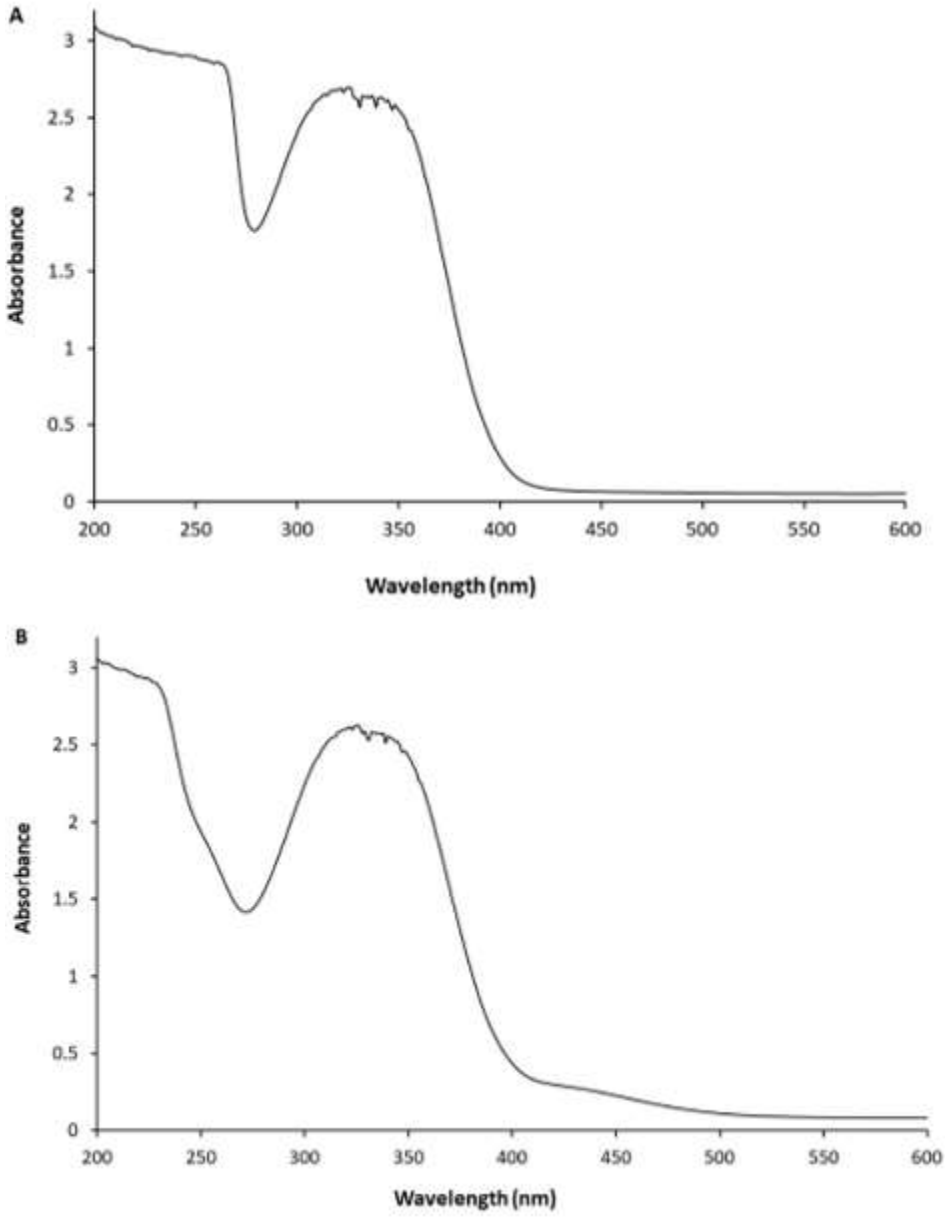

Figure 4.8. Using DTNB reagent for Csp3 quantification in the unfolded state in the presence of 8 M urea and 6 M guanidine hydrochloride.

Ellman's reagent reacts with sulfhydryl groups and produces a measurable yellow colour. The test tube contained reaction buffer, protein solution, DTNB solution and 6 M guanidine or 8 M urea. Then the DTNB-sulfhydryl complexes in this solution was quantified in spectrophotometer by measuring the absorbance at the wavelength of 412nm and using extinction coefficient 14,150 M^{-1} cm^{-1} . The experimental process was performed under anaerobic conditions inside an anaerobic chamber.

Unfortunately, during analysis of multiple preparations of Csp3 protein, it was observed that the calculated values of the Csp3 protein concentration that was obtained using these three approaches was inconsistent. This was nonetheless consistent with the previous results that were obtained with *Neisseria* Csp1 (Chapter 3). It was therefore difficult to continue experiments which aimed to estimate the Cu(I) binding stoichiometry of the Csp3 protein until this problem of Csp3 protein quantitation was resolved.

As previously, in an effort to resolve this conflict between multiple assays of protein quantitation, a sample of recombinant Csp3 was sent for a quantitative amino acid analysis by Alta Biosciences Ltd. The results obtained from Alta Biosciences are shown in Table 4.1.3A, which shows the abundance of each of the individual amino acids, along with the amino acid content in the known sequence of the *Salmonella* Csp3 protein, followed by the estimation of Csp3 concentration on the basis of each of the individual amino acids.

As previously, this analysis was performed on a batch of Csp3 protein which had previously been quantified using the three methods described above. Based on the report which was received from Alta Biosciences Ltd, giving quantities of 16 out of the 20 amino acids (excluding phenylalanine, tryptophan, lysine and arginine), this allowed us to calculate an average measured protein concentration from the amino acid analysis. This, in turn, allowed us to then generate correction factors from this analysis relative to the other three methods employed.

Amino acid		nmole/ml	µg/ml	mg/ml	AA content Csp3	[Estimated Csp3in µM]
Cysteic acid						
Hydroxyproline						
Aspartic acid	D	63.9	7.36	0.00736	9	7.1
Threonine	T	12.6	1.27	0.00127	6	2.1
Serine	S	32.2	2.81	0.00281	7	4.6
Glutamic acid	E	106	13.6	0.0136	13	8.153846
Proline	P	10.5	1.02	0.00102	2	5.25
Glycine	G	19.2	1.1	0.0011	4	4.8
Alanine	A	109	7.77	0.00777	25	4.36
Cystine	C	21.7	4.82	0.00482	14	1.55
Valine	V	20	1.98	0.00198	6	3.333333
Methionine	M	34.3	4.5	0.0045	4	8.575
Isoleucine	I	32.3	3.66	0.00366	1	32.3
Leucine	L	53.5	6.05	0.00605	12	4.458333
Tyrosine	Y	14.8	2.42	0.00242	3	4.933333
Phenylalanine	F	11.6	1.71	0.00171	0	0
Histidine	H	43.7	6	0.006	12	3.641667
Tryptophan	W	-	-	-	0	-
Lysine	K	29.8	3.82	0.00382	7	4.257143
Arginine	R	37.2	5.82	0.00582	3	12.4
Totals		652	75.7	0.0757		7.039527

Table 4.1.3A. Amino acid analysis yield of Csp3

A sample of purified Csp3 was measured by A280, Bradford, and DTNB. An aliquot of that sample, which was estimated by Bradford assay to be approximately 30 µM, was analysed for total amino acid composition by Alta Biosciences Ltd. Each number in this table represents the measured concentration of amino acids (nmole/ml, µg/ml, mg/ml) and the relative amino acids compositions of Csp3 (AA content), which enabled us to calculate the Csp3 concentration derived from each individual amino acid (Estimated Csp3). An average of these values, with the exception of phenylalanine, histidine, tryptophan, lysine and arginine, was used to generate correction factors for the other quantitation techniques (Table 4.1.3B).

Four different methods of protein measurement were therefore used in an effort to minimise the error in the concentration value.

Protein measurement method	Protein concentration in (µM)
1- Bradford assay	30 µM
2-Uv/vis spectroscopy	8.5 µM
3-DTNB	15 µM
4-Amino acid analysis	7.04 µM

Table 4.1.3B. Protein measurement outcomes

The data presented in this table show the Csp3 quantity measured using the four different methods used. These data were obtained from a single biological sample (n=1).

As in the case of Csp1 (Chapter 3), these four different methods were employed in an effort to find an optimal method for measuring the concentration of *Salmonella* Csp3. Amino acid analysis is the 'gold standard' for protein concentration determination. This method measures directly up to 20 amino acids, reducing experimental error. The alternative methods each have advantages and disadvantages, in terms of cost, accuracy and ease of measurement, as described in Chapter 3. However, table 4.1.3B indicated that each of these measurement approaches showed discrepancies from one another . As with Csp1, we aimed to use the average of the amino acid analysis, regarded as most accurated, to generate correction factors for the alternative and more accessible methods in an effort to improve the accuracy of these techniques.

4.2.4. Determination of metal stoichiometry

Previous studies (Vita et al., 2016; Vita et al., 2015) have estimated the approximate Cu(I)-binding of Csp homologues using spectroscopic and chromatographic methods. Those studies estimated stoichiometries 15 to 20 copper ions per monomer for *Mt*Csp3 and of 17 to 21 copper ions per monomer for *Bs*Csp3, and a lower stoichiometry of 12-14 copper ions per monomer for the periplasmic *Mt*Csp1. Crystal structures of copper-loaded samples of two of these homologues demonstrated binding of 19 copper ions bound at the core of the *Mt*Csp3 monomer, and 13 copper

ions bound at the core of the *Mt*Csp1 monomer (Vita et al., 2016; Vita et al., 2015), consistent with the stoichiometries estimated by the spectroscopic and chromatographic methods.

In the previous section we used several methods of measuring the protein concentration because we aimed to estimate the copper binding stoichiometry of Csp3 *in vitro* which means determination of the number of copper ions that can bind to the recombinant Csp3protein. Utilising the methods described for estimating Csp3 protein quantitation, we used two methods for determining how much copper it was capable to bind, as with *Ng*Csp1 (Chapter 3). One method used UV/visible spectroscopy to monitor binding of Cu(I) to the cysteines of Csp3, and the other involved direct detection of the amount of copper bound to Csp3 after resolution through a chromatography column.

Again, for these experiments, the cells from which this protein was purified were grown in M9 medium in an effort to produce apo protein, to avoid copper contamination of the purified protein that would interfere with stoichiometric measurements. As had happened before, however, we observed that we were not able to make apo protein, even when we grew the cells in M9 medium, as the purified protein was generally found to contain 1-2 mole equivalents of copper as determined by ICP-MS, using Bradford assay data for protein measurements corrected by a factor derived from the amino acid analysis.

The binding of copper to proteins via cysteine bonding can be detected via UV-visible spectroscopy. In the same experiment with Csp1, the limitation was the limited amount of the protein available for these experiments due to protein instability. Csp3 was found to be more stable, alleviating this issue a little. Furthermore, we had observed that we were unable to saturate Csp1 (Chapter 3). The experimental design was therefore modified to include higher copper concentrations for solving the issue of lack of saturation seen in Csp1 experiments (Figure 3.9). In these experiments, the concentrations of copper added were 0, 24, 48, 120 and 180 equivalents. Each sample, in triplicate, was incubated overnight in an anaerobic chamber (section 2.10). Then

after this incubation period, the absorbance of each sample was determined at 210 – 350 nm where copper-binding features are anticipated using the UV/visible spectrophotometer.

The results (Figure 4.9). demonstrated a remarkable increase of absorbance in the presence of Cu(I) ions after incubation 24, 48, and 120 mole equivalents of copper, as compared to negative control with no added copper. This result indicated the coordination of a large number of copper ions by recombinant Csp3. According to Meghana et al., 2015, Vita et al., 2015 and Vita et al., 2016, these results are indicative of characteristic ligand-to-metal charge transfer transition from Cys to Cu(I).

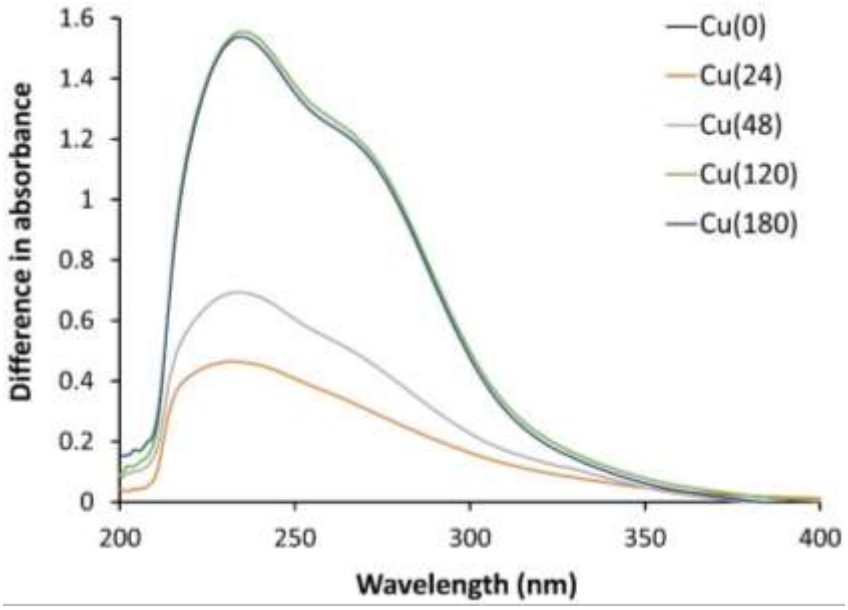

Figure 4.9. UV/visible spectroscopy detects binding of Cu(I) ions to *Salmonella* Csp3.

In order to evaluate the binding of Cu(I) ions with Csp3 protein via UV-visible spectroscopy, various copper concentrations were used (0, 24, 48, 120 and 180 molar equivalents). The starting concentration of Csp3 that was used was 10 µM, as determined by Bradford assay using a correction factor derived from quantitative amino acid analysis. Each sample was incubated overnight in the presence of a specific concentration of copper inside an anaerobic chamber for equilibration purposes in 20mM Tris, 150mM NaCl pH 8.5. The next day, the UV/visible spectrum

of each sample was collected. The difference spectra are shown, which were calculated by subtracting the absorbance of the apo sample (i.e. with no added copper) from each of the copper-loaded samples (hence why the zero copper spectrum is a flat line at 0). The spectra showed a significant increase in absorbance in the presence of Cu(I) ions, consistent with binding of Cu(I) ions to Cys residues in Csp3. However, the figure showed that the absorbance kept increasing, up to the addition of what was intended to be 120 mole equivalents of copper. Nonetheless, there was evidence of copper saturation of Csp3 in this experiment, in contrast to the data obtained with Csp1 (Figure 3.9). The data presented in this figure is derived from a single biological replicate. This experiment was repeated two further times and, on both occasions, there was evidence of protein precipitation at high copper concentration but consistently all three replicates suggested copper stoichiometry substantially greater than 20.

The results from the UV/visible spectroscopy experiment demonstrated that the absorbance in the region of the spectrum diagnostic of copper binding to Cys residues increased in intensity until 120 mole equivalents of Cu(I) were added (Figure 4.9). No evidence of protein precipitation was observed, even at high copper stoichiometries. At this point, the spectrum saturated, and no further increases in absorbance were observed at higher additions of Cu(I). Further increase in concentration, such as 180 equivalents, caused no increase in absorbance indicating that saturation point was achieved at 120. This is in contrast to the data obtained with *N. gonorrhoeae* Csp1 (Figure 3.9).

However, that did not necessarily mean that the binding capacity of *Salmonella* Csp3 is 120 molar equivalents of Cu(I). These data indicate that it is something higher than 48 and less than 120, as the titration graph showed. All the Csp proteins that have been studied so far have a capacity between 13 and 24, and the Csp3s between 21 and 24, so we don't really believe that the capacity is more than 48. However, Csp3 with 120 equivalent of Cu(I) showed maximum absorbance as compared to the other concentrations tested, suggesting this was the copper saturation point of the protein in this assay. Given the problems we have observed in accurately measuring the protein

concentration, both for *N. gonorrhoeae* Csp1 (Chapter 3) and here for *Salmonella* Csp3, it seems likely that an error in the protein concentration determination may be responsible for the discrepancy between the observed and expected value for copper binding stoichiometry.

Nonetheless, the result of this experiment was a clear indication that copper binds to sulfur when Cu(I) is titrated into Csp3, as expected. Furthermore, we did manage to saturate the protein with copper, in contrast to the equivalent experiments with *Neisseria* Csp1, but we cannot be certain of the final stoichiometry.

The binding of Csp3 to copper ions was further investigated by resolving bound and unbound metal from these titrated samples using the gel filtration chromatography assay, as previously applied to *N. gonorrhoeae* Csp1. Again, I employed an analytical Superdex 200 10/300 column that was previously equilibrated and resolved in the buffer of 10 mM Hepes, 150 mM NaCl, pH 7.0. We decided to eliminate the sample incubated with 180 Cu(I) equivalents, both because we were expecting it will look the same as that incubated with 120 equivalents, and because, looking at the test tube, it was obvious that there was some precipitate. Even though the extent of precipitation was less in the case of Csp3 compared with prior experiments with Csp1, we did not want to load a precipitate into the column as this could damage it.

The result from the size exclusion chromatographs (Figure 4.10) showed that the Csp3 protein, as measured from A280nm during the AKTA runs, eluted from the column again at a volume of 14-15 ml, as was the case for Csp1. SDS-PAGE analysis confirmed the presence of Csp3 in this peak (Figure 4.10, inset). The elution profile looked very similar for each of these samples, consistent with the idea that the mass of Csp3 did not change as it was titrated with copper. The absorbance increased with increasing copper incubation relative to the control, to which no copper was added. This is consistent with the observation that the protein absorbance at A280 increases in a copper dependent manner, as was seen in the UV/visible titration (Figure 4.9), which also showed the absorbance in this region of the spectrum increasing as the copper was increased.

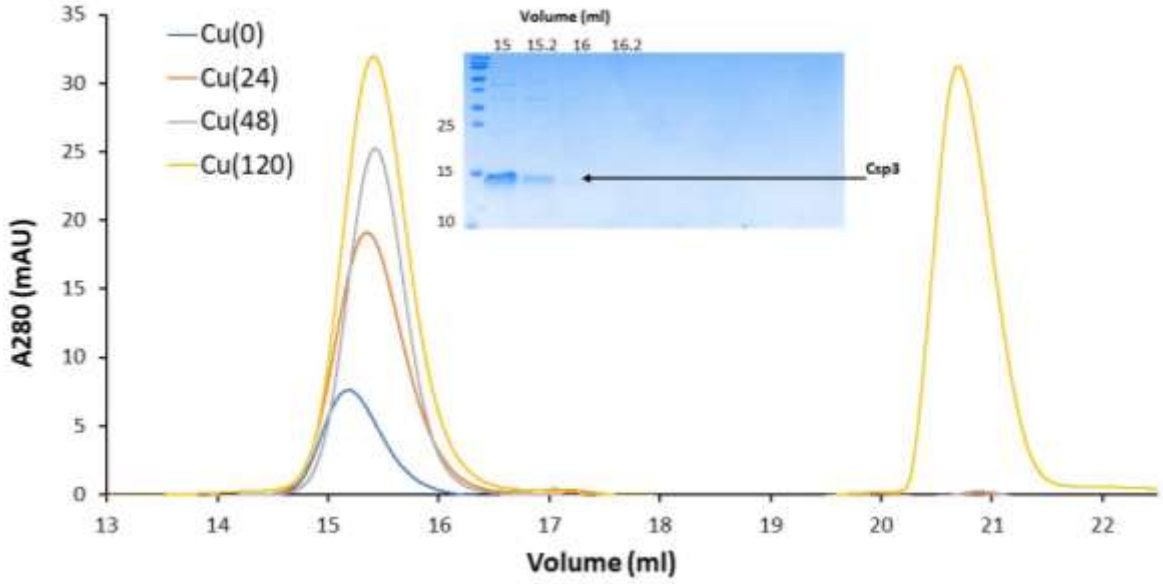

Figure 4.10 Size exclusion chromatography to resolve copper treated bound and unbound copper from Csp3 samples

Samples of recombinant Csp3 protein (10 µM, as determined by Bradford assay) were incubated in the presence of 0, 24, 48, or 120 mole equivalents of Cu(I) in an anaerobic chamber overnight and used for UV/visible spectroscopy (Figure 4.9). Each sample was subsequently injected (0.5 ml) onto a size exclusion column, Superdex S200 10/300, which was equilibrated and resolved in 10 mM Hepes, 150 mM NaCl pH 7.0 on an ÄKTA pure purification system at room temperature. Each trace shows the absorbance at 280nm, reflecting protein eluting from the column, which is moderated by binding of Cu(I) (Figure 3.9), increasing intensity. Subsequent SDS-PAGE analysis of these fractions from the sample treated with 48 equivalents Cu(I) is shown as an inset, demonstrating that the protein eluted around 15 ml. This experiment was performed on three biological replicates, but only a representative set of chromatograms are shown.

The fractions collected during the size exclusion chromatography, as shown in Figure 4.10, were subjected to elemental analysis by ICP-MS (Figure 4.11) to determine how much copper co-

migrated with the Csp3 protein. The fractions from 14 to 21 ml were analysed to measure metal content and the protein content of these fractions were measured by Bradford, corrected using the correction factor derived from the quantitative amino acid analysis.

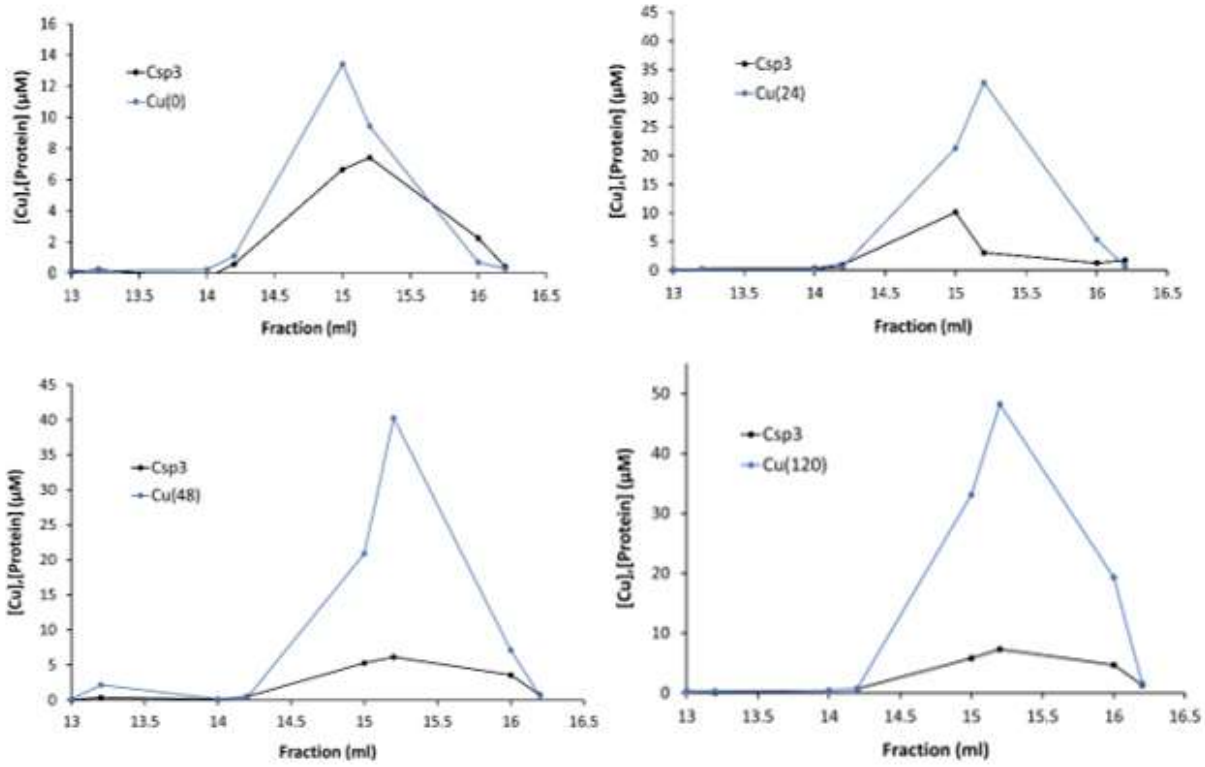

Figure 4.11. Measurement of copper co-migrating with Csp3 in SEC by ICP-MS

Samples of *Salmonella* Csp3 (10μM) that had been incubated with varying molar equivalents of Cu(I) (0, 24, 48 and 120) and resolved by analytical SEC (Figure 4.10). The resulting fractions (0.5 ml) were analysed by ICP-MS to measure copper content and by Bradford assay to estimate protein concentration. The data presented here are from a single biological replicate, which was the same set of samples as shown for the experiment in Figure 4.9. A similar experiment was performed two further times and a similar result was obtained on each occasion. Fractions numbers were converted to ml as per AKTA software.

The result of the stoichiometry by ICP-MS when 120 equivalents of copper was added was 6.2 in this assay. In a further replicate, where 24 equivalents of copper were added, the stoichiometry measured by ICP-MS was 41.9. These absolute numbers should be interpreted carefully again here, though, due to known issues with quantification of the protein (Table 4.1.3B), which causes particularly severe problems when trying to quantify low concentrations of protein, as in this case after it has been diluted while resolving through SEC.

Overall, we found that the data from UV/visible spectroscopy and SEC analysis was consistent in terms of the absorbance of the Csp3 protein in the presence of Cu(I). After size exclusion the absorbance in the Csp3-containing fractions was greatly increased (Figure 4.10), consistent with the increased absorbance of the copper-loaded protein form observed in UV/visible spectroscopy (Figure 4.9). However, there was less consistency in the measurement of the copper-binding stoichiometry. Nonetheless, in the ICP-MS results, it was found out that more copper was detected in the peak Csp3-containing fractions as copper was increased from 24 to 48 Cu(I) equivalents (Figure 4.11), although there was not a significant increase in the detected copper between 48 and 120 equivalents, as we would have expected from the UV/visible spectroscopy data (Figure 4.9). As discussed before, the most challenging step in this study was measuring the protein accurately (Table 4.1.3B), so it is possible that both datasets have been most impacted by inaccuracy in this measurement. From the beginning of the copper titration experiment, it might have based on an inaccurate protein concentration. Alternatively, measurements of the copper by ICP-MS may not have been accurate, although this is less likely due to the internal controls that are inherent to this quantitative technique using internal standards in the analysis. Taken together, the results suggest a stoichiometry greater than 20, which would again contrast with the previous data from other homologues (Vita et al., 2015; Vita et al., 2016), but the variability prevented us from defining the precise stoichiometry.

In conclusion, measuring the stoichiometry of *Salmonella* Csp3 was really challenging. Accurately measuring the concentration of apo protein was difficult, as was previously seen for *N. gonorrhoeae* Csp1 (Chapter 3). However, the positive result was that my data showed that the

recombinant Csp3 protein did bind a lot of copper ions, as anticipated. The stoichiometry is best estimated as being between 48 to 120 equivalents.

4.2.5. Effect of Cu/ Zn/Ag binding

As previously tested for *N. gonorrhoeae* Csp1, in this experiment aimed to test the hypothesis other metals, silver and zinc, which have some similar properties to copper, could bind to the recombinant Csp3 protein. This experiment was also designed to investigate the whether the hypothesised binding of zinc and silver ions would subsequently interfere with binding of copper to the Csp3 protein.

In this experiment, we measured the concentration of Csp3 protein by Bradford assay using a correction factor derived from the amino acid analysis (Table 4.1.3B). Using the same experimental design as described for the equivalent experiment with Csp1 (section 3.2.5), the metal ions were incubated with aliquots of Csp3 protein under anaerobic conditions overnight. Protein samples were incubated either alone with Cu(I), Ag(I) or Zn(II) ions (1 mole equivalent), or were exposed to two metals sequentially (1 equivalent of either silver or zinc, followed by a 1 h incubation period, followed by subsequent challenge with 10 equivalents of copper). After overnight incubation, the samples were each resolved by size exclusion chromatography (Superdex 200 10/300 in the buffer of 10 mM Hepes /50 mM NaCl pH7.0) and then the eluted fractions were used for metal analysis by using inductively coupled plasma mass-spectroscopy (ICP-MS).

The chromatographs from size exclusion chromatography (Figure 4.12) showed that the protein eluted as a peak across the same region as previously (~15 ml). The addition of Cu(I) alone, as a positive control, led to a large increase in the absorbance at A280nm, consistent with the UV/visible spectroscopy data (Figure 4.9). Interestingly, addition of silver ions also increased the protein's absorbance, whereas addition of Zn did not. Crucially, subsequent addition of Cu(I) to

samples that were previously incubated with either silver or zinc did result in a jump in absorbance, which suggests binding of neither metal prevented subsequent copper binding (Figure 4.12).

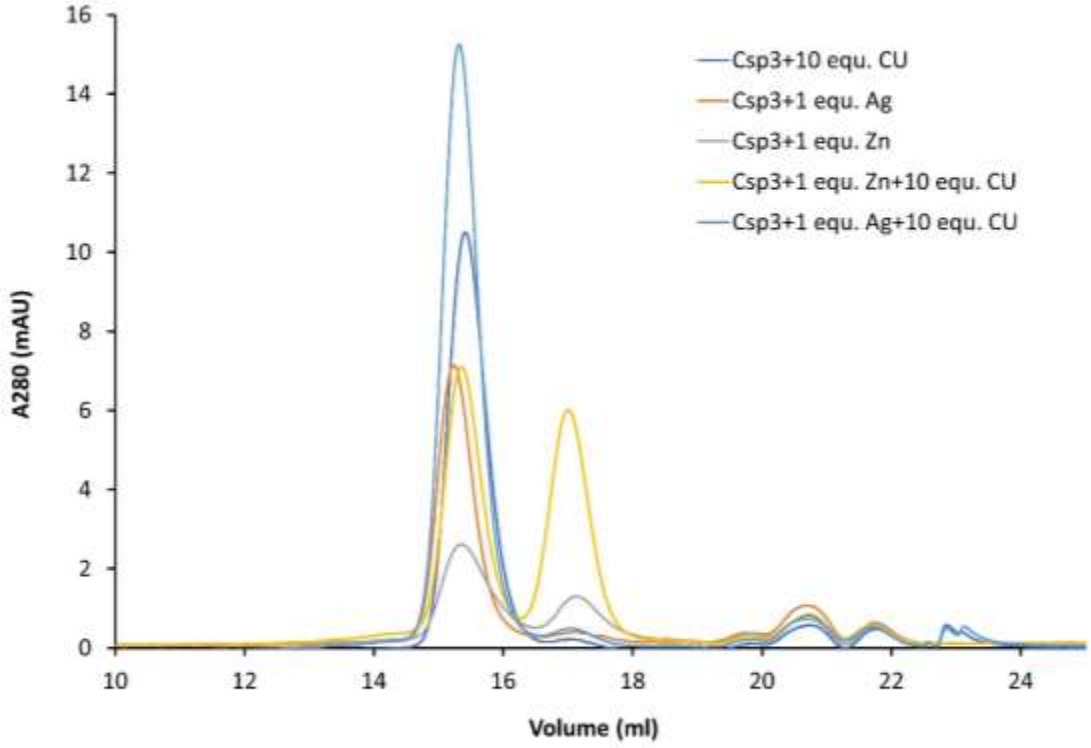

Figure 4.12. Size exclusion chromatogram of Csp3 treated with Cu/Ag/Zn.

Samples of purified Csp3 (5µM) were mixed with either ten equivalents of Cu(I), or with one equivalent of Ag(I) or Zn(II). Two further samples were treated first with Ag(I) or with Zn(II), incubated for one hour, and then challenged with ten equivalents Cu(I). All of the samples were incubated overnight inside an anaerobic chamber, followed by resolving by analytical size exclusion chromatography on Superdex S200 10/300 in 10 mM Hepes,50 mM NaCl pH 7.0. The absorbance traces, A280nm, are shown. The data presented here are from a single biological replicate n=1.

Next, we analysed the metal content of size exclusion chromatography eluted fractions by ICP-MS, The analysed samples in the positive control experiment showed that the protein was associated with copper that had bound to Csp3 (Figure 4.13). We were expecting high concentrations of copper eluting at 15 ml based on size exclusion chromatogram that showed this

as the peak fraction (Figure 4.12), however the ICP-MS result indicated only a little more than 1 equivalent of copper in this fraction. Therefore tis indicated a low stoichiometry, but nonetheless demonstrated copper binding to Csp3 as expected from this control. In the experiment in which Csp3 was incubated with 1 equivalent of silver nitrate (Figure 4.13), the ICP-MS analysis detected some silver eluting at 15ml. This indicated that Ag(I) ions did bind to Csp3, as we hypothesised it would as silver has similar coordination preferences and is located above copper in the periodic table. The third metal, zinc (Figure 4.13), was hard to interpret. Although there was an indication of a small 'peak' of zinc detected in the fraction in which the protein was present, the data were negative, suggesting the zinc concentrations detected in these fractions was lower than those detected in the blank solution used for calibrating the ICP-MS instrument.

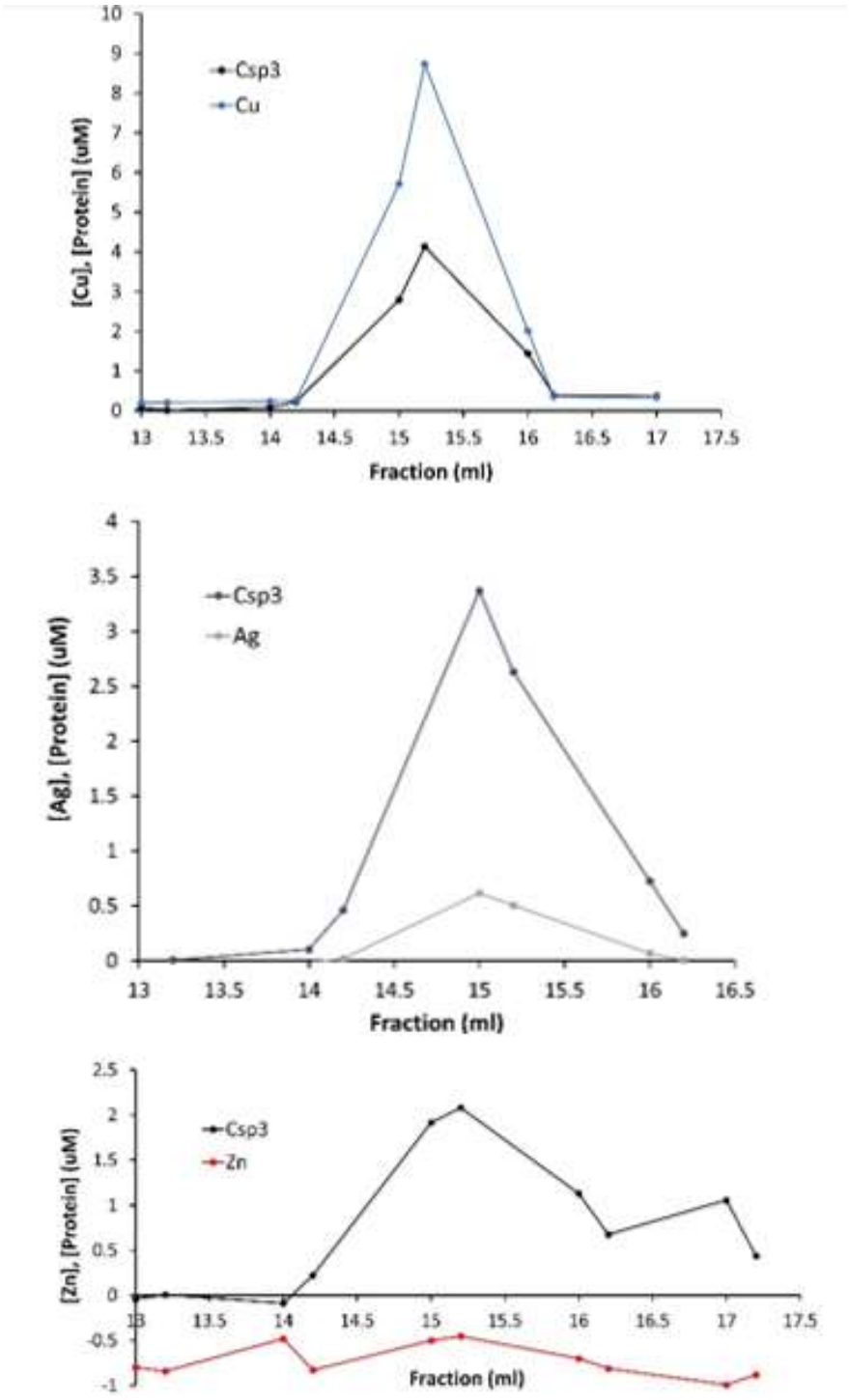

Figure 4.13. Binding of Cu, Ag and Zn to recombinant Csp3 using ICP-MS.

Protein samples of Csp3, incubated with either ten equivalents of Cu(I), or one equivalent of either Ag(I) or Zn(II), were resolved by analytical SEC on a Superdex S200 10/300 column in 10 mM Hepes, 150 mM NaCl, pH 7.0. The resulting fractions

of SEC (Figure 3.12) were prepared for metal analysis by using ICP-MS (Section 2.8). Protein concentration in those fractions were measured with Bradford assay. This experiment was performed once, n=1.

The SEC fractions obtained from samples representing the second stage of this experiment, where Salmonella Csp3 was incubated in combination with two metals, were also analysed by ICP-MS (Figure 4.14). The result of metal analysis, as shown in Figure 4.14, indicated that copper was detected bound to Csp3, in both samples. This suggests that any binding of silver or zinc to Csp3 (Figure 4.13) did not prevent the ability of copper ions to subsequently fill up the protein tube. Interestingly, we nonetheless detected some silver ions (and a hint of zinc ions) present in the fractions that contained Csps, which might indicate that those ions are able to bind to the protein in a way that does not prevent subsequent binding of copper ions. This may suggest that these ions bind around the opening of the tube, at the entrance, but do not block entry of copper ions into the tube, or that they can enter the tube and move down it such that copper added afterwards is able to fill up the tube.

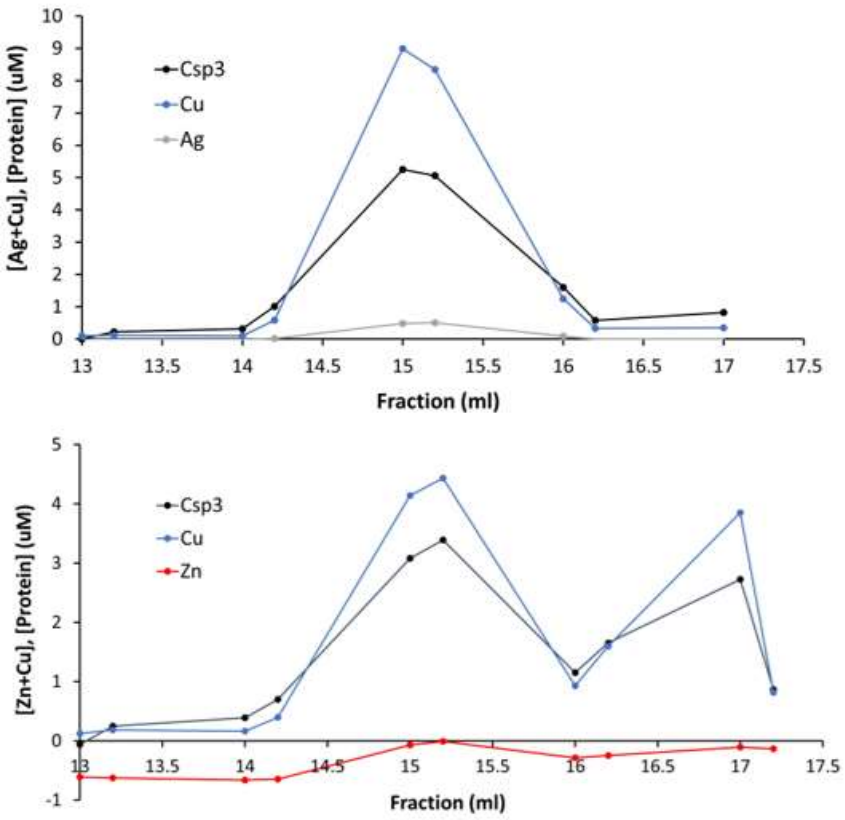

Figure 4.14. Binding of Cu, after incubation with Ag and Zn, to recombinant Csp3 using ICP-MS.

Protein samples of *Salmonella* Csp3 were initially incubated with one equivalent of either Ag(I) or Zn(II) for one hour, and then were challenged by subsequent addition of ten equivalents of Cu(I), followed by incubation overnight in an anaerobic chamber. The samples were subsequently resolved by analytical SEC on a Superdex S200 10/300 column in 10 mM Hepes, 150 mM NaCl, pH 7.0. The resulting fractions of SEC (Figure 4.12) were prepared for metal analysis by using ICP-MS (Section 2.8). Protein concentration in those fractions were measured with Bradford assay. This experiment was performed once, n=1.

4.3 Discussion

Many organisms including bacteria have characteristic Cu(I) resistance systems that enable them to avoid its toxic effect in biological systems. Previously, it was considered that bacteria do not have cytosolic copper enzymes as there is no known metabolic requirement for cytosolic copper and few identified copper-binding metallothioneins in bacteria.

Recent experimental investigation demonstrated the presence of a new family of copper storage proteins in the bacterial cytosol in methanotrophic bacteria. These proteins showed the highest binding capacity with Cu ions (Vita et al., 2016). These proteins have conserved Cys residues that localise to the centre of a 'tube' formed by the characteristic four-helix bundle structure of Csp3s to coordinate with a large number of copper ions. The apparent range of stoichiometry of these metalloproteins is different to Csp1s, the putative periplasmic homologues of these copper storage proteins. The tetrameric Csp3s have the ability to bind with up to 80 copper ions (Straw et al., 2018; Vita et al., 2016).

In this study, we were able to successfully express and purify the recombinant form of Csp3 from *Salmonella*. The results of the purification indicated that the protein was selectively eluted from anion exchange chromatography (Figure 4.2). The protein eluted from the AEC was then subjected to gel-filtration chromatography on a Superdex 200 column for a further purification step. The data from Figure 4.4 of size exclusion chromatography determined that the Csp3 protein eluted around 90 ml, which was further confirmed through the analysis of SDS -PAGE that showed the purified Csp3 protein in these fractions with very few contaminants.

One of the main tasks in my project was finding the most accurate method for quantifying the copper storage proteins, As demonstrated in Chapter 3, this was highly problematic for measuring the concentration of the Csp1 protein from Neisseria gonorrhoeae. Unfortunatly, my work

demonstrated that this protein quantitation step is still one of the biggest challenges in this field, but it is essential to build a strategy to answer this question to be able to measure the metal binding to the Csp proteins, as in this project. Table 4.1.3B presented the data acquired by multiple methods for protein quantitation that have been used in this study. Each method that was used has strengths and weakness, and each depends on the protein composition. For instance, quantification using A280 is primarily a tryptophan measurement, with further small contributions from phenylalanine and tyrosine, and Csp3 does not contain any tryptophan residues. Conversely, DTNB seemed to be a good method to quantify Csp3. This assay is a method that measures the number of cysteines, so it is not surprising that this method was effective given the high number of Cys residues in Csp proteins (Table 4.1.3A). However, there difficulties with this method. It depends on being able to routinely maintain good anaerobic conditions, which we had access to via use of a nitrogen atmosphere glovebox, but we met some complications through instrumental error that meant that the chamber was not always functioning and working at the level we needed it to be. This made it impractical to use the chamber every time in the protein calculations. Finally, we felt that the only solution for this issue available to us was to use the Bradford assay. We did triplicate technical replication when using Bradford assays during the study specifically to try to decrease the possible error. The results from the Bradford assays were then corrected using a correction factor derived from the quantitative amino acid analysis, as shown in Table 4.1.3B. Nonetheless, it is highly likely that inaccuracies in my protein quantitation assays led to significant errors for calculation of copper stoichiometry. If we had more time and resources, this approach may have been more successful if we had modified the experiment to apply it to a much larger number of samples, e.g. ten independent biological replicates. Alternatively, we should have used exclusively the DTNB assay, which was the approach that yielded data closest to those obtained from quantitative amino acids analysis (Table 4.1.3B).

The spectroscopic study showed that the spectral feature of Csp3 protein in the wavelength range 250-350 nm was increased in intensity in the presence of Cu (I). This increase was observed when the protein was incubated with 24 and 48 mole equivalents. However, as with Csp1, we observed further increases in absorbance in the 250-350 nm range on further addition of Cu (120 equivalents), although here there were no further absorbance increases observed after the final

addition of copper (180 equivalents), indicating it achieved a saturation state after 120 equivalents. Nonetheless, these values imply a stoichiometry significantly higher than would be expected based on previous studies of Csp3 proteins (Vita et al., 2016). This indicates, once again, that our protein quantitation was insufficiently accurate to determine a true copper binding stoichiometry. Nonetheless, this study determined that overexpressed Csp3 accumulates much copper, and this finding is similar to that reported by Dennison et al. 2018 and Vita et al. 2016 in case of *Bs*Csp3 recombinant overexpressed protein. It has also been supported by Straw et al. 2017 who showed that Csp3 from *S. lividans* binds a large number of copper ions and enables cells to grow under high stress of copper.

The challenging step we have encountered purifying both proteins was knowing exactly how much protein was present in the samples. The likely explanation of the stoichiometry data was that the protein concentrations determined were inaccurate and that led to underestimation of the protein concentration and overestimation of the stoichiometry. A further possibility was the incubation period. Initial experiments used a short incubation period (data not shown), where we incubated the samples for only a few hours, but the data were variable and unreliable. We altered the protocol with longer incubation time, where the samples were left overnight for equilibration purposes, and this approach was used in all data shown in this chapter. However, this step has a drawback. The Cu(I) precipitates, which may not have been observed at the time through the frosted tube, and that may have caused problems in the binding assay, with the copper ions not properly mixing with the protein in solution. A further possibility might be that the anaerobic chamber, which was supposed to ensure an anaerobic environment for the reaction, might not have been sufficiently anaerobic during this experiment. Even small levels of leaking of oxygen ions could impact on the result, as both Cu(I) and the Cys residues in the protein are susceptible to oxidation.

When considering the functional properties of Csp3 it is very important to keep in mind that this association with copper is due to the presence of lots of Cys residues. The spectroscopy data clearly demonstrate binding of Cu(I) ions to Cys residues. Therefore, this investigation is also in

agreement with the previous study of Vita et al. 2016 and Vita et al., 2015. The presence of cysteine residues could allow the protein to bind with a number of other d^{10} electronic configuration metal ions such as Zn and Ag, which could be expected to harm its role in detoxification of copper. The study indicated that the protein eluted similarly in the presence of Zn, Ag and Cu (Figure 4.12), suggesting that the presence of these metals did not substantially alter the quaternary structure of Csp3. Dennison et al. in 2018 reported that the effect of no other metal ions, such as manganese, iron and zinc, were evaluated on a homologue of this protein. So, this is a novel aspect of my study, in which binding of zinc and silver ions, alone or in combination with copper, were determined. The data, as with Csp1, demonstrated some binding of silver ions to Csp3, whereas incubation with zinc alone did not firmly demonstrate that the Zn(II) bound to the protein (Figure 4.13). Importantly however, subsequent incubation of protein with Cu(I) after prior incubation with Zn or Ag demonstrated that neither metal inhibits binding of Cu(I), presumably meaning these metals can only bind in a manner that leaves the opening of the Csp tube available for copper insertion.

In conclusion, the results from the present research proved that the tetrameric Csp3 protein has strong binding capacity with copper ions, and can also bind another metal ion, silver ions, and potentially also zinc.

Chapter 5: Crystal Structure of Copper Storage Proteins

5.1. Introduction

Metal ions provide proteins with access to a wider range of chemistry, enabling enzymes to catalyse chemical reactions that would be impossible by using solely organic molecules (De Graaf et al., 2009). However, most of these metal ions can also contribute towards toxicity of cells. Copper is well known for its essential role in many important processes including the processes of photosynthesis as well as respiration (Nalewajko and Olaveson, 1995) as it is a cofactor for key enzymes that take part in these processes.

In the past few years, the mechanism of cellular toxicity of copper has been reassessed. Now, it is not attributed to the production of reactive oxygen species (Choudhury et al., 2017) instead being shown to be driven by the potential of copper to bind tightly with the active sites of metalloenzymes (Dennison et al., 2018), especially those that contain iron-sulphur clusters. This not only contributes to the loss of activity of the mis-metallated protein but also releases iron which in turn can effectively produce reactive oxygen species. This is the main reason why “free”, hydrated copper ions must not be present in cells, both within prokaryotes and in eukaryotes (Lopez et al., 2019). The availability of copper appears to be constrained largely by the use of high affinity sites in proteins (Cremer et al., 2018). Understanding how such proteins sequester and ‘buffer’ copper within the cell is important to understanding how cells regulate copper, and in optimising the exploitation of copper toxicity in medicine.

Cells use a number of homeostatic proteins to enable safe handling of copper ions which include transporters, sensors, metallochaperones, and copper insertion proteins, each of which have high specificity and high affinity for copper (Zhang et al., 2019). Many of these homeostatic proteins are conserved between prokaryotic and eukaryotic organisms. The primary mechanism by which bacteria, and also eukaryotes, regulate their cytosolic copper concentration is through the activity of the P-type ATPase family proteins, generally called CopA. CopA plays its role in copper homeostasis through removing cytosolic copper by pumping copper ions across membranes.

Recent studies from the last decade have suggested that some bacteria have the additional potential to store copper safely by using a highly novel approach, by binding Cu(I) ions to a newly described family of copper storage proteins (Vita et al 2015 and Vita et al 2016). As yet, no gene encoding a Csp protein has been identified in any eukaryote. Csp proteins come in two 'flavours' that are defined by their subcellular localisation. Cytosolic homologues of the Csps, termed Csp3, are the more widespread and abundant class of the Csps, whereas periplasmic homologues, termed Csp1, are much more rare in bacterial genomes.

The copper storage proteins that have been previously characterised so far, namely two Csps from *M. trichosporium* OB3b, one from *Bacillus subtilis*, and a further homologue from *Streptomyces lividans*, share conserved structural features (Straw et al., 2018; Vita et al., 2016; Vita et al., 2015). It was reported that all Csps proteins are formed of a tetrameric complex structure of four individual monomers, each of which folds to form a four helix bundle (Vita et al. 2015). Each monomer is abundant in cysteine residues (more than 10% of the total residues), which are all located within the four helices, and positioned in such a way that allows all of the thiol groups of those Cys side chains point into the centre of the 'tube' that is formed by the bundle structure (Figure 1.4). Structures of the apo-forms of these proteins shows that these Cys residues do not form disulphide bonds, but are maintained in their free thiol form, such that the proteins appear to be relatively stable even in aerobic conditions (Vita et al., 2015). Structures of copper-loaded forms of these proteins reveal that the 'tube' in the bundle becomes filled with Cu(I) ions, with each ion coordinated to the Cys residues (as well as to some Met or His residues near the opening of the tube) in 2-, 3- or 4-coordinate copper binding sites (Vita et al., 2015; Vita et al., 2016). It has been proposed, in each case, that the structures demonstrate that the tube has one 'open' end and the other end is 'closed' by the presence of hydrophobic residues, therefore a likely mechanism of copper loading and unloading into the Csp proteins has been suggested via entry to the tube through solely this open end (Vita et al. 2015).

The Csps share some functional similarities with the metallothioneins. These are small, Cys-rich proteins that tightly coordinate metals, buffering excess metal to avoid toxicity. These are extensive and well-characterised in eukaryotes, but less so in bacteria. The protein SmtA (Seifipour

et al., 2017) which is present in the cyanobacterium *Synechococcus* PCC 7942, forms a metal cluster containing up to four zinc ions, which are bound to nine cysteine sulfurs along with two histidine nitrogens (Calvo et al., 2017). However, despite some similarities, a lot of structural studies were conducted and found that metallothioneins form their structure only in the presence of the metal ion, whereas Csps adopt the same structure as apo- proteins as copper-loaded (Emsley and Lindon, 2018)(Gülbakan et al., 2018). Notably, the structural fold of metallothionein is not related to that of the Csps.

The discovery and initial characterisation of the copper biochemistry of Csps was originally made in methanotrophic bacteria. These Gram-negative organisms tend to require a very large amount of copper in order to metabolise methane using the membrane-bound copper-dependent enzyme particulate methane monooxygenase, pMMO (Khadka et al., 2018). This enzyme is responsible for catalysing the conversion of methane to methanol in almost all of the methanotrophs (Bjorck et al., 2018), suggesting that pMMO's mononuclear copper active site (Oord et al., 2018) makes up a large proportion of total protein content in the cell. When there is a decline in the copper levels available, some methanotrophs have the additional capability to use the soluble methane monooxygenase, SMMO, which performs the same reaction but via an unrelated enzyme that consists of a dinuclear iron active site (Semrau and DiSpirito, 2019). Cucially, even in the organisms that possess both pMMO and sMMO, the 'switchover' between these copper-dependent and iron-dependent methane monooxygenases is regulated by copper (Banerjee et al., 2019).

The requirement to use a large number of copper ions per cell makes these organisms a focal point for recent studies to identify novel mechanisms of bacterial copper-handling. For example, copper acquisition by these oorganisms involves methanobactin (Mbn) (DiSpirito et al., 2016), which is a small copper-chelating molecule that can be considered as comparable to iron-binding siderophores, and for this reason it is termed as a chalkophore (Wang et al., 2017). Methanobactin is a modified peptide that is a crucial component of a highly specific copper-uptake system (Semrau and DiSpirito, 2019), secreted into the growth medium to acquire this metal ion under copper restricted conditions.

Although it is unsurprising that the novel family of Csps were initially discovered in methanotrophic bacteria, due to their very high cellular copper demand, Csps are not unique to these bacteria. Genes encoding Csp proteins are present in diverse (but not every) bacterial genomes, both in Gram negative and Gram positive bacteria (Vita et al., 2015). The conservation of the Cys residues in Csp family proteins strongly argues they will all bind significant numbers of Cu(I) ions (Straw et al., 2018), but whether they all share identical structures and/or binding/release mechanisms is unclear at this stage because so few Csp homologues have been characterised.

5.2. Result

5.2.1. Structure of the Csp3 copper storage protein from *Salmonella enterica sv.* Typhi

A preparation of *Salmonella* Csp3 protein was purified (see chapters 2 and 4), concentrated to 20 mg ml^{-1} protein concentration, and used in initial high throughput crystallisation trials. A single high-quality crystal was obtained, and was used for data collection at the Diamond synchrotron, UK. Once diffraction data was collected, the crystal structure was solved using molecular replacement methods by Dr Arnaud Baslé, Newcastle.

As anticipated, the Salmonella Csp3 complex forms a tetramer (Figure 5.1). The orientation of the four monomeric molecules of Csp3 in the tetramer was similar to what we have seen previously in the crystal structures of other members of this family (Vita et al., 2016; Vita et al., 2015; Baslé et al., 2017). These results agreed with a previous study by Vita et al. 2016, who revealed that multiple copper storage proteins are structurally tetrameric in nature.

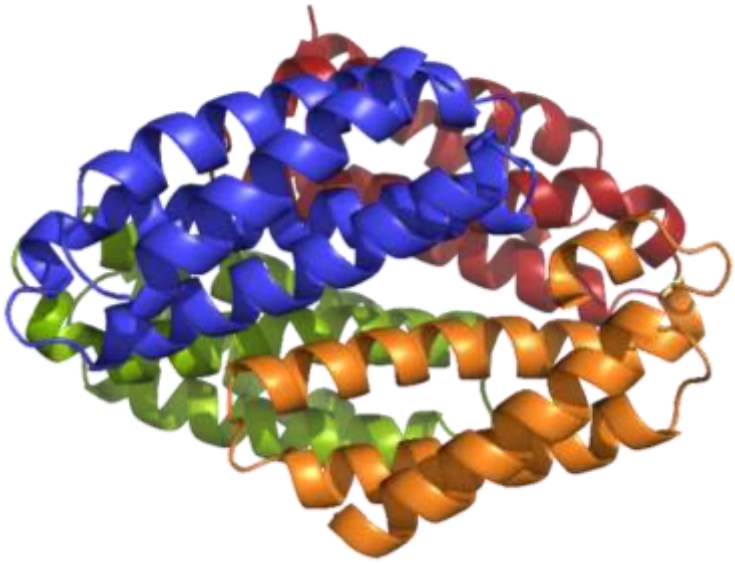

Figure 5.1. The crystal structure of *Salmonella* copper storage protein Csp3.

A side-view of the tetramer of the *Salmonella* Csp3 structure, shown in the ribbon representation, with each monomer coloured differently (blue, green, orange and red). The single copper ion that was detected in each monomer has been omitted for clarity. The orientation of the four molecules in the tetramer is similar to that observed previously in other Csp structures.

Vita and colleagues in 2016 demonstrated that the monomeric Csp3 is made up of a four-helix bundle, with 73% of the protein's residues found within alpha helical secondary structure. As shown in (Figure 5.2), showing just one monomer that was extracted from the previous tetramer, the *Salmonella* Csp3 protein also adopts the four helix bundle structure.

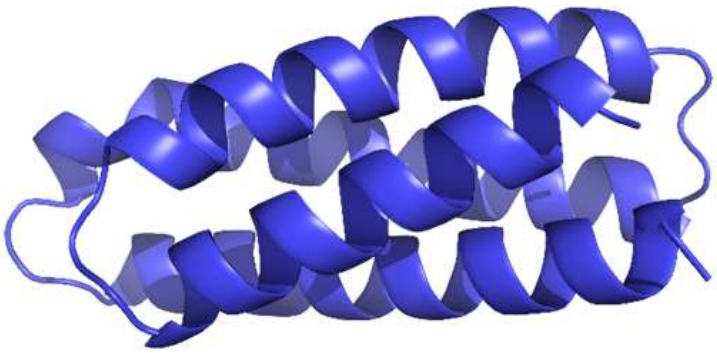

Figure 5.2. A Csp3 monomer extracted out of the tetramer structure.

This figure illustrates the side-view of a single monomer, shown in the ribbon representation, coloured blue. The four-helix bundle structure of the Csp monomer can be clearly seen. No copper is shown.

Previous structures have illustrated that all of the Cys residues in Csp family proteins point into the core of the helical bundle, where they are able to line the 'tube' formed by the bundle and coordinate the copper ions stored. As shown in (Figure 5.3), the structure of *Salmonella* Csp3 shows exactly the same arrangement as the previous structures, with the cysteine residues pointing into the core of the tube. All of the Cys residues are shown, pointing into the tube, and also shown are the Met/His residues that are localised at the end of the tube that has been hypothesised to be the opening for Cu(I) ions to enter/leave the tube are also illustrated in ball-and-stick representation. Interestingly, there are additional Met/His residues located at the opposite end of the tube, as shown in (Figure 5.3).

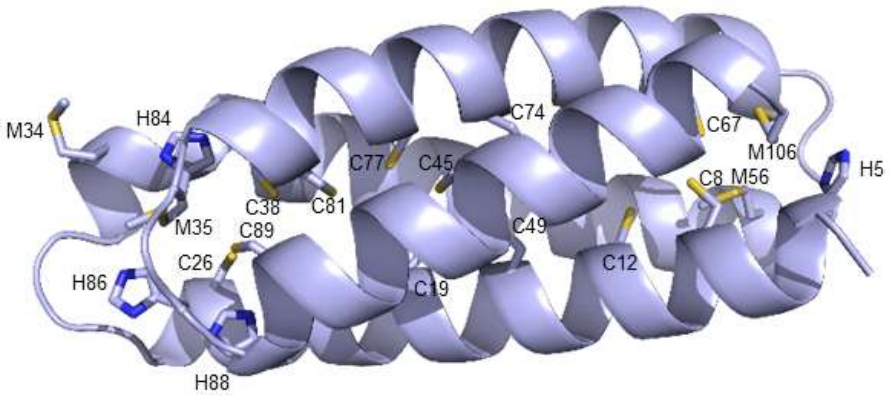

Figure 5.3. Complete monomer structure of *Salmonella* Csp3 structure.

Structure of the Csp3 monomer, with all of the putative copper binding ligands shown. This figure illustrates the side-view of the monomer, shown in the ribbon representation, with the backbone coloured light blue. The location of all of the Cys residues, and also the Met/His residues that may act as copper ligands at either end, are shown in ball-and-stick representation.

The observation that there are His/Met residues at both ends of the SeCsp3 tube is in contrast to the previously characterised Csp structures. In the first structure (Vita et al., 2015), one end of the tube possessed entirely hydrophobic residues and the copper-coordinating cysteine residues nearest this end of the tube were not solvent-accessible, thus it was presumed therefore that this end of the tube had to be closed. The other end of the tube had methionine residues that were solvent-accessible in the apo structure, were copper ligands in the fully copper-loaded structures, and even the cysteine residues closest to this end of the tubewere solvent-accessible. For these reasons, it was presumed that this end had to be the open end through which copper ions could enter. In a subsequent study that characterised the structure of the first Csp3 protein (Vita et al., 2016), a similar arrangement of metal ligands were observed, with one end open to solvent and the other end closed by hydrophobic residues, except that the ligands at the open end were histidine in this case, rather than Met residues in Csp1.

This concept is illustrated in figure 5.3; the end of the tube on the left hand side possesses histidine and methionine in positions similar to those observed in previous structures. This is

consistent with that end of the tube being the ‘open end’. However, the *Salmonella* Csp3 structure also has histidine and methionine residues at the other end of the tube, shown in figure 5.3 on the right hand side, and it is possible that the cysteine residues are also solvent-accessible at this end. This leads us to hypothesise that both ends of the *Salmonella* Csp3 tube could be open. The presence of histidine or methionine at the ends is also illustrated in figure 5.4, which shows a different view of this structure, illustrating how the Met/His residues at both ends appear to be pointing outwards and therefore may be available to interact with incoming Cu(I) ions. These results potentially contradict results from previous structures of the copper storage protein from *Methylosinus* and *Bacillus*, which determined that only few a Met/His residues are present at one end. However, the other end is considered closed.

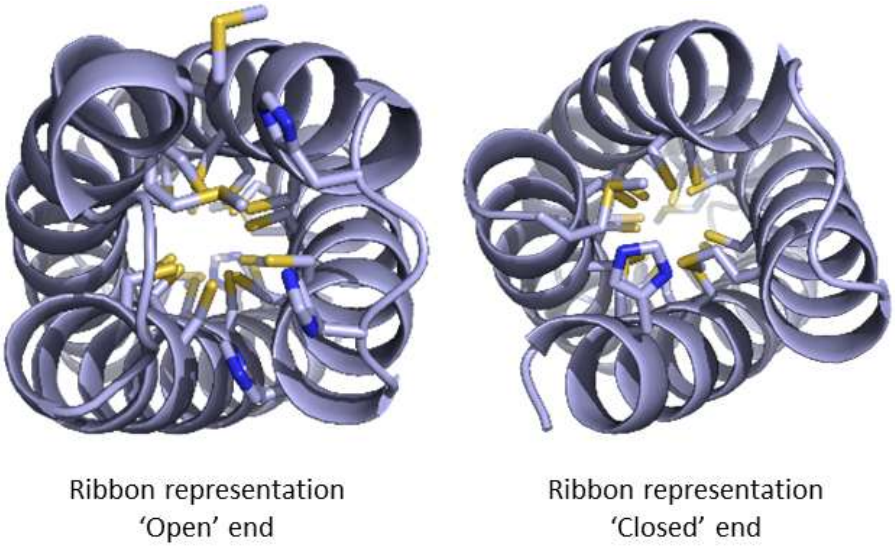

Figure 5.4. The view of ends of one monomer, showing the arrangements of potential ligands at both ends of the Csp3 tube.

The *Salmonella* Csp3 structure is shown in the ribbon representation, coloured blue, but here from an angle that is looking down the tube. The image on the left is fromthe ‘open’ end, based on previous literature and on the presence of conserved Met/His residues. The image on the right is the ‘closed’ end of the tube, but interestingly this end also contains some potential copper binding Met/His residues, raising the

possibility that both ends of this tube could actually be ‘open’. The Cys/Met/His residues are in ball-and-stick representation. The sulfur atoms of the Cys/Met residues are in yellow and nitrogen atoms of His residues are in dark blue.

To clarify this point, presented in (Figure 5.5) are equivalent views of the monomer as those shown in (Figure 5.4), but this time using a space-filling representation. From these images, it is clear that the nitrogen of the His residues at both ends of the tube are solvent exposed. This same surface representation viewed from each side of the tube shows that these potential copper-coordinating atoms could be exposed to solvent.

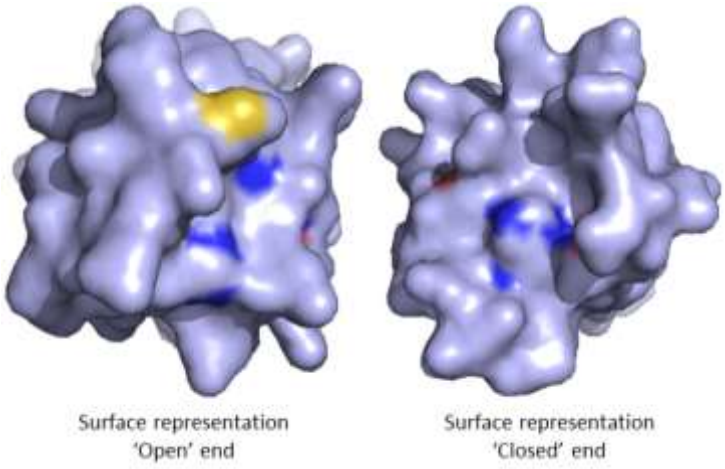

Figure 5.5. A surface representation of the Csp3 monomer from both ends.

The end-on views of the monomer, as shown in figure 5.4, are shown here in a surface representation. The general surface of the protein is coloured light blue. These figures illustrate the views from either end of the tube, with the end considered the ‘open’ end on the left and the ‘closed’ end on the right. The sulfur atoms of the Met residues are shown in yellow, the nitrogens of His residues in blue, and oxygen atoms in the backbone of these residues in red.

The overall structure this *Salmonella* Csp3 protein can now be compared with those of previously characterised Csp structures (Figure 5.6). This comparison demonstrates that the overall structure

is highly conserved, as is the observation that all cysteine residues in all of these proteins go down the centre of the tube. A previous comparison of Csp1/Csp3 from *M. trichosporium* structurally revealed that the Met/His residues are located exclusively at one end of the tube, with these residues being Met in Csp1 and His in Csp3 (Vita et al., 2016; Vita et al., 2015). That argues that both Csp1 and Csp3 *of M. trichosporium* have one closed end and one open end, as can be seen in (Figure 5.6). In the *Salmonella* Csp3 structure presented here, methionine and histidine residues seem to be present at both ends of the tube, suggesting both ends may be opened and accessible. Interestingly, this was also the case in the prior structure of Csp3 from *Bacillus subtilis*, yet this hypothesis was never suggested in the original paper (Vita et al., 2016). My data raise the hypothesis that this end may also be accessible to Cu(I). Indeed, this hypothesis would also be consistent with the data demonstrating that binding of silver ions did not prevent subsequent access of copper to the tube, potentially indicating binding of Ag(I) to only one end of the tube.

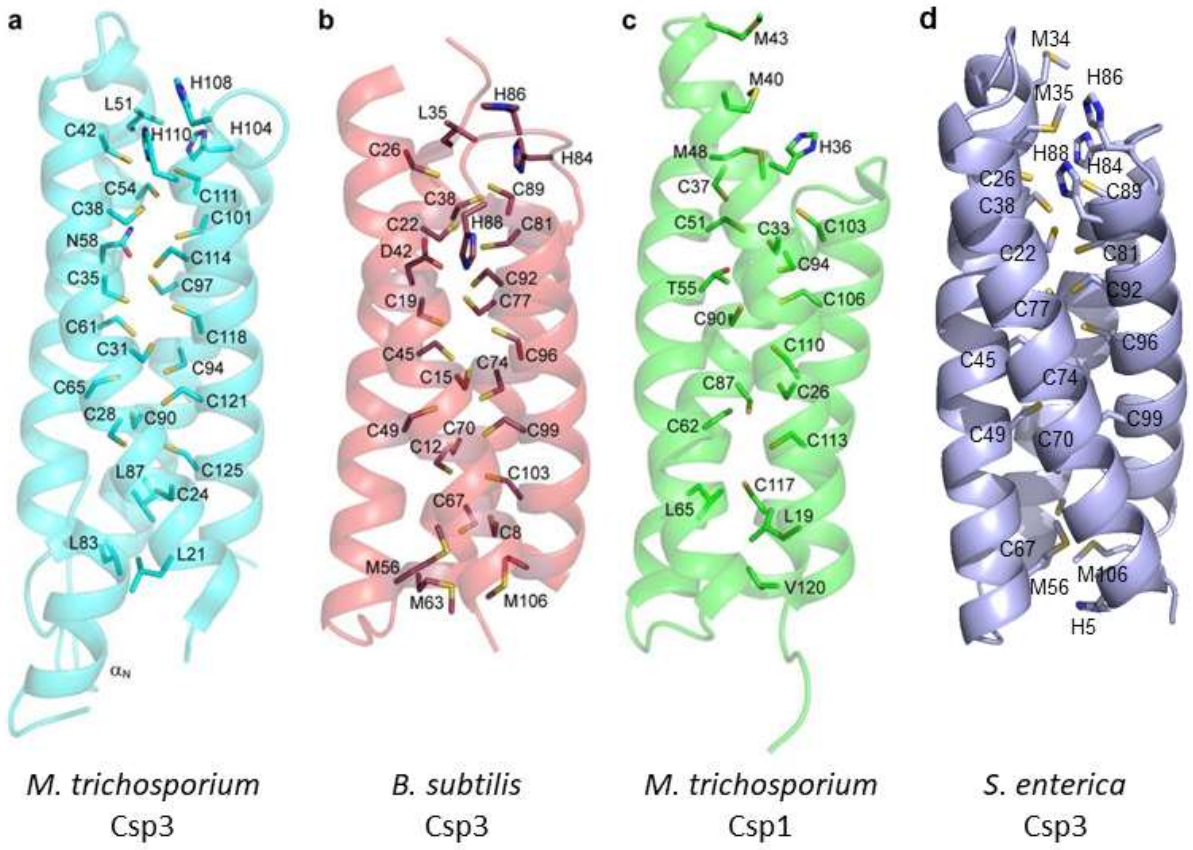

Figure 5.6. Comparison of Csp structures that have been characterised.

This figure illustrates the view of each of the monomers of known Csp structures. Each is shown in the ribbon representation, with the *Salmonella* Csp3 (from this work) coloured light blue. This figure was adapted from Vita et al., 2016 by addition of the new data for *Salmonella* Csp3, illustrating similarity of Csp structures.

Despite having expressed this protein inside *E. coli* cells cultured in a minimal medium, with no added copper, nonetheless we detected one metal ion in each monomer of the crystal structure. Consistent with this observation, subsequent elemental analysis of the Csp3 preparation by ICP-MS also determined the presence of ~ 1 mole equivalent of copper (data not shown). This copper must therefore have co-purified with the protein after acquisition within the *E. coli* expression host, as no copper was added to the protein during or after purification.

The single metal ion that was observed in the crystal structure of *Salmonella* Csp3 was modelled as a copper ion. The copper binding site, shown in (Figure 5.7), shows the copper coordinating to Cys22, Cys26, Cys89 and His88. This is significant as it shows binding near to the entrance to the tube (Figure 5.7).

Figure 5.7. Binding of a single copper ion to *Salmonella* Csp3.

This figure illustrates the presence of a single metal ion, modelled as a copper atom, in the crystal structure of SeCsp3 (shown as a ribbon in green). This copper is bound close to one end of the monomer tube (left panel) and is localised within the tube formed by the four-helix bundle (central panel). The metal ion is coordinated by three Cys and one His residue (right panel), which likely represents the copper site nearest this entrance to the tube.

A previous study by Baslé and co-workers solved the structure of copper protein *Mt*Csp3 with two coppers inside the tube (Baslé et al., 2017). They showed that, after adding two copper ions, it partially occupied four sites in the centre of the tube (but each one is not fully occupied in the crystal - giving an average of copper moving around between four sites). The crucial point here is that the location of the binding sites for copper when the protein only contains low levels of copper ions is different between Csp3 from *Salmonella enterica* sv. Typhi (presented here) and the Csp3 protein from *M. trichosporium.* Data presented here demonstrate that adding a small amount of copper to the Csp3 from *Salmonella enterica* sv. Typhi resulted that in copper remaining at the opening of the tube. On the other hand, when adding a small amount of copper to *Mt*Csp3, it moved further into the tube and seemed to be localised at its centre(Baslé et al., 2017).

5.2.2. Model structure of the Csp1 from *Neisseria gonorrhoeae*

Unfortunately, despite efforts to crystallise the *N. gonorrhoeae* Csp1 protein, in both apo- and Cu(I)-loaded form, no diffraction quality crystals were obtained. This precluded structural determination for this protein within the timescale of this study.

In order to glean some insight into the probable structure of the gonococcal Csp1 protein, this structure was modelled. Instead of modelling the structure on that of the *Salmonella* Csp3 determined here, it was more appropriate to use the previously determined structure of Csp1 from *M. trichosporium* OB3b (Vita et al., 2015). This is closer in homology, but is also more likely to

be a functional homologue, as both of these proteins contain a putative Tat recognition sequence and thus are expected to be exported into the periplasm of their respective cells.

The structure of *N. gonorrhoeae* Csp1 was modelled using SWISS-model, using its default settings. The structure of *M. trichosporium* OB3b Csp1 was identified by SWISS as the most suitable structural model, as anticipated. As expected, the prediction demonstrated a likely tetramer, composed of monomers that form four-helix bundle structures (Figure 5.8).

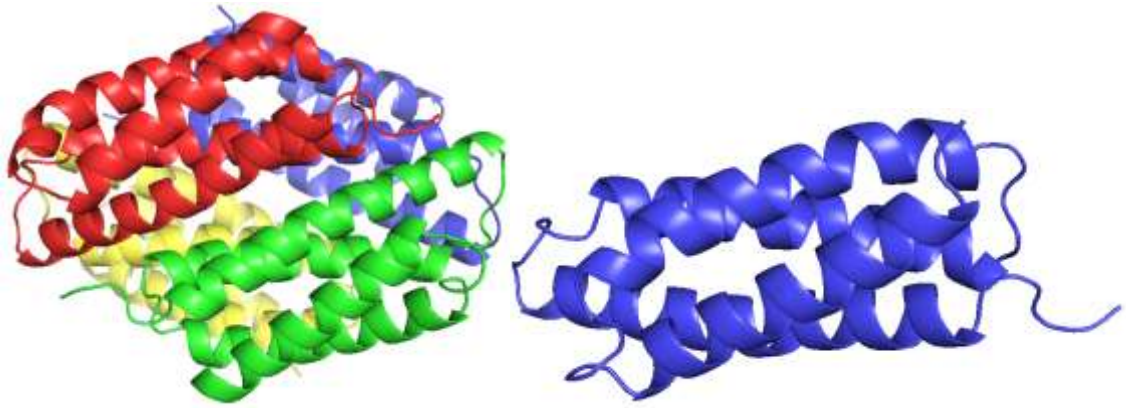

Figure 5.8. Modelled structure of *N. gonorrhoeae* Csp1, based on MtCsp1.

The sequence of *N. gonorrhoeae* Csp1, lacking its first 24 amino acids that are predicted (SignalP) to encode its Tat-targeting signal sequence, was used to model a likely structure using SWISS Model (https://swissmodel.expasy.org/). The SWISS Model search tool identified the *M. trichosporium* OB3b Csp1 structure (PDB ID = 5FJD; Vita *et al.*, 2015) as the best possible template, and this was used to generate the model using the default parameters in SWISS. The resulting model was visualised using Pymol.

When the conserved residues that are predicted to bind to the copper ions within this Csp structure were localised (Figure 5.9), a similar arrangement was observed as seen in the *Salmonella* Csp3 and in prior Csp structures (Vita *et al.*, 2015; Vita *et al.*, 2016). All of the Cys

residues are located on the interior of the tube formed by the four-helix bundle, whereas the Met/His residues localise to one end of the tube, hypothesised to be the 'open' end of the tube.

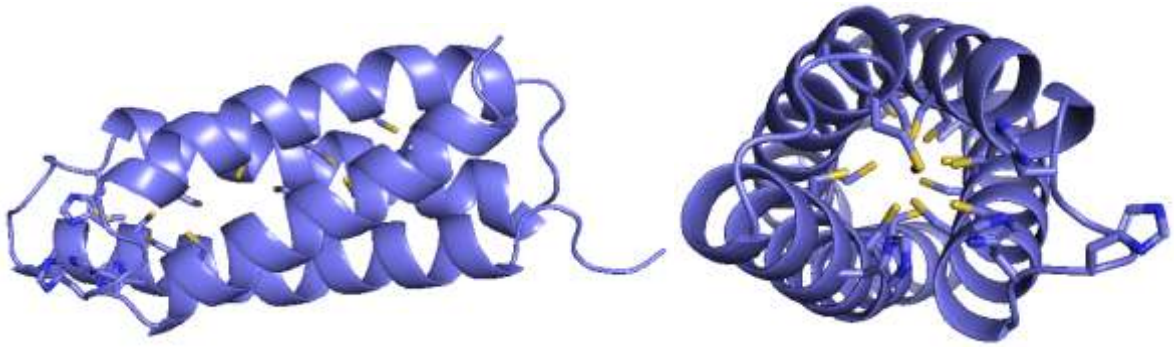

Figure 5.9. Location of putative metal ligands within the monomer of the model structure of *N. gonorrhoeae* Csp1.

Localisation of the Cys/Met/His residues within a monomer of the modelled structure of *N. gonorrhoeae* Csp1 demonstrated their likely localisation in conserved positions within this protein. The Cys residues are all localised within the tube formed by the four-helix bundle, as shown on the left in the side-on view of a monomer of the modelled structure, whereas the Met/His localise to the opening of the tube, shown in the end-on view of the monomer, shown on the right.

5.3. Discussion.

In this chapter, I have described the structure of Csp3 from *Salmonella* as determined by X-ray crystallography, as well as a model structure of Csp1 from *Neisseria gonorrhoeae*. Consistent with the previous studies that have characterised structures of members of this family (Vita et al., 2015; Vita et al., 2016; Straw et al., 2018), the determined structure of the cytosolic Csp3 protein from *Salmonella* exhibits the conserved four-helix bundle for the monomer (Figure 5.2). Four of these monomers come together to form the tetrameric complex (Figure 5.1), again as expected from prior studies.

To gain an understanding of the likely Cu(I) coordination by *Salmonella* Csp3, we localised the spatial positions of each of the residues hypothesised to bind metal ions, based on prior structural studies. We found that all of the Cys residues in the *Salmonella* Csp3 sequence are located within the interior of the tube formed by the four-helix bundle (Figure 5.3). This is consistent with the fully loaded structure being analogous to those studied previously (Vita et al., 2015; Vita et al., 2016), in which the tube fills with a large number of Cu(I) ions.

Conversely, there are several other residues that are capable of coordinating Cu(I) ions that are localised at the end of the tube (Figure 5.3). In *M. trichosporium* OB3b Csp1, these residues were exclusively Met (Vita et al., 2015) whereas they were exclusively His residues in *M. trichosporium* OB3b Csp3 (Vita et al., 2016), and it was postulated that this may reflect a key difference between periplasmic and cytosolic Csp homologues, as these two proteins exhibited substantially different off-rates for dissociation of Cu(I) (Vita et al., 2015; Vita et al., 2016). However, the residues found in the *Salmonella* protein at the 'open' end, i.e. the end of the tube that is always exposed to solvent in all characterised Csp proteins to date, were a mixture of Met and His residues (Figure 5.3).

Furthermore, we identified a number of these potential Cu(I)-coordinating Met/His residues at both ends of the tube in *Salmonella* Csp3 (Figures 5.3, 5.4). This is in contrast to the Csp proteins studied from *M. trichosporium* OB3b, which exhibit hydrophobic residues at the opposite end, which was hypothesised to be the 'closed' end of the tube (Figure 5.6). Interestingly, a similar arrangement was observed in *B. subtilis* Csp3, with hydrophilic residues at both ends, although this was not commented on in the publication (Vita et al., 2016). Nonetheless, such an arrangement, visualised in (Figure 5.4), raises the possibility that both ends of the Csp3 tube may be solvent-exposed and 'open' in the *Salmonella* Csp3, and also perhaps the *B. subtilis* Csp3. This interesting possibility may indicate that Cu(I) ions may be able to enter and leave the *Salmonella* Csp3 tube through either end.

Future work should aim to test the hypothesis that both ends of the tube of the *Salmonella* Csp3 tube may be open for entry/exit of Cu(I) ions. This hypothesis could be tested using an *in vitro* approach using site-directed mutagenesis. Mutated recombinant forms of this protein could be synthesised, in which: (i) the classical 'open' end of the tube has been mutated, with all Met/His residues in this region mutated to non-coordinating alanine (Ala); (ii) the opposite, 'closed' end of the tube has been mutated, with all Met/His residues int his region mutated to Ala; and (iii) all Met/His residues at both ends of the tube have been mutated to Ala. Production of these three mutated Csp3 forms, as well as the wild type protein, would enable *in vitro* experiments to test for Cu(I) binding to each form. If only one end of the tube is open, then the variants (i) and (iii) would fail to load with copper, whereas variant (ii) would load with copper exactly the same as wild type. On the other hand, if both ends are open we should observe that only variant (iii) fails to load with copper. Furthermore, we might expect to observe kinetic differences in copper dissociation from variants (i) and (ii). Crucially, variant (iii) would act as an important negative control in these experiments. Such experiments are currently planned by the Waldron lab.

Despite expressing the *Salmonella* Csp3 inside *E. coli* cells under metal-limited conditions in a minimal medium, we nonetheless observed a single metal ion within the structure of Csp3 (Figure 5.7). This was consistent with ICP-MS data on the preparation used for crystallisation which suggested approximately one mole equivalent of copper was present (data not shown). Nonetheless, this single copper ion's location was very interesting. A previous study that solved structures of partially loaded Csps suggested that, when loaded with two equivalents of Cu(I), the *M. trichosporium* OB3b Csp3 showed the presence of the two metal ions at the centre of the tube occupying four distinct sites, suggesting that the copper is able to occupy these sites interchangeably. In our case, however, we identified a single copper site occupied, which was localised at one end of the tube, specifically close to the 'open' end of the tube. This suggests that copper-loading is different between these two proteins, and perhaps shows significant diversity between the Csp family. Future studies should aim to test the mechanism of loading, perhaps by using similar structural approaches to that used previously (Basle et al., 2017), with diverse members of this novel family. The observation that a single copper ion locaises near the entrance

to the tube in this structure also raises questions about how the rest of the tube gets filled up, as it must require displacement of this first copper ion in order to add more coppers to the tube.

Finally, in the absence of successful crystallisation of *the N.* gonorrhoeae Csp1, we generated a structural model of this protein, based on the predicted mature form after cleavage of its pre-sequence, using SWISS Model. This software predicted a similar overall structure of this protein to those of Salmonella Csp3, determined here, and to those determined in prior studies (Vita et al., 2015; Vita et al., 2016; Straw et al., 2018). It also formed a four-helix bundle monomer, which formed tetramers, and which contained all of its Cys residues within the core of the tube. It only possessed Met/His residues at one end of the tube. Future studies should aim to determine the real structure of this protein and compare it with this model, to determine how effective such modelling is for the Csp proteins

Chapter 6. General Discussion

6.1. Over-expression, purification and quantification of *N. gonorrhoeae* Csp1 Protein

The simple and efficient prokaryotic system, i.e. *E. coli* was utilized for large scale production and expression of the recombinant form of the Csp1 protein from *Neisseria gonorrhoea*. The expression and purification results were in agreement with those of Vita et al. 2016, Tarasava et al. 2018 and Straw et al. 2017 as they also utilized *E. coli* for expression of their targeted recombinant proteins for metal binding studies. The *N. gonorrhoeae* Csp1 protein (13.6 kDa) was purified initially using anion exchange chromatography, and the purification results were determined by running the resulting protein samples on SDS-PAGE. Fractions for SDS-PAGE analysis were selected by identifying the most intense A280nm peak to contain the Csp1 protein, as this was highly overexpressed in cell lysates, and by comparison to published data (Vita et al., 2015; Vita et al., 2016). The SDS-PAGE results showed a partially purified band of Csp1 protein of ~13 kDa size, based on its migration relative to molecular weight standards of known mass, but with some other non-targeted protein bands also present in the gels. These impurities were removed by a second dimension of separation using size exclusion chromatography. Again, the likely Csp1 peak was identified from the most intense peak in the A280nm trace. After that, the purification results were again determined on SDS- PAGE.

Overall, by using the anion exchange and size exclusion chromatography, the yield of purified Csp1 was found to be quite low, despite the protein having been well expressed in *E. coli*. Furthermore, the protein concentration was observed to decline over time when the purified protein sample was left in the refrigerator over the course of several days, suggesting the *N. gonorrhoeae* Csp1 protein was relatively unstable. Notably, this problem was far less pronounced for the *S. enterica* Csp3 protein, which was purified in higher yields and was found to be a little more stable at refrigerated temperatures. This instability of Csp1 was not observed in previous studies of Csp proteins (Vita et al., 2015; Vita et al., 2016). This led to a shortage of viable Csp1 protein, which caused the main problem during this part of my study. To enhance the study of such unstable proteins, in the future the conditions will need to be optimized to obtain higher yield of recombinant purified protein and to maximise its stability over periods of time in the fridge. For

example, adjusting the pH or using high salt concentrations in order to ensure that the sample remains stable during storage for use in subsequent experiments. By achieving this, improvements may also be observed in subsequent protein quantification using existing techniques through improving the signal-noise in quantitative analyses, which would be helpful to get more precise data on metal binding stoichiometry.

Unfortunately, a major hindrance to the subsequent study of the metal-binding properties of the *N. gonorrhoeae* Csp1 protein was in the difficulty of accurately measuring the protein concentration of samples of purified recombinant protein. Multiple methods were employed for quantitation, but each method employed had drawbacks. The ideal method for quantification would have been the routine use of quantitative amino acid analysis. This is considered the gold standard, because it enables us to simultaneously measure the abundance of a number (~15) different amino acids, giving a good signal:noise ratio on the measurement. However, we did not possess the relevant instrumentation for such routine analysis in the department. As a result, we contracted this analysis to an external commercial company. Therefore, using this method routinely would have been prohibitively expensive, and would have been very time-consuming as we would have had to ship samples daily or weekly to the company and await the results before proceeding. This would in turn have made even worse the stability problem observed with Csp1. An alternative would have been to use the DTNB assay routinely, as was used in prior studies (Vita et al., 2015; Vita et al., 2016). However, while this had been our planned strategy, we had systematic issues with our anaerobic glovebox during this study, which prevented this anaerobic chamber being used every day, as would have been needed to use DTNB as the standard method for protein quantification.

Instead, we decided to use a more simple protein assay, using either A280nm alone or through the standardised Bradford assay, and then to amend the resulting data using correction factors that were obtained by comparison of these methods with the more accurate quantitative amino acid analysis (Table 3.1.3B). The absorbance of a protein at 280nm is predominantly a function of the number of tryptophan residues present in the protein, with more minor contributions to the absorbance at this wavelength being made by other aromatic residues, phenylalanine and tyrosine. Unfortunately, the Csp1 protein does not contain any Trp residues, and therefore we concluded

that the use of A280nm corrected by the amino acid analysis data was likely to be problematic. Instead, we employed the Bradford assay routinely. This assay exploits the binding of a colorimetric dye to positively charged residues – predominantly arginine residues, with a further contribution from lysine and histidine residues – and the concentration of an unknown protein sample is determined by comparison to identically treated samples of a BSA standard solution. This approach was not guaranteed to be without error, but was our best option at the time given the cost and simplicity. A correction factor was applied based on comparative analysis by Bradford and amino acid analysis of an identical protein sample (Table 3.1.3B).

6.2. Copper content in the purified protein and its removal

We found variable amounts of copper in the Csps throughout this study. In initial experiments, when we started by expressing *N. gonorrhoeae* Csp1 inside *E. coli* cells that were cultured in rich LB medium, the amount of copper detected in the purified protein by ICP-MS analysis was ~9.5 µM in a 3.8 µM sample of Csp1 as determined by ICP-MS, which equates to approximately 2.5 mole equivalents. This suggested that the copper content of LB medium must be high enough to result in significant copper accumulation inside *E. coli* cells, resulting in its sequestration inside the overexpressed heterologous protein in the cytosol. In an effort to remove this bound copper, we incubated a sample of Csp1 with an excess (0.5 mM) of the high affinity Cu(I) chelator, bathocuproine disulfonate (BCS), but we detected no significant decline in the Csp1 copper content after several days incubation and subsequent removal of the BCS.

Therefore, we decided to use M9 as a minimal growth medium to reduce the amount of copper available to the *E. coli* cells during culture, thereby reducing cellular copper content and therefore, hopefully, reducing the number of copper ions that would be incorporated into the Csp1 protein during expression inside *E. coli* cells. However, despite this approach, we still detected some copper, 1.5 µM of copper in a sample containing 0.36 µM of Csp1 as determined by ICP-MS. Significantly, this observation indicated that, even when the cells are grown in medium that contained extremely low levels of contaminating copper, some of the trace amounts of copper that are inevitably present as low-level contaminants in the media components nonetheless gets into

the cells, and the affinity of the Csp proteins for copper must be high enough that it can find these few atoms of copper in the *E. coli* cytosol.

We were unable to remove copper from Csp, however I moved to using M9 as growth medium in an effort to prevent it from getting any copper during expression. Consequently, that led to some limited reduction of the amount of copper, but it was still not perfect. Previous studies have looked at copper removal from Csps (Vita et al., 2016; Vita et al., 2015). They showed that when Csp1 or Csp3 was exposed to high affinity copper chelators such as BCS, that copper can be removed but only very slowly. Furthermore, they showed that *Mt* Csp1 released copper more quickly than *Mt*Csp3, in which only ~20% of Cu(I) could be removed after 85 h exposure to excess BCS. We therefore decided that a sensible strategy was to try to prevent copper getting into the expressed protein in the first place rather than trying to extract copper out of it after expression.

6.3. Csp1 copper binding properties

The Csp1 protein from *N. gonorrhoeae* is constituted of ~30% cysteine residues. The presence of cysteine residues facilitates these proteins to bind with a large number of copper ions. When the Csp proteins were first characterised (Vita et al., 2015), this feature was interpreted as indicating a probable role of these proteins, not only in metal storage for later use, but also potentially in defence mechanism and detoxification of toxic copper. Similar results were also reported by Tarasava and colleagues in 2016 about metallothionein (MT) from *Triticum astevum*. The MT protein showed association with a large diversity of metal ions.

The data shown in the thesis demonstrates that numerous copper ions did bind to Csp1 but we were unable to determine the precise stoichiometry. As a result of the difficulties already discussed of low yield of protein after being purified, and subsequent protein precipitation/instability, as well as great difficulties experienced in accurately quantifying this protein, created a discrepancy between experiments for determination of copper binding stoichiometry and the results that were anticipated based on prior studies of Csp1 from *Methylosinus trichosporium* OB3b (Vita et al.,

2015). However, we did nonetheless see copper binding to sulfur in our UV/visible spectroscopy experiments due to detection of ligand-to-metal charge transfer absorptions in the wavelength range of 250-350 nm (Vita et al., 2015; Vita et al., 2016). Binding of copper to Csp1 was observed through multiple additions of copper by UV/visible spectroscopy, and by subsequent separation of unbound copper through size exclusion and ICP-MS. As discussed, the instability of Csp1 was main issue in this study, however a suggestion to avoid this issue in the future is to optimise storage conditions, aiming to stabilizing the protein through changing the pH or the salt concentration for example. Better protein stability would enable us to use larger amounts of protein for the copper titration, improving the signal-no-noise ratio. As a result of this increased availability of the recombinant protein, experiments would be able to be performed using high concentration of protein. Csp1 would be titrated with various copper concentrations under different conditions/parameters that might be very helpful for better determination of copper-Csp1 stoichiometry.

6.4. Csp1 silver and zinc binding

The *N. gonorrhoeae* Csp1 protein also showed some limited evidence of binding to other metal ions, particularly silver, in addition to copper in this *in vitro* study. In this experiment we investigated the effect of adding silver, zinc, and copper, individually or in combination through adding silver or zinc followed by copper. The positive control for this experiment was the addition of was copper alone, with the expected observation in the ICP-MS data that copper should bind to Csp1 protein in large quantities. Unfortunately, that did not happen, with the result that the data for binding of the other metals are impossible to draw firm conclusions. The Csp1 protein did nonetheless show some limited evidence of association with the silver ions in this experiment, but the data must be interpreted with caution due to the positive control in the experiment. In conclusion, the data did not show conclusively whether the metals did bind or not.

The reasons for this disappointing outcome are many and have already been outlined, such as the protein's unstable nature and the relatively low yield of protein concentration that limited the amount of protein that could be used in these experiments, and the difficulties in the quantitative

protein measurement. Therefore, the suggested solutions to improve the experimental design will be for the overexpressed protein to be produced in larger quantities via using further optimized conditions for expression and improved stability. Improvements to the methods for measurement of the protein concentration, improving accuracy by using different measurement techniques or increased replication, is essential. After that, more experimental work would be performed not only with various concentrations of zinc and silver but also with a diversity of other transition metal ions. Such a study would be able to properly define the actual stoichiometry and ability of the protein to bind metals other than copper.

6.5. Over-expression and Purification of Csp3 Protein

The *Salmonella enterica* Csp3 recombinant protein was also cloned and expressed in the *E. coli* prokaryotic system, just like the gonorrhoeal Csp1 protein. In the case of Csp3, the experimental study found that Csp3 recombinant protein was efficiently overexpressed in higher yield as compared to Csp1 under the same conditions. The *Salmonella* Csp3 protein was also purified via anion exchange and size exclusion chromatography using the same approaches and conditions as described for the *N. gonorrhoeae* Csp1, and the purified band was visualized on SDS-PAGE as being highly pure after the chromatographic separation steps.

Vita and his research group in 2016 determined that the overexpressed Csp3s accumulate more copper than the only characterised Csp1. One of the challenging tasks, as with *Neisseria* Csp1, was to determine the exact concentration of the target protein after purification. The strategy followed to tackle this problem was to use results from the Bradford assay to calculate the protein concentration with a correction factor introduced through the quantitative amino acid analysis, in the same way described for the quantitation of *Ng*Csp1. The interpretation of final outcomes, however, were again not encouraging, suggesting this quantitation introduced an error into the result for binding stoichiometry of copper with protein.

As with *Ng*Csp1, we routinely detected the presence of trace quantities of copper in preparations, despite expressing this protein inside cells cultured in M9 minimal medium. For example, one preparation contained 13.42 µM copper in 6.65 µM of *Se*Csp3, as determined by ICP-MS and Bradford with amino acid analysis correction. This approximates to one mole equivalent, although the stoichiometric measurements suggest that the protein concentration measured here may be in error by as much as 2-fold. The presence of one equivalent of copper is clearly illustrated in the Csp3 crystal structure, in which a single copper atom was detected (Figure 5.9).

6.6. Csp3 Copper binding properties

The UV/visible spectroscopy results showed a remarkable increase of absorbance in the 250-350 nm wavelength range when *Salmonella* Csp3 was incubated in the presence of Cu(I) ions as compared to negative control with no Cu(I) added. The spectral feature kept increasing on the UV/visible trace until 120 equivalents of copper had been added, but did not increase further after a further addition of copper. The implication was that the protein was fully occupied after addition of 120 equivalents, indicating the complete coordination of metal ions with recombinant Csp3. Meghana et al., 2015 and Vita et al., 2015 obtained results that are found to be in agreement with our data, demonstrating a high absorbance value due to characteristic ligand-to-metal charge transfer transition from Cys to Cu(I). However, that does not mean that the copper binding capacity of *Se*Csp3 is 120 Cu(I) ions per monomer, which would be significantly higher than the stoichiometry observed with previously characterised Csps (Vita et al., 2016). Within the parameters of our experiment, the stoichiometry is something higher than 48 and less than 120 coppers, but obvious error within our protein quantitation data would suggest a reduction in this number by at least 2-fold. In addition, size exclusion chromatography results showed some consistency with the UV/visible data in terms of the absorbance of the eluted protein increasing with increasing amounts of copper in the incubation. Moreover, by using ICP-MS to determine metal content after this fractionation, it was found out that there was no more copper found in the peak fractions between after incubation with 120 mole equivalents Cu(I) as there was after incubation with 48 equivalents, suggesting that the 48 equivalents incubation was approaching saturation.

In conclusion, measuring the stoichiometry of Cu(I) binding to the *Salmonella* Csp3 was very challenging, as was the case with the *Neisseria* Csp1. Measuring the abundance of apo protein was difficult for technical reasons associated with the various methods of measuring protein concentration. Although yield and stability of Csp3 was improved relative to Csp1, these experiments would nonetheless have been improved with more protein material available. Even after growing the cells expressing the Csp3 protein in M9 medium, the resulting purified recombinant protein was contaminated with low levels of copper, and copper ions would have further interfered with protein quantitation using A280nm. In future studies, optimisation of conditions to make lots more of the Csp3 protein using a better optimised protocol for expression and for stable storage, and thus using much more protein in the experiments, might solve the issue and minimize the error in protein measurements and therefore in stoichiometry calculations.

6.7. Csp3 copper/silver/zinc binding

As with *Ng*Csp1, I tested for evidence of binding of Ag(I) or Zn(II) ions to the *Se*Csp3 protein. The result from this experiment was that all metal-treated samples eluted in the same region of the chromatogram, demonstrating that incubation with any of these three ions did not lead to a significant change in the quaternary structure of Csp3. We observed some copper bound to Csp3, and also some silver, suggesting the latter is capable of binding to Csp3. However, we were not able to show that zinc as free form associated with Csp3. After sequential incubation of Csp3 in the presence of first zinc and then copper, followed by size exclusion and metal analysis, the results indicated that copper binding was observed to Csp3 after exposure to zinc, which showed that the presence of zinc did not prevent copper from filling up the protein tube. In the equivalent experiment with silver, we detected substantial copper but also detected some silver ions associated with the protein, which might signify that those silver ions bind around the tube entrance but not in a way that blocks access of copper ions to the tube.

In conclusion, for improvement of these data, overexpressed protein would need to be produced in much larger quantities via using optimized expression and purification conditions, as previously described. This would enable us to measure the protein concentration more accurately by using

different measurement techniques, and then use higher concentrations of Csp3 protein to repeat these experiments. After that, more experimental work would be performed, not only with various concentrations of zinc and silver to validate whether these bind to Csp3, but also with a diversity of other transition metal ions. Such a study would properly define the actual stoichiometry and wider metal binding properties of the Csps.

6.8. The structure and function of Csps in pathogenic bacteria

Copper is vital metal for aerobic organisms, which is involved in redox enzymatic reactions. The Imlay group in 2009 (Macomber and Imlay, 2009) investigated the emerging mechanisms of cellular toxicity of copper, in which copper damages Fe-S clusters. This mechanism not only diminished the reactivity of the mis-metallated protein but also discharges iron that can produce ROS. Due to this toxicity mechanism, free copper metallic ions were found to be restricted in prokaryotic and as well as in eukaryotic system (Changela et al., 2003). Copper binding proteins specifically regulate copper homeostasis to prevent copper toxicity while ensuring copper supply to enzymes that need it. Both prokaryotes and eukaryotes have evolved P-type ATPase copper exporting proteins and cytosolic copper metallochaperones in response to excess of copper (Festa and Thiele, 2011).

Dennison and colleagues identified the Csps as a novel family of copper storage proteins that are widely distributed in bacterial genomes (Vita et al., 2015; Vita et al., 2016). Most Csps in bacteria are anticipated to be cytosolic (Csp3), whereas only a few Csp homologues possess a signal peptide for translocation out of the cytoplasm (Csp1/2).

Many other bacteria also contain a Csp3 protein which are predicted to have similar type of structure. These proteins are presumed to have the same kind of copper binding capabilities. A goal of the Waldron lab is to determine what the functions of these Csp proteins are in pathogenic microbes. Copper is important in immune function, for example it is used by macrophages to kill bacteria. Our hypothesis is that Csps absorb copper and prevent toxicity during conditions of excess copper, leading to safe accumulation of copper inside Csp stores at the host-pathogen

interface. But this could be purely through sequestering excess copper to prevent toxicity, or as a storage protein, where both binding of copper under high copper conditions and subsequent release of copper under low copper conditions is crucial for Csp function. My goal was to demonstrate whether the Csp proteins from *Salmonella* and *Neisseria* behave in a similar way to the ones that have been previously characterised from *M. trichosporium* OB3b and *B. subtilis*. My contribution to this work is that my data has demonstrated the *Salmonella* Csp3 protein has a similar structure to the previously characterised proteins, and that both Csps from *Salmonella* and *Neisseria* did bind copper in high levels. Interestingly, I also provided preliminary evidence that Csp3 did bind to silver, and possibly also zinc ions, but that this did not necessarily interfere with copper binding.

Csp3 from *Salmonella enterica* sv. Typhi was found to be tetrameric, consisting of four monomers that folds to adopt a four-helix bundle structure. Each monomer was found to contain one copper atom, which must have co-purified with the protein from *E. coli* during expression. These results agreed with (Vita et al., 2016), which also revealed that these copper binding proteins are structurally tetrameric in nature. In that study, the crystal structure of both apo- and copper-loaded Csp3 were both found to adopt the same structure tetramer.

Our crystal structure showed that that Cys26, Cys 89 and His88 were coordinated to bind with the single copper ion. This copper ion was coordinated near the putative site of entrance to the Csp3 monomer. However, experimental work of Basle and colleagues in 2017 contradicted our results and suggested that *Mt*Csp3, when loaded with just two equivalents of copper, exhibited four binding sites which are present at the core of the monomer tube. The copper was proposed to move around between these four sites and did not fully occupy the one site. This may represent an important difference between the coordination of low equivalents of copper between these two proteins, and perhaps among the wider Csp family. Furthermore, this may indicate differences between Csps in the mechanism by which they fill up with copper, which should be investigated more fully in future studies.

The monomer structure extracted from the crystal structure of the *Salmonella* Csp3 tetramer showed a four-helix bundle that formed a tube-like molecule, with cysteine residues lining the inside. These results are also found agree with previous results in *M. trichosporium* OB3b and *B. subtilis*, whose Csp proteins possess many Cys residues pointing into the core of the tube formed within the monomer. So, this property indicated the potential capability to accommodate approximately up to 80 Cu ions per tetramer.

The surface representation of the Csp3 monomer indicated the possibility that both ends of the Csp3 tube may be open. This is distinct from the proteins from *M. trichosporium* OB3b, in which one side is considered as an open end and the other side as a closed one**.** The crystal structure that contained a single copper ion in this study also proved that this sole copper interacted with cysteine residues of the putative open end. Further investigation will be needed to study the mechanism by which copper gets in and out of the tube.

If I had had more time in the laboratory, we could have tested that this hypothesis by making site-directed mutant variants of the *Salmonella* Csp3 protein and comparing its copper-binding properties to those of the wild type protein. I would have done this by making a variant protein in which all of the methionines and histidines in the putative open end had been mutated to amino acids that will not bind copper (e.g. alanine), another mutant in which all the methionine and histidine residues in the putative closed end had been converted to alanine, and a third mutant in which these residues at both ends had been mutated to alanine. I would then express them all in BL21, purify them and quantify them, then test their relative ability to bind copper. We would incubate them with a fixed amount of copper, based on their concentration (mole equivalents), and then we would resolve each by size exclusion chromatography. Finally, the resulting fractions would be analysed by ICP-MS for copper and for protein by Bradford assay (or even better, an improved assay for protein quantitation). The expectation would be that the wild type will bind copper, as expected, and would thus act as a positive control. If the tube is only open at one end, then the mutant in which we have mutated to copper-binding residues at this end should not bind copper at all, and the one in which all the copper-binding residues at the closed end were mutated would still bind copper. The one with both ends deleted will not bind any copper, and thus would act as a negative control. On the other hand, if both ends are open, then the one with mutations at

the open end will still bind copper because the copper ions will be able to enter through the closed end's opening, and the one with the deletion on the closed end will still bind copper because the copper ions will be able to enter through the open end's opening. Only the double mutant, with both ends mutated, will bind no copper.

In terms of comparison, the previous copper proteins that have been previously structurally characterised are similar in having the open end, which possesses methionine and histidine residues. Csp3 from *M. trichosporium* has these methionine and histidines present only at one end, with the other end closed by hydrophobic residues. Based on the reported results in Vita et al., 2016, indeed, an argument was made the cytosolic proteins use primarily histidine residues t this open end and the periplasmic proteins use predominantly methionine at this opening. The Csp3 from *Salmonella enterica* uses both histidine and methionine at the open end, and similar residues are present at the other, closed end. Interestingly, this arrangement is also present in the *Bacillus* Csp3.

Copper storage proteins are a new protein family that have been reported by Newcastle University scientists in 2015, therefore they have not been studied sufficiently enough to fully understand how these proteins work. It remains unclear how Csp3 functions in copper homeostasis, and whether their function is integrated with any of the proteins known to function in bacterial copper homeostasis such as CopA, CopZ, or the sensors (CsoR, CueR). The only thing has been studied has been whether or not apo *Bs*CopZ can extract copper from *Bs*Csp3 (Vita et al., 2016), which it can although only very slowly. We do know that the bacterial copper homeostatic system is integrated, for example CopA and CopZ function together in effluxing copper, and the expression of the copper homeostasis genes are generally combined into a functional regulon, regulated by a copper sensor, to ensure they're coordinated together. There remain other important questions about the exact role of Csp1 and Csp3 in bacteria, in particular the reason for homologues of these proteins to be localised in different cellular compartments. The answer so far remains unclear, but we hypothesise that this may be for the purpose of supplying Csp-stored copper ions to copper-requiring enzymes that are also differently localised to these bacterial compartments. This may be the reason for there being three distinct Csps in *M. trichosporium*, which is proposed to contain additional subcellular compartments. In summary, it is clear that organisms use Csps in different compartments but the reason remains unknown.

Future studies will need to determine whether the function of Csp proteins in bacterial copper homeostasis relies on the function of other proteins of bacterial copper homeoastsis, such as CopA, CopZ or CueR. The proposed experiment to test this hypothesis would be to compare the phenotype a Csp deletion strain of a bacterium when combined with deletion of those other proteins. For example, does the cell produce more CopA in the absence of Csp? This would imply that copper sequestration by Csp was keeping copper away from the sensor that regulates CopA. Or does the opposite happen, that CopA functions worse in the absence of Csp, i.e. the transporter provides less benefit to a bacterium growing in high copper in a Csp deletion strain? Consequently, that would imply that Csp works synergistically with CopA. Importantly, such experiments should be performed both in non-pathogenic and pathogenic microbes, as it is possible that Csps play different roles in pathogens as they do in non-pathogens

6.9. Potential role of Csps in bacterial virulence

So far, no group has performed virulence experiments to determine whether genes encoding copper storage proteins play an important role in virulence of any pathogenic bacterium. The unavailability of evidence for a role of Csp proteins in virulence makes it currently impossible therefore to draw conclusions on this question. However, we could hypothesise that Csps may play a role in bacterial virulence because it is known that other aspects of bacterial copper homeostasis are crucial for virulence.

Vita and colleagues in 2016 published data that showed that a *Bacillus subtilis* strain lacking its Csp (*Bs*Csp3) has a growth phenotype when cultured in high copper conditions. However, this copper-dependent growth phenotype is very weak and was only observed in late stationary phase of growth. Yet that bacterium has already a characterised copper homeostatic system (consisting of CopA, CopZ and the regulator, CsoR), so this weak phenotype may be a reflection that there is another homeostatic system that dominates or compensates for loss of cCsp3. Therefore, the critical experiment that is required to clarify the function of Csp proteins is not to simply study the

phenotype of Csp-delete strains, but also to study, for example, a *c*copA double deletion, or even a *csp copA copZ* treble deletion strain.

In unpublished data from our lab, my colleague Louisa Stewart made a *csp1*-delete strain of *Neisseria gonorrhoea*. She has not observed a strong growth phenotype of this strain during *in vitro* culture in high copper conditions (unpublished data, personal communication). Likewise, another colleague, Francesca Focarelli, has done similar experiments with *Salmonella* and she also observed no significant phenotype when the *csp3*-delete strain was cultured in high copper conditions (unpublished data, personal communication). This implies that either these proteins play no role in defending their respective cells from copper toxicity, or perhaps that neither gene is expressed during *in vitro* culture conditions. Consequently, the implication is that just comparing the growth of the strain in which *csp* is deleted to the growth of the wild type parent during *in vitro* culture is not the way to understand Csp function. Future studies must use such strains in ex vivo and in vivo infections experiments to determine if these strains show reduced ability to survive attack by the immune system during infection. Nonetheless, I would argue that all of that evidence, in *Bacillus*, *Salmonella*, and *Neisseria*, of the weakness of growth phenotypes of *csp* deletion strains *in vitro* indicates that most likely role for Csp is in storing nutrient copper, not simply in preventing copper toxicity.

6.10. Copper toxicity in bacteria and copper homeostasis genes as antimicrobial targets

Copper, being a heavy metal, can create oxidative stress by making reactive oxygen species (ROS) in cells including bacteria (Svenningsen et al., 2017). ROS can result in protein oxidation, lipid peroxidation and damage to nucleic acid (Solioz et al., 2010). However, copper metal was shown to be more toxic under anaerobic reducing conditions than aerobic conditions (Macomber & Imlay, 2009), demonstrating that ROS cannot be the sole mechanism for copper toxicity in bacteria. Cu(I) is a soft metal and has high affinity for thiolates and subsequently it was shown that copper toxicity can also be caused by it destabilizing iron–sulfur clusters in bacteria (Macomber and Imlay, 2009). Dihydroxy-acid dehydratase (IlvD), in the common branched-chain amino acid synthesis pathway, isopropylmalate dehydratase (LeuC) in the leucine-specific branch, fumarase A (FumA) in the tricarboxylic acid cycle and 6-phosphogluconate dehydratase in the pentose phosphate pathway

(Edd) were found to be inactivated as a result of copper toxicity leading toward the lethal damage (Macomber and Imlay, 2009).

On the other hand, bacteria have evolved mechanisms to prevent copper toxicity. These mechanisms involve primarily transmembrane copper export, moving this ion from the cytoplasm into the periplasmic space or into the extracellular milieu (Rensing et al., 2000), as well as sequestration of copper by metallochaperones and metallothioneins, and oxidation of Cu(I) by multi-copper oxidases to make the less toxic Cu(II) ion (Ladomersky and Petris, 2015). CopA in *E .coli* and *Neisseria gonorrhoeae*, and the homologues CopA and GolT in *Salmonella enteric* are the proteins that play the major role in efflux of copper from cytosol to the periplasmic region (Andersson et al., 2014). *E. coli* CueO (named CuiD in *Salmonella*) is an oxidase that is believed to play a role in oxidizing periplasmic Cu(I) to Cu(II), probably to slow down its accidental entry into the cytoplasm (Grass and Rensing, 2001). Induction of CopA and CueO strongly occur when cells are exposed to moderate levels of copper (Rensing et al., 2000; Outten et al., 2001; Munson et al., 2000). Higher levels additionally activate the Cus system, that moves copper from the periplasm back to the extracellular environment (Munson et al., 2000). There are many reports which reflect that bacterial growth is stunted as a result of copper toxicity (Djoko et al., 2012).

Copper has been in use as an antimicrobial agent against a different number of bacteria. Copper surfaces have been used in healthcare services (clinics, hospitals and diagnostic) to kill bacteria (Prado et al., 2012; Arendsen et al., 2019). It can be used in several forms i.e. solution of copper compounds, powdered and composites (Montero et al., 2019). There are some examples, like door handles and surfaces with direct contact, that may be replaced with copper metal (Palza et al., 2018). It will release the copper ions that cause disruption and damage to bacterial cell walls and membranes as a result of oxidative stress and will kill the bacteria due to toxicity (Grass et al., 2011; Besaury et al., 2013). However, the bacteria may get copper resistance because of enhancing capacity for copper detoxification (Vincent et al., 2016). Copper is also used by the immune system as a weapon to fight infecting bacteria (see Introduction).

Antibiotics generally use one of five approaches, such as cell wall disruption, inhibition of translation (protein synthesis), cell membrane alteration, inhibition of DNA and RNA synthesis or antimetabolite activity (Kapoor et al., 2017; O'Connell, 2001). *Neisseria gonorrhoeae* and *Salmonella* are among the major threats to human health and have been targeted for new antibiotic development.

CopA, and perhaps also copper storage proteins (Csps), are major proteins that effect detoxification of copper in bacteria. *Salmonella* has CopA and Csp3 as a defence against copper toxicity (Giachino and Waldron, 2020). CopA can be targeted for antibiotic development in Gram-negative bacteria (Mandal et al., 2002). Damage to CopA in bacteria leads to their sensitivity to copper and bacteria can be killed more easily when *copA* is inactivated (White et al., 2009). CopA targeted antibiotics could be potentially used for diseases in humans as CopA is highly conserved among bacteria. However, this could be predicted to result in side-effects, as CopA has human homologues, ATP7A and ATP7B, which may also be inhibited by drug molecules that target bacterial CopA. Conversely, Csps such as those in *N. gonorrhoeae* and *Salmonella* could be better antibiotic targets without side effects to humans, as there is no homologue to Csp in human genome.

Our lab has acquired data in *Salmonella* that indicates that Salmonella Csp really is important to fight immune cells, as strains lacking *csp3* are more sensitive to killing by macrophages *in vitro*. This indicates it might be a suitable drug target. No data has yet been acquired that indicates whether or not *N. gonorrhoeae* Csp1 could also be a drug target, so further experiments are needed to determine this.

REFERENCES

Abou Zeid, C. & Kaler, S. G. 2019. Normal Human Copper Metabolism. *Wilson Disease.* Elsevier.

Achard, M. E., Tree, J. J., Holden, J. A., Simpfendorfer, K. R., Wijburg, O. L., Strugnell, R. A., Schembri, M. A., Sweet, M. J., Jennings, M. P. & McEwan, A. G. 2010. The multi-copper-ion oxidase CueO of Salmonella enterica serovar Typhimurium is required for systemic virulence. *Infection and immunity,* 78(5)**,** pp 2312-2319.

Ahmed, A. M., Younis, E. E., Ishida, Y. & Shimamoto, T. 2009. Genetic basis of multidrug resistance in Salmonella enterica serovars Enteritidis and Typhimurium isolated from diarrheic calves in Egypt. *Acta tropica,* 111(2)**,** pp 144-149.

Alquethamy, S. F., Khorvash, M., Pederick, V. G., Whittall, J. J., Paton, J. C., Paulsen, I. T., Hassan, K. A., McDevitt, C. A. & Eijkelkamp, B. A. 2019. The role of the CopA copper efflux system in Acinetobacter baumannii virulence. *International journal of molecular sciences,* 20(3)**,** pp 575.

Anastasiadou, D., Psomas, G., Kalogiannis, S., Geromichalos, G., Hatzidimitriou, A. G. & Aslanidis, P. 2019. Bi-and trinuclear copper (I) compounds of 2, 2, 5, 5-tetramethyl-imidazolidine-4-thione and 1, 2-bis (diphenylphosphano) ethane: Synthesis, crystal structures, in vitro and in silico study of antibacterial activity and interaction with DNA and albumins. *Journal of inorganic biochemistry,* 198(110750.

Andersson, M., Mattle, D., Sitsel, O., Klymchuk, T., Nielsen, A. M., Møller, L. B., White, S. H., Nissen, P. & Gourdon, P. 2014. Copper-transporting P-type *ATPases* use a unique ion-release pathway. *Nature structural & molecular biology,* 21(1)**,** pp 43-48.

Andrei, A., Öztürk, Y., Khalfaoui-Hassani, B., Rauch, J., Marckmann, D., Trasnea, P.-I., Daldal, F. & Koch, H.-G. 2020. Cu Homeostasis in Bacteria: The Ins and Outs. *Membranes,* 10(9)**,** pp 242.

Arendsen, L. P., Thakar, R. & Sultan, A. H. 2019. The use of copper as an antimicrobial agent in health care, including obstetrics and gynecology. *Clinical microbiology reviews,* 32(4)**,** pp e00125-18.

Arenz, S. & Wilson, D. N. 2016. Bacterial Protein Synthesis as a Target for Antibiotic Inhibition. *Cold Spring Harbor perspectives in medicine,* 6(9)**,** pp a025361.

Arguello, J. M., Raimunda, D. & Padilla-Benavides, T. 2013. Mechanisms of copper homeostasis in bacteria. *Frontiers in cellular and infection microbiology,* 3(73.

Arredondo, M. & Núñez, M. T. 2005. Iron and copper metabolism. *Molecular aspects of medicine,* 26(4-5)**,** pp 313-327.

Axelsen, K. B. & Palmgren, M. G. 1998. Evolution of substrate specificities in the P-type ATPase superfamily. *Journal of molecular evolution,* 46(1)**,** pp 84-101.

Axelsen, K. B. & Palmgren, M. G. 2001. Inventory of the superfamily of P-type ion pumps in Arabidopsis. *Plant physiology,* 126(2)**,** pp 696-706.

Baker, J., Sengupta, M., Jayaswal, R. K. & Morrissey, J. A. 2011. The Staphylococcus aureus CsoR regulates both chromosomal and plasmid-encoded copper resistance mechanisms. *Environmental microbiology,* 13(9)**,** pp 2495-2507.

Balamurugan, K. & Schaffner, W. 2006. Copper homeostasis in eukaryotes: teetering on a tightrope. *Biochimica et Biophysica Acta (BBA)-Molecular Cell Research,* 1763(7)**,** pp 737-746.

Balasubramanian, R., Smith, S. M., Rawat, S., Yatsunyk, L. A., Stemmler, T. L. & Rosenzweig, A. C. 2010. Oxidation of methane by a biological dicopper centre. *Nature,* 465(7294)**,** pp 115-119.

Banci, L., Bertini, I., Cantini, F., Migliardi, M., Natile, G., Nushi, F. & Rosato, A. 2009. Solution structures of the actuator domain of ATP7A and ATP7B, the Menkes and Wilson disease proteins. *Biochemistry,* 48(33)**,** pp 7849-7855.

Banci, L., Bertini, I., Ciofi-Baffoni, S., Kozyreva, T., Zovo, K. & Palumaa, P. 2010. Affinity gradients drive copper to cellular destinations. *Nature,* 465(7298)**,** pp 645-648.

Banci, L., Bertini, I., Del Conte, R., Markey, J. & Ruiz-Dueñas, F. J. 2001. Copper trafficking: the solution structure of Bacillus subtilis CopZ. *Biochemistry,* 40(51)**,** pp 15660-15668.

Bandyopadhyay, U., Das, D. & Banerjee, R. K. 1999. Reactive oxygen species: oxidative damage and pathogenesis. *Current science,* 658-666.

Barry, A., Jones, R., Thornsberry, C., Ayers, L. W., Gerlach, E. & Sommers, H. 1984. Antibacterial activities of ciprofloxacin, norfloxacin, oxolinic acid, cinoxacin, and nalidixic acid. *Antimicrobial Agents and Chemotherapy,* 25(5)**,** pp 633.

Baslé, A., El Ghazouani, A., Lee, J. & Dennison, C. 2018. Insight into metal removal from peptides that sequester copper for methane oxidation. *Chemistry (Weinheim an der Bergstrasse, Germany),* 24(18)**,** pp 4515.

Baslé, A., Platsaki, S. & Dennison, C. 2017. Visualizing Biological Copper Storage: The Importance of Thiolate-Coordinated Tetranuclear Clusters. *Angewandte Chemie,* 129(30)**,** pp 8823-8826.

Bäumler, A. & Fang, F. C. 2013. Host specificity of bacterial pathogens. *Cold Spring Harbor perspectives in medicine,* 3(12)**,** pp a010041.

Berks, B. C., Sargent, F. & Palmer, T. 2000. The Tat protein export pathway. *Molecular microbiology,* 35(2)**,** pp 260-274.

Besaury, L., Bodilis, J., Delgas, F., Andrade, S., De la Iglesia, R., Ouddane, B. & Quillet, L. 2013. Abundance and diversity of copper resistance genes cusA and copA in microbial communities in relation to the impact of copper on Chilean marine sediments. *Marine pollution bulletin,* 67(1-2)**,** pp 16-25.

Bleves, S., Viarre, V., Salacha, R., Michel, G. P., Filloux, A. & Voulhoux, R. 2010. Protein secretion systems in Pseudomonas aeruginosa: a wealth of pathogenic weapons. *International Journal of Medical Microbiology,* 300(8)**,** pp 534-543.

Borkow, G. & Gabbay, J. 2009. Copper, an ancient remedy returning to fight microbial, fungal and viral infections. *Current Chemical Biology,* 3(3)**,** pp 272-278.

Braymer, J. J. & Giedroc, D. P. 2014. Recent developments in copper and zinc homeostasis in bacterial pathogens. *Current opinion in chemical biology,* 19(59-66.

Bult, C. J., White, O., Olsen, G. J., Zhou, L., Fleischmann, R. D., Sutton, G. G., Blake, J. A., FitzGerald, L. M., Clayton, R. A. & Gocayne, J. D. 1996. Complete genome sequence of the methanogenic archaeon, Methanococcus jannaschii. *Science,* 273(5278)**,** pp 1058-1073.

Burkhead, J. L., Gogolin Reynolds, K. A., Abdel-Ghany, S. E., Cohu, C. M. & Pilon, M. 2009. Copper homeostasis. *New Phytologist,* 182(4)**,** pp 799-816.

Caldelari, I., Mann, S., Crooks, C. & Palmer, T. 2006. The Tat pathway of the plant pathogen Pseudomonas syringae is required for optimal virulence. *Molecular plant-microbe interactions,* 19(2)**,** pp 200-212.

Calderone, V., Dolderer, B., Hartmann, H.-J., Echner, H., Luchinat, C., Del Bianco, C., Mangani, S. & Weser, U. 2005. The crystal structure of yeast copper thionein: the solution of a long-lasting enigma. *Proceedings of the National Academy of Sciences,* 102(1)**,** pp 51-56.

Cao, L., Caldararu, O., Rosenzweig, A. C. & Ryde, U. 2018. Quantum refinement does not support dinuclear copper sites in crystal structures of particulate methane monooxygenase. *Angewandte Chemie International Edition,* 57(1)**,** pp 162-166.

Carstens, C. K., Salazar, J. K. & Darkoh, C. 2019. Multistate outbreaks of foodborne illness in the United States associated with fresh produce from 2010 to 2017. *Frontiers in microbiology,* 10(2667.

Chang, F.-M. J., Coyne, H. J., Cubillas, C., Vinuesa, P., Fang, X., Ma, Z., Ma, D., Helmann, J. D., García-de los Santos, A. & Wang, Y.-X. 2014. Cu (I)-mediated allosteric switching in a copper-sensing operon repressor (CsoR). *Journal of Biological Chemistry,* 289(27)**,** pp 19204-19217.

Changela, A., Chen, K., Xue, Y., Holschen, J., Outten, C. E., O'Halloran, T. V. & Mondragón, A. 2003. Molecular basis of metal-ion selectivity and zeptomolar sensitivity by CueR. *Science,* 301(5638)**,** pp 1383-1387.

Chappell, L., Kaiser, P., Barrow, P., Jones, M. A., Johnston, C. & Wigley, P. 2009. The immunobiology of avian systemic salmonellosis. *Veterinary immunology and immunopathology,* 128(1-3)**,** pp 53-59.

Checa, S. K., Espariz, M., Audero, M. E. P., Botta, P. E., Spinelli, S. V. & Soncini, F. C. 2007. Bacterial sensing of and resistance to gold salts. *Molecular microbiology,* 63(5)**,** pp 1307-1318.

Choi, J. H., Keum, K. C. & Lee, S. Y. 2006. Production of recombinant proteins by high cell density culture of Escherichia coli. *Chemical engineering science,* 61(3)**,** pp 876-885.

Choudhury, F. K., Rivero, R. M., Blumwald, E. & Mittler, R. 2017. Reactive oxygen species, abiotic stress and stress combination. *The Plant Journal,* 90(5)**,** pp 856-867.

Cobine, P. A., Ojeda, L. D., Rigby, K. M. & Winge, D. R. 2004. Yeast contain a non-proteinaceous pool of copper in the mitochondrial matrix. *Journal of Biological Chemistry,* 279(14)**,** pp 14447-14455.

Coburn, B., Li, Y., Owen, D., Vallance, B. A. & Finlay, B. B. 2005. Salmonella enterica serovar Typhimurium pathogenicity island 2 is necessary for complete virulence in a mouse model of infectious enterocolitis. *Infection and immunity,* 73(6)**,** pp 3219.

Control, C. f. D. & Prevention (2012). Update to CDC's sexually transmitted diseases treatment guidelines, 2010: oral cephalosporins no longer a recommended treatment for gonococcal infections. MMWR. Morbidity and mortality weekly report, 61(31)**,** 590-594.

Corbett, D., Schuler, S., Glenn, S., Andrew, P. W., Cavet, J. S. & Roberts, I. S. 2011. The combined actions of the copper-responsive repressor CsoR and copper-metallochaperone CopZ modulate CopA-mediated copper efflux in the intracellular pathogen Listeria monocytogenes. *Molecular microbiology,* 81(2)**,** pp 457-472.

Cornelis, P., Wei, Q., Andrews, S. C. & Vinckx, T. 2011. Iron homeostasis and management of oxidative stress response in bacteria. *Metallomics,* 3(6)**,** pp 540-549.

Cotruvo Jr, J. A., Aron, A. T., Ramos-Torres, K. M. & Chang, C. J. 2015. Synthetic fluorescent probes for studying copper in biological systems. *Chemical Society Reviews,* 44(13)**,** pp 4400-4414.

Cremer, P. S., Flood, A. H., Gibb, B. C. & Mobley, D. L. 2018. Collaborative routes to clarifying the murky waters of aqueous supramolecular chemistry. *Nature chemistry,* 10(1)**,** pp 8-16.

Dai, Y., Yang, Z., Cheng, S., Wang, Z., Zhang, R., Zhu, G., Wang, Z., Yung, B. C., Tian, R. & Jacobson, O. 2018. Toxic reactive oxygen species enhanced synergistic combination therapy by self-assembled metal-phenolic network nanoparticles. *Advanced Materials,* 30(8)**,** pp 1704877.

Darwin, K. H. 2015. Mycobacterium tuberculosis and copper: a newly appreciated defense against an old foe? *Journal of Biological Chemistry,* 290(31)**,** pp 18962-18966.

Dassama, L. M., Kenney, G. E., Ro, S. Y., Zielazinski, E. L. & Rosenzweig, A. C. 2016. Methanobactin transport machinery. *Proceedings of the National Academy of Sciences,* 113(46)**,** pp 13027-13032.

Dassama, L. M., Kenney, G. E. & Rosenzweig, A. C. 2017. Methanobactins: from genome to function. *Metallomics,* 9(1)**,** pp 7-20.

De Graaf, A. J., Kooijman, M., Hennink, W. E. & Mastrobattista, E. 2009. Nonnatural amino acids for site-specific protein conjugation. *Bioconjugate chemistry,* 20(7)**,** pp 1281-1295.

De Keyzer, J., Van Der Does, C. & Driessen, A. 2003. The bacterial translocase: a dynamic protein channel complex. *Cellular and Molecular Life Sciences CMLS,* 60(10)**,** pp 2034-2052.

Dennison, C., David, S. & Lee, J. 2018. Bacterial copper storage proteins. *Journal of Biological Chemistry,* 293(13)**,** pp 4616-4627.

Desai, P. T., Porwollik, S., Long, F., Cheng, P., Wollam, A., Clifton, S. W., Weinstock, G. M. & McClelland, M. 2013. Evolutionary genomics of Salmonella enterica subspecies. *MBio,* 4(2)**,** pp.

Dieye, Y., Ameiss, K., Mellata, M. & Curtiss, R. 2009. The Salmonella Pathogenicity Island (SPI) 1 contributes more than SPI2 to the colonization of the chicken by Salmonella enterica serovar Typhimurium. *BMC microbiology,* 9(1)**,** pp 1-14.

Djoko, K. Y., Cheryl-lynn, Y. O., Walker, M. J. & McEwan, A. G. 2015. The role of copper and zinc toxicity in innate immune defense against bacterial pathogens. *Journal of Biological Chemistry,* 290(31)**,** pp 18954-18961.

Djoko, K. Y., Franiek, J. A., Edwards, J. L., Falsetta, M. L., Kidd, S. P., Potter, A. J., Chen, N. H., Apicella, M. A., Jennings, M. P. & McEwan, A. G. 2012. Phenotypic characterization of a copA mutant of Neisseria gonorrhoeae identifies a link between copper and nitrosative stress. *Infection and immunity,* 80(3)**,** pp 1065-1071.

Dougan, G. & Baker, S. 2014. Salmonella enterica serovar Typhi and the pathogenesis of typhoid fever. *Annual review of microbiology,* 68(317-336.

Doyle, M. E. 2015. Multidrug-resistant pathogens in the food supply. *Foodborne Pathogens and Disease,* 12(4)**,** pp 261-279.

Drees, S. L., Beyer, D. F., Lenders-Lomscher, C. & Lübben, M. 2015. Distinct functions of serial metal-binding domains in the E scherichia coli P 1 B-ATP ase CopA. *Molecular microbiology,* 97(3)**,** pp 423-438.

Drees, S. L., Klinkert, B., Helling, S., Beyer, D. F., Marcus, K., Narberhaus, F. & Lübben, M. 2017. One gene, two proteins: coordinated production of a copper chaperone by differential transcript formation and translational frameshifting in Escherichia coli. *Molecular microbiology,* 106(4)**,** pp 635-645.

Edwards, J. L. 2010. Neisseria gonorrhoeae survival during primary human cervical epithelial cell infection requires nitric oxide and is augmented by progesterone. *Infection and immunity,* 78(3)**,** pp 1202-1213.

El Ghazouani, A., Basle, A., Firbank, S. J., Knapp, C. W., Gray, J., Graham, D. W. & Dennison, C. 2011. Copper-binding properties and structures of methanobactins from Methylosinus trichosporium OB3b. *Inorganic chemistry,* 50(4)**,** pp 1378-1391.

Emsley, J. W. & Lindon, J. C. 2018. *NMR spectroscopy using liquid crystal solvents*: Elsevier.

Eng, S.-K., Pusparajah, P., Ab Mutalib, N.-S., Ser, H.-L., Chan, K.-G. & Lee, L.-H. 2015. Salmonella: a review on pathogenesis, epidemiology and antibiotic resistance. *Frontiers in Life Science,* 8(3)**,** pp 284-293.

Eschenbach, D. A., Buchanan, T. M., Pollock, H. M., Forsyth, P. S., Alexander, E. R., Lin, J.-s., Wang, S.-p., Wentworth, B. B., McCormack, W. M. & Holmes, K. K. 1975. Polymicrobial etiology of acute pelvic inflammatory disease. *New England Journal of Medicine,* 293(4)**,** pp 166-171.

Evangelopoulou, G., Kritas, S., Govaris, A. & Burriel, A. R. 2013. Animal salmonelloses: a brief review of "host adaptation and host specificity" of *Salmonella spp*. *Veterinary world,* 6(10)**,** pp 703.

Festa, R. A. & Thiele, D. J. 2011. Copper: an essential metal in biology. *Current Biology,* 21(21)**,** pp R877-R883.

Festa, R. A. & Thiele, D. J. 2012. Copper at the front line of the host-pathogen battle. *PLoS Pathogen,* 8(9)**,** pp.

Frain, K. M., Robinson, C. & van Dijl, J. M. 2019. Transport of Folded Proteins by the Tat System. *The Protein Journal,* 38(4)**,** pp 377-388.

Francis, M. S. & Thomas, C. J. 1997. Mutants in the CtpA copper transporting P-type ATPase reduce virulence ofListeria monocytogenes. *Microbial pathogenesis,* 22(2)**,** pp 67-78.

Franke, S., Grass, G., Rensing, C. & Nies, D. H. 2003. Molecular analysis of the copper-transporting efflux system CusCFBA of Escherichia coli. *Journal of bacteriology,* 185(13)**,** pp 3804-3812.

Freudl, R. 2018. Signal peptides for recombinant protein secretion in bacterial expression systems. *Microbial Cell Factories,* 17(1)**,** pp 1-10.

Fu, Y., Chang, F.-M. J. & Giedroc, D. P. 2014. Copper transport and trafficking at the host–bacterial pathogen interface. *Accounts of chemical research,* 47(12)**,** pp 3605-3613.

Galán, J. E. 2001. Salmonella interactions with host cells: type III secretion at work. *Annual review of cell and developmental biology,* 17(1)**,** pp 53-86.

Gaballa, A., Cao, M. & Helmann, J. D. (2003). Two MerR homologues that affect copper induction of the Bacillus subtiliscopZA operon. Microbiology, 149(12)**,** 3413-3421.

Gaballa, A. & Helmann, J. D. (2003). Bacillus subtilis CPx-type ATPases: characterization of Cd, Zn, Co and Cu efflux systems. Biometals, 16(4)**,** 497-505.

Gerber, J., Neumann, K., Prohl, C., Mühlenhoff, U. & Lill, R. 2004. The yeast scaffold proteins Isu1p and Isu2p are required inside mitochondria for maturation of cytosolic Fe/S proteins. *Molecular and cellular biology,* 24(11)**,** pp 4848-4857.

Gerlach, R. G. & Hensel, M. 2007. Salmonella pathogenicity islands in host specificity, host pathogen-interactions and antibiotics resistance of Salmonella enterica. *Berliner und Munchener tierarztliche Wochenschrift,* 120(7/8)**,** pp 317.

Giachino, A. & Waldron, K. J. 2020. Copper tolerance in bacteria requires the activation of multiple accessory pathways. *Molecular microbiology,* 114(3)**,** pp 377-390.

Gold, B., Deng, H., Bryk, R., Vargas, D., Eliezer, D., Roberts, J., Jiang, X. & Nathan, C. 2008. Identification of a copper-binding metallothionein in pathogenic mycobacteria. *Nature chemical biology,* 4(10)**,** pp 609-616.

Gómez-Gallego, T., Benabdellah, K., Merlos, M. A., Jiménez-Jiménez, A. M., Alcon, C., Berthomieu, P. & Ferrol, N. 2019. The Rhizophagus irregularis genome encodes two CTR copper transporters that mediate Cu import into the cytosol and a CTR-like protein likely involved in copper tolerance. *Frontiers in plant science,* 10(604.

Gómez-Mendikute, A. & Cajaraville, M. 2003. Comparative effects of cadmium, copper, paraquat and benzo [a] pyrene on the actin cytoskeleton and production of reactive oxygen species (ROS) in mussel haemocytes. *Toxicology in vitro,* 17(5-6)**,** pp 539-546.

Grass, G. & Rensing, C. 2001. CueO is a multi-copper oxidase that confers copper tolerance in Escherichia coli. *Biochemical and biophysical research communications,* 286(5)**,** pp 902-908.

Grass, G., Rensing, C. & Solioz, M. 2011. Metallic copper as an antimicrobial surface. *Applied and environmental microbiology,* 77(5)**,** pp 1541-1547.

Grass, G., Thakali, K., Klebba, P. E., Thieme, D., Müller, A., Wildner, G. n. F. & Rensing, C. 2004. Linkage between catecholate siderophores and the multicopper oxidase CueO in Escherichia coli. *Journal of bacteriology,* 186(17)**,** pp 5826-5833.

Gu, W. & Semrau, J. D. 2017. Copper and cerium-regulated gene expression in Methylosinus trichosporium OB3b. *Applied microbiology and biotechnology,* 101(23)**,** pp 8499-8516.

Gudipaty, S. A. & McEvoy, M. M. 2014. The histidine kinase CusS senses silver ions through direct binding by its sensor domain. *Biochimica et Biophysica Acta (BBA)-Proteins and Proteomics,* 1844(9)**,** pp 1656-1661.

Gupta, S., Read, S. A., Shackel, N. A., Hebbard, L., George, J. & Ahlenstiel, G. 2019. The role of micronutrients in the infection and subsequent response to hepatitis C virus. *Cells,* 8(6)**,** pp 603.

Hartman, H. B., Fell, D. A., Rossell, S., Jensen, P. R., Woodward, M. J., Thorndahl, L., Jelsbak, L., Olsen, J. E., Raghunathan, A. & Daefler, S. 2014. Identification of potential drug targets in Salmonella enterica sv. Typhimurium using metabolic modelling and experimental validation. *Microbiology,* 160(6)**,** pp 1252-1266.

Hassan, R., Whitney, B., Williams, D., Holloman, K., Grady, D., Thomas, D., Omoregie, E., Lamba, K., Leeper, M. & Gieraltowski, L. 2019. Multistate outbreaks of Salmonella infections linked to imported Maradol papayas–United States, December 2016–September 2017. *Epidemiology & Infection,* 147(

Hasselbach, W. 1961. Die Calciumpumpe der'Erschlaffungsgrana'des Muskels und ihre Abhangigkeit von der ATP-Spaltung [The calcium pump of the" relaxing granules" of muscle and its dependence on ATP-splitting]. *Biochem Z.,* 333(518-528.

Haynes, C. A. & Gonzalez, R. 2014. Rethinking biological activation of methane and conversion to liquid fuels. *Nature chemical biology,* 10(5)**,** pp 331-339.

Health, U. D. o. & Services, H. 2012. Sexually transmitted disease surveillance 2012. *National Center for HIV/AIDS VH, STD and TB Prevention, ed. Washington, DC: US Department of Health and Human Services*.

Hedemann, M. S., Mikkelsen, L. L., Naughton, P. & Jensen, B. B. 2005. Effect of feed particle size and feed processing on morphological characteristics in the small and large intestine of pigs and on adhesion of Salmonella enterica serovar Typhimurium DT12 in the ileum in vitro. *Journal of Animal Science,* 83(7)**,** pp 1554-1562.

Heithoff, D. M., Conner, C. P., Hanna, P. C., Julio, S. M., Hentschel, U. & Mahan, M. J. 1997. Bacterial infection as assessed by in vivo gene expression. *Proceedings of the National Academy of Sciences,* 94(3)**,** pp 934-939.

Hill, S. A., Masters, T. L. & Wachter, J. 2016. Gonorrhea-an evolving disease of the new millennium. *Microbial cell,* 3(9)**,** pp 371.

Hood, M. I. & Skaar, E. P. 2012. Nutritional immunity: transition metals at the pathogen–host interface. *Nature Reviews Microbiology,* 10(8)**,** pp 525-537.

Horn, N. & Tümer, Z. 1999. Molecular genetics of intracellular copper transport. *The Journal of Trace Elements in Experimental Medicine: The Official Publication of the International Society for Trace Element Research in Humans,* 12(4)**,** pp 297-313.

Howell, S. B., Safaei, R., Larson, C. A. & Sailor, M. J. 2010. Copper transporters and the cellular pharmacology of the platinum-containing cancer drugs. *Molecular pharmacology,* 77(6)**,** pp 887-894.

Ibarra, J. A. & Steele-Mortimer, O. 2009. Salmonella--the ultimate insider. Salmonella virulence factors that modulate intracellular survival. *Cellular microbiology,* 11(11)**,** pp 1579-1586.

Ibarra, J. A. & Steele-Mortimer, O. 2009. Salmonella–the ultimate insider. Salmonella virulence factors that modulate intracellular survival. *Cellular microbiology,* 11(11)**,** pp 1579-1586.

Isah, M. B., Goldring, J. D. & Coetzer, T. H. 2020. Expression and copper binding properties of the N-terminal domain of copper P-type ATPases of African trypanosomes. *Molecular and biochemical parasitology,* 235(111245.

Jajere, S. M. 2019. A review of Salmonella enterica with particular focus on the pathogenicity and virulence factors, host specificity and antimicrobial resistance including multidrug resistance. *Veterinary world,* 12(4)**,** pp 504.

Jerse, A. E., Wu, H., Packiam, M., Vonck, R. A., Begum, A. & Garvin, L. E. 2011. Estradiol-treated female mice as surrogate hosts for Neisseria gonorrhoeae genital tract infections. *Frontiers in microbiology,* 2(107.

Jiang, H., Chen, Y., Jiang, P., Zhang, C., Smith, T. J., Murrell, J. C. & Xing, X.-H. 2010. Methanotrophs: multifunctional bacteria with promising applications in environmental bioengineering. *Biochemical Engineering Journal,* 49(3)**,** pp 277-288.

Jones, M. A., Hulme, S. D., Barrow, P. A. & Wigley, P. 2007. The Salmonella pathogenicity island 1 and Salmonella pathogenicity island 2 type III secretion systems play a major role in pathogenesis of systemic disease and gastrointestinal tract colonization of Salmonella enterica serovar Typhimurium in the chicken. *Avian Pathology,* 36(3)**,** pp 199-203.

Kalyuzhnaya, M. G., Puri, A. W. & Lidstrom, M. E. 2015. Metabolic engineering in methanotrophic bacteria. *Metabolic engineering,* 29(142-152.

Kapoor, G., Saigal, S. & Elongavan, A. 2017. Action and resistance mechanisms of antibiotics: A guide for clinicians. *Journal of anaesthesiology, clinical pharmacology,* 33(3)**,** pp 300.

Khor, B., Gardet, A. & Xavier, R. J. 2011. Genetics and pathogenesis of inflammatory bowel disease. *Nature,* 474(7351)**,** pp 307-317.

Kiley, P. J. & Beinert, H. 2003. The role of Fe–S proteins in sensing and regulation in bacteria. *Current opinion in microbiology,* 6(2)**,** pp 181-185.

Kim, B.-E., Nevitt, T. & Thiele, D. J. 2008. Mechanisms for copper acquisition, distribution and regulation. *Nature chemical biology,* 4(3)**,** pp 176-185.

Kim, E.-H., Nies, D. H., McEvoy, M. M. & Rensing, C. 2011. Switch or funnel: how RND-type transport systems control periplasmic metal homeostasis. *Journal of bacteriology,* 193(10)**,** pp 2381-2387.

Kim, H. J., Graham, D. W., DiSpirito, A. A., Alterman, M. A., Galeva, N., Larive, C. K., Asunskis, D. & Sherwood, P. M. 2004. Methanobactin, a copper-acquisition compound from methane-oxidizing bacteria. *Science,* 305(5690)**,** pp 1612-1615.

Knapp, J. S., Ohye, R., Neal, S. W., Parekh, M. C., Higa, H. & Rice, R. J. 1994. Emerging in vitro resistance to quinolones in penicillinase-producing Neisseria gonorrhoeae strains in Hawaii. *Antimicrobial Agents and Chemotherapy,* 38(9)**,** pp 2200-2203.

Knauert, S. & Knauer, K. 2008. The role of reactive oxygen species in copper toxicity to two freshwater green algae 1. *Journal of phycology,* 44(2)**,** pp 311-319.

Krentz, B. D., Mulheron, H. J., Semrau, J. D., DiSpirito, A. A., Bandow, N. L., Haft, D. H., Vuilleumier, S., Murrell, J. C., McEllistrem, M. T. & Hartsel, S. C. 2010. A comparison of methanobactins from Methylosinus trichosporium OB3b and Methylocystis strain SB2 predicts methanobactins are synthesized from diverse peptide precursors modified to create a common core for binding and reducing copper ions. *Biochemistry,* 49(47)**,** pp 10117-10130.

Ladomersky, E., Khan, A., Shanbhag, V., Cavet, J. S., Chan, J., Weisman, G. A. & Petris, M. J. 2017. Host and pathogen copper-transporting P-type ATPases function antagonistically during Salmonella infection. *Infection and immunity,* 85(9)**,** pp e00351-17.

Ladomersky, E. & Petris, M. J. 2015. Copper tolerance and virulence in bacteria. *Metallomics,* 7(6)**,** pp 957-964.

Leone, P. A., Hynes, N. A. & McGovern, B. H. (2013). Epidemiology, pathogenesis, and clinical manifestations of Neisseria gonorrhoeae infection. UpToDate, Basow, DS (Ed), UpToDate, Waltham, MA.

Lai, N. Y., Musser, M. A., Pinho-Ribeiro, F. A., Baral, P., Jacobson, A., Ma, P., Potts, D. E., Chen, Z., Paik, D. & Soualhi, S. 2020. Gut-innervating nociceptor neurons regulate Peyer's patch microfold cells and SFB levels to mediate Salmonella host defense. *Cell,* 180(1)**,** pp 33-49. e22.

Lamas, A., Miranda, J. M., Regal, P., Vázquez, B., Franco, C. M. & Cepeda, A. 2018. A comprehensive review of non-enterica subspecies of Salmonella enterica. *Microbiological research,* 206(60-73.

Laufer, A., Grass, J., Holt, K., Whichard, J., Griffin, P. M. & Gould, L. 2015. Outbreaks of Salmonella infections attributed to beef–United States, 1973–2011. *Epidemiology & Infection,* 143(9)**,** pp 2003-2013.

Leitzinger, C. 2017. *Mitochondrial copper overload in a rat model for Wilson disease is paralleled by upregulated COX17 and can be restored using the bacterial peptide methanobactin.* Technische Universität München.

Lenz, J. D. & Dillard, J. P. 2018. Pathogenesis of Neisseria gonorrhoeae and the host defense in ascending infections of human fallopian tube. *Frontiers in immunology,* 9(2710.

Liu, T., Ramesh, A., Ma, Z., Ward, S. K., Zhang, L., George, G. N., Talaat, A. M., Sacchettini, J. C. & Giedroc, D. P. 2007. CsoR is a novel Mycobacterium tuberculosis copper-sensing transcriptional regulator. *Nature chemical biology,* 3(1)**,** pp 60-68.

Lombardi, A. 2015. Simple structure, complex function. *Nature chemical biology,* 11(10)**,** pp 760-761.

Lonergan, Z. R. & Skaar, E. P. 2019. Nutrient zinc at the host–pathogen interface. *Trends in biochemical sciences,* 44(12)**,** pp 1041-1056.

López-Marqués, R. L., Poulsen, L. R., Hanisch, S., Meffert, K., Buch-Pedersen, M. J., Jakobsen, M. K., Pomorski, T. G. & Palmgren, M. G. 2010. Intracellular targeting signals and lipid specificity determinants of the ALA/ALIS P4-ATPase complex reside in the catalytic ALA α-subunit. *Molecular biology of the cell,* 21(5)**,** pp 791-801.

Lopez, J. S., Lee, L. & Mackey, K. R. 2019. The toxicity of copper to Crocosphaera watsonii and other marine phytoplankton: a systematic review. *Frontiers in Marine Science,* 5(511.

Lucas, C. E., Sugawa, C., Riddle, J., Rector, F., Rosenberg, B. & Walt, A. J. 1971. Natural history and surgical dilemma of stress gastric bleeding. *Archives of surgery,* 102(4)**,** pp 266-273.

Lutsenko, S., Barnes, N. L., Bartee, M. Y. & Dmitriev, O. Y. 2007. Function and regulation of human copper-transporting ATPases. *Physiological reviews,* 87(3)**,** pp 1011-1046.

Lutsenko, S., Jayakanthan, S. & Dmitriev, O. Y. 2019. Molecular Architecture of the Copper-Transporting ATPase ATP7B. *Clinical and Translational Perspectives on WILSON DISEASE,* 33-43.

Lutsenko, S. & Petris, M. 2003. Function and regulation of the mammalian copper-transporting ATPases: insights from biochemical and cell biological approaches. *The Journal of membrane biology,* 191(1)**,** pp 1-12.

Ma, Q., Zhai, Y., Schneider, J. C., Ramseier, T. M. & Saier Jr, M. H. 2003. Protein secretion systems of Pseudomonas aeruginosa and P. fluorescens. *Biochimica et Biophysica Acta (BBA)-Biomembranes,* 1611(1-2)**,** pp 223-233.

Macomber, L. & Imlay, J. A. 2009. The iron-sulfur clusters of dehydratases are primary intracellular targets of copper toxicity. *Proceedings of the National Academy of Sciences,* 106(20)**,** pp 8344-8349.

Macomber, L., Rensing, C. & Imlay, J. A. 2007. Intracellular copper does not catalyze the formation of oxidative DNA damage in Escherichia coli. *Journal of bacteriology,* 189(5)**,** pp 1616-1626.

Maisey, K., Nardocci, G., Imarai, M., Cardenas, H., Rios, M., Croxatto, H. B., Heckels, J. E., Christodoulides, M. & Velasquez, L. A. 2003. Expression of proinflammatory cytokines and receptors by human fallopian tubes in organ culture following challenge with Neisseria gonorrhoeae. *Infection and immunity,* 71(1)**,** pp 527-532.

Mandal, A. K., Cheung, W. D. & Argüello, J. M. 2002. Characterization of a Thermophilic P-type Ag+/Cu+-ATPase from the ExtremophileArchaeoglobus fulgidus. *Journal of Biological Chemistry,* 277(9)**,** pp 7201-7208.

McCall, K. A., Huang, C.-c. & Fierke, C. A. 2000. Function and mechanism of zinc metalloenzymes. *The Journal of nutrition,* 130(5)**,** pp 1437S-1446S.

McCoy, L. S., Xie, Y. & Tor, Y. 2011. Antibiotics that target protein synthesis. *Wiley Interdisciplinary Reviews: RNA,* 2(2)**,** pp 209-232.

Meghana, S., Kabra, P., Chakraborty, S. & Padmavathy, N. 2015. Understanding the pathway of antibacterial activity of copper oxide nanoparticles. *RSC advances,* 5(16)**,** pp 12293-12299.

Meydan, S., Klepacki, D., Karthikeyan, S., Margus, T., Thomas, P., Jones, J. E., Khan, Y., Briggs, J., Dinman, J. D. & Vázquez-Laslop, N. 2017. Programmed ribosomal frameshifting generates a copper transporter and a copper chaperone from the same gene. *Molecular cell,* 65(2)**,** pp 207-219.

Miao, E. A., Scherer, C. A., Tsolis, R. M., Kingsley, R. A., Adams, L. G., Bäumler, A. J. & Miller, S. I. 1999. Salmonella typhimurium leucine-rich repeat proteins are targeted to the SPI1 and SPI2 type III secretion systems. *Molecular microbiology,* 34(4)**,** pp 850-864.

Misba, L. & Khan, A. U. 2019. Photodynamic Therapy Against Bacterial Biofilm: Role of Reactive Oxygen Species. *Oxidative Stress in Microbial Diseases.* Springer.

Montero, D. A., Arellano, C., Pardo, M., Vera, R., Gálvez, R., Cifuentes, M., Berasain, M. A., Gómez, M., Ramírez, C. & Vidal, R. M. 2019. Antimicrobial properties of a novel copper-based composite coating with potential for use in healthcare facilities. *Antimicrobial Resistance & Infection Control,* 8(1)**,** pp 3.

Müller, D., Bayer, K. & Mattanovich, D. 2006. Potentials and limitations of prokaryotic and eukaryotic expression systems for recombinant protein production–a comparative view. *Microbial Cell Factories,* 5(1)**,** pp 1-2.

Müller, M. & Bernd Klösgen, R. 2005. The Tat pathway in bacteria and chloroplasts. *Molecular membrane biology,* 22(1-2)**,** pp 113-121.

Munson, G. P., Lam, D. L., Outten, F. W. & O'Halloran, T. V. 2000. Identification of a copper-responsive two-component system on the chromosome of Escherichia coli K-12. *Journal of bacteriology,* 182(20)**,** pp 5864-5871.

Nalewajko, C. & Olaveson, M. M. 1995. Differential responses of growth, photosynthesis, respiration, and phosphate uptake to copper in copper-tolerant and copper-intolerant strains of Scenedesmus acutus (Chlorophyceae). *Canadian Journal of Botany,* 73(8)**,** pp 1295-1303.

Ng, L.-K. & Martin, I. E. 2005. The laboratory diagnosis of Neisseria gonorrhoeae. *Canadian Journal of Infectious Diseases and Medical Microbiology,* 16(1)**,** pp 15-25.

O'Connell, D. 2001. Mechanisms of antibiotic action and resistance. *Trends in Microbiology,* 9(9)**,** pp 410.

Ochman, H. & Groisman, E. A. 1996. Distribution of pathogenicity islands in Salmonella spp. *Infection and immunity,* 64(12)**,** pp 5410.

Odermatt, A., Suter, H., Krapf, R. & Solioz, M. 1993. Primary structure of two P-type ATPases involved in copper homeostasis in Enterococcus hirae. *Journal of Biological Chemistry,* 268(17)**,** pp 12775-12779.

Ong, S. T., Ho, J. Z. S., Ho, B. & Ding, J. L. (2006). Iron-withholding strategy in innate immunity. Immunobiology, 211(4)**,** 295-314.

Organization, W. H. 2012. Global action plan to control the spread and impact of antimicrobial resistance in Neisseria gonorrhoeae.

Osborne, A. R., Rapoport, T. A. & van den Berg, B. 2005. Protein translocation by the Sec61/SecY channel. *Annu. Rev. Cell Dev. Biol.*, 21(529-550.

Osman, D., Waldron, K. J., Denton, H., Taylor, C. M., Grant, A. J., Mastroeni, P., Robinson, N. J. & Cavet, J. S. 2010. Copper homeostasis in Salmonella is atypical and copper-CueP is a major periplasmic metal complex. *Journal of Biological Chemistry,* 285(33)**,** pp 25259-25268.

Outten, F. W., Huffman, D. L., Hale, J. A. & O'Halloran, T. V. 2001. The independent cue and cusSystems confer copper tolerance during aerobic and anaerobic growth inEscherichia coli. *Journal of Biological Chemistry,* 276(33)**,** pp 30670-30677.

Palmer, T. & Berks, B. C. 2003. Moving folded proteins across the bacterial cell membrane. *Microbiology,* 149(3)**,** pp 547-556.

Palmer, T., Sargent, F. & Berks, B. C. 2005. Export of complex cofactor-containing proteins by the bacterial Tat pathway. *Trends in Microbiology,* 13(4)**,** pp 175-180.

Palmgren, M. G. & Axelsen, K. B. 1998. Evolution of P-type ATPases. *Biochimica et Biophysica Acta (BBA)-Bioenergetics,* 1365(1-2)**,** pp 37-45.

Palza, H., Nuñez, M., Bastías, R. & Delgado, K. 2018. In situ antimicrobial behavior of materials with copper-based additives in a hospital environment. *International journal of antimicrobial agents,* 51(6)**,** pp 912-917.

Petersen, C. & Møller, L. B. 2000. Control of copper homeostasis in Escherichia coli by a P-type ATPase, CopA, and a MerR-like transcriptional activator, CopR. *Gene,* 261(2)**,** pp 289-298.

Polishchuk, R. & Lutsenko, S. 2013. Golgi in copper homeostasis: a view from the membrane trafficking field. *Histochemistry and cell biology,* 140(3)**,** pp 285-295.

Pontel, L. B., Audero, M. E. P., Espariz, M., Checa, S. K. & Soncini, F. C. 2007. GolS controls the response to gold by the hierarchical induction of Salmonella-specific genes that include a CBA efflux-coding operon. *Molecular microbiology,* 66(3)**,** pp 814-825.

Pontel, L. B. & Soncini, F. C. 2009. Alternative periplasmic copper-resistance mechanisms in Gram negative bacteria. *Molecular microbiology,* 73(2)**,** pp 212-225.

Porcheron, G., Garénaux, A., Proulx, J., Sabri, M. & Dozois, C. M. 2013. Iron, copper, zinc, and manganese transport and regulation in pathogenic Enterobacteria: correlations between strains, site of infection and the relative importance of the different metal transport systems for virulence. *Frontiers in cellular and infection microbiology,* 3(90.

Porowińska, D., Wujak, M., Roszek, K. & Komoszyński, M. 2013. Prokaryotic expression systems. *Postepy higieny i medycyny doswiadczalnej (Online),* 67(119-129.

Porter, W. L. 1993. Paradoxical behavior of antioxidants in food and biological systems. *Toxicology and Industrial Health,* 9(1-2)**,** pp 93-122.

Pountney, D. L., Schauwecker, I., Zarn, J. & Vasak, M. 1994. Formation of mammalian Cu8-metallothionein in vitro: evidence for the existence of two Cu (I) 4-thiolate clusters. *Biochemistry,* 33(32)**,** pp 9699-9705.

Prado, V., Vidal, R. & Durán, C. 2012. Aplicación de la capacidad bactericida del cobre en la práctica médica. *Revista médica de Chile,* 140(10)**,** pp 1325-1332.

Puig, S. & Thiele, D. J. 2002. Molecular mechanisms of copper uptake and distribution. *Current opinion in chemical biology,* 6(2)**,** pp 171-180.

Purves, J., Thomas, J., Riboldi, G. P., Zapotoczna, M., Tarrant, E., Andrew, P. W., Londoño, A., Planet, P. J., Geoghegan, J. A. & Waldron, K. J. 2018. A horizontally gene transferred copper resistance locus confers hyper-resistance to antibacterial copper toxicity and enables survival of community acquired methicillin resistant Staphylococcus aureus USA300 in macrophages. *Environmental microbiology,* 20(4)**,** pp 1576-1589.

Quillin, S. J. & Seifert, H. S. 2018. Neisseria gonorrhoeae host adaptation and pathogenesis. *Nature Reviews Microbiology,* 16(4)**,** pp 226-240.

Quintana, J., Novoa-Aponte, L. & Argüello, J. M. 2017. Copper homeostasis networks in the bacterium Pseudomonas aeruginosa. *Journal of Biological Chemistry,* 292(38)**,** pp 15691-15704.

Radford, D. S., Kihlken, M. A., Borrelly, G. P., Harwood, C. R., Le Brun, N. E. & Cavet, J. S. 2003. CopZ from Bacillus subtilis interacts in vivo with a copper exporting CPx-type ATPase CopA. *FEMS microbiology letters,* 220(1)**,** pp 105-112.

Rae, T., Schmidt, P., Pufahl, R., Culotta, V. & O'halloran, T. 1999. Undetectable intracellular free copper: the requirement of a copper chaperone for superoxide dismutase. *Science,* 284(5415)**,** pp 805-808.

Rankin, S., Li, Z. & Isberg, R. R. 2002. Macrophage-induced genes of Legionella pneumophila: protection from reactive intermediates and solute imbalance during intracellular growth. *Infection and immunity,* 70(7)**,** pp 3637-3648.

Rensing, C., Fan, B., Sharma, R., Mitra, B. & Rosen, B. P. 2000. CopA: an Escherichia coli Cu (I)-translocating P-type ATPase. *Proceedings of the National Academy of Sciences,* 97(2)**,** pp 652-656.

Rensing, C. & Grass, G. 2003. Escherichia coli mechanisms of copper homeostasis in a changing environment. *FEMS microbiology reviews,* 27(2-3)**,** pp 197-213.

Ridge, P. G., Zhang, Y. & Gladyshev, V. N. 2008. Comparative genomic analyses of copper transporters and cuproproteomes reveal evolutionary dynamics of copper utilization and its link to oxygen. *PloS one,* 3(1)**,** pp e1378.

Robinson, C. & Bolhuis, A. 2004. Tat-dependent protein targeting in prokaryotes and chloroplasts. *Biochimica et Biophysica Acta (BBA)-Molecular Cell Research,* 1694(1-3)**,** pp 135-147.

Robinson, J. D. 1997. Structure and Relatives of the Na+/K+-ATPase. *Moving Questions.* Springer.

Robinson, N. J. & Winge, D. R. 2010. Copper metallochaperones. *Annual review of biochemistry,* 79(537-562.

Rodríguez-Tirado, C., Maisey, K., Rodríguez, F. E., Reyes-Cerpa, S., Reyes-López, F. E. & Imarai, M. 2012. Neisseria gonorrhoeae induced disruption of cell junction complexes in epithelial cells of the human genital tract. *Microbes and infection,* 14(3)**,** pp 290-300.

Rosenzweig, A. C., Frederick, C. A. & Lippard, S. J. 1993. Crystal structure of a bacterial non-haem iron hydroxylase that catalyses the biological oxidation of methane. *Nature,* 366(6455)**,** pp 537-543.

Samanovic, M. I., Ding, C., Thiele, D. J. & Darwin, K. H. 2012. Copper in microbial pathogenesis: meddling with the metal. *Cell host & microbe,* 11(2)**,** pp 106-115.

Santiviago, C. A., Fuentes, J. A., Bueno, S. M., Trombert, A. N., Hildago, A. A., Socias, L. T., Youderian, P. & Mora, G. C. 2002. The Salmonella enterica sv. Typhimurium smvA, yddG and ompD (porin) genes are required for the efficient efflux of methyl viologen. *Molecular microbiology,* 46(3)**,** pp 687-698.

Schlief, M. L. & Gitlin, J. D. 2006. Copper homeostasis in the CNS. *Molecular neurobiology,* 33(2)**,** pp 81-90.

Schwan, W. R., Warrener, P., Keunz, E., Stover, C. K. & Folger, K. R. 2005. Mutations in the cueA gene encoding a copper homeostasis P-type ATPase reduce the pathogenicity of Pseudomonas aeruginosa in mice. *International Journal of Medical Microbiology,* 295(4)**,** pp 237-242.

Seeger, M. A., Schiefner, A., Eicher, T., Verrey, F., Diederichs, K. & Pos, K. M. 2006. Structural asymmetry of AcrB trimer suggests a peristaltic pump mechanism. *Science,* 313(5791)**,** pp 1295-1298.

Seifipour, M., Emadi-Baygi, M., Saffar, B. & Abolmaali, S. 2017. Evaluation of smtA expression and E. coli survival against cadmium ions. *International Journal of Environmental Science and Technology,* 14(3)**,** pp 481-486.

Semrau, J. D., Jagadevan, S., DiSpirito, A. A., Khalifa, A., Scanlan, J., Bergman, B. H., Freemeier, B. C., Baral, B. S., Bandow, N. L. & Vorobev, A. 2013. Methanobactin and MmoD work in concert to act as the 'copper-switch'in methanotrophs. *Environmental microbiology,* 15(11)**,** pp 3077-3086.

Shafeeq, S., Yesilkaya, H., Kloosterman, T. G., Narayanan, G., Wandel, M., Andrew, P. W., Kuipers, O. P. & Morrissey, J. A. 2011. The cop operon is required for copper homeostasis and contributes to virulence in Streptococcus pneumoniae. *Molecular microbiology,* 81(5)**,** pp 1255-1270.

Sharma, A., Gupta, P. & Prabhakar, P. K. 2019. Endogenous repair system of oxidative damage of DNA. *Current Chemical Biology,* 13(2)**,** pp 110-119.

Sharma, A., Sharma, D. & Verma, S. K. 2018. In silico study of iron, zinc and copper binding proteins of Pseudomonas syringae pv. lapsa: emphasis on secreted metalloproteins. *Frontiers in microbiology,* 9(1838.

Shi, X., Festa, R. A., Ioerger, T. R., Butler-Wu, S., Sacchettini, J. C., Darwin, K. H. & Samanovic, M. I. 2014. The copper-responsive RicR regulon contributes to Mycobacterium tuberculosis virulence. *MBio,* 5(1)**,** pp e00876-13.

Singh, S. K., Grass, G., Rensing, C. & Montfort, W. R. 2004. Cuprous oxidase activity of CueO from Escherichia coli. *Journal of bacteriology,* 186(22)**,** pp 7815-7817.

Slayman, C. L., Lu, C. Y.-H. & Shane, L. 1970. Correlated changes in membrane potential and ATP concentrations in Neurospora. *Nature,* 226(5242)**,** pp 274-276.

Smith, A. D., Logeman, B. L. & Thiele, D. J. 2017. Copper acquisition and utilization in fungi. *Annual review of microbiology,* 71(597-623.

Solioz, M. 2018a. *Copper and bacteria: evolution, homeostasis and toxicity*: Springer.

Solioz, M. 2018b. Copper homeostasis in gram-negative bacteria. *Copper and Bacteria.* Springer.

Solioz, M., Abicht, H. K., Mermod, M. & Mancini, S. 2010. Response of Gram-positive bacteria to copper stress. *JBIC Journal of Biological Inorganic Chemistry,* 15(1)**,** pp 3-14.

Solioz, M. & Stoyanov, J. V. 2003. Copper homeostasis in Enterococcus hirae. *FEMS microbiology reviews,* 27(2-3)**,** pp 183-195.

Stephenson, K. 2005. Sec-dependent protein translocation across biological membranes: evolutionary conservation of an essential protein transport pathway. *Molecular membrane biology,* 22(1-2)**,** pp 17-28.

Stoyanov, J. V., Hobman, J. L. & Brown, N. L. 2001. CueR (YbbI) of Escherichia coli is a MerR family regulator controlling expression of the copper exporter CopA. *Molecular microbiology,* 39(2)**,** pp 502-512.

Straw, M. L., Chaplin, A. K., Hough, M. A., Paps, J., Bavro, V. N., Wilson, M. T., Vijgenboom, E. & Worrall, J. A. 2018. A cytosolic copper storage protein provides a second level of copper tolerance in Streptomyces lividans. *Metallomics,* 10(1)**,** pp 180-193.

Svenningsen, N. B., Damgaard, M., Rasmussen, M., Pérez-Pantoja, D., Nybroe, O. & Nicolaisen, M. H. 2017. Cupriavidus pinatubonensis AEO106 deals with copper-induced oxidative stress before engaging in biodegradation of the herbicide 4-chloro-2-methylphenoxyacetic acid. *BMC microbiology,* 17(1)**,** pp 1-10.

Takaya, A., Tomoyasu, T., Matsui, H. & Yamamoto, T. 2004. The DnaK/DnaJ chaperone machinery of Salmonella enterica serovar Typhimurium is essential for invasion of epithelial cells and survival within macrophages, leading to systemic infection. *Infection and immunity,* 72(3)**,** pp 1364.

Taneja, N. 2007. Changing epidemiology of shigellosis and emergence of ciprofloxacin-resistant Shigellae in India. *Journal of clinical microbiology,* 45(2)**,** pp 678.

Theil, E. C. 2011. Ferritin protein nanocages use ion channels, catalytic sites, and nucleation channels to manage iron/oxygen chemistry. *Current opinion in chemical biology,* 15(2)**,** pp 304-311.

Thung, T., Mahyudin, N., Basri, D., Radzi, C. W. M., Nakaguchi, Y., Nishibuchi, M. & Radu, S. 2016. Prevalence and antibiotic resistance of Salmonella Enteritidis and Salmonella Typhimurium in raw chicken meat at retail markets in Malaysia. *Poultry Science,* 95(8)**,** pp 1888-1893.

Tottey, S., Waldron, K. J., Firbank, S. J., Reale, B., Bessant, C., Sato, K., Cheek, T. R., Gray, J., Banfield, M. J. & Dennison, C. 2008. Protein-folding location can regulate manganese-binding versus copper-or zinc-binding. *Nature,* 455(7216)**,** pp 1138-1142.

Ugboko, H. & De, N. 2014. Mechanisms of Antibiotic resistance in Salmonella typhi. *Int J Curr Microbiol App Sci,* 3(12)**,** pp 461-76.

Ulrich, K. & Jakob, U. 2019. The role of thiols in antioxidant systems. *Free Radical Biology and Medicine,* 140(14-27.

Unemo, M. & Shafer, W. M. 2011. Antibiotic resistance in Neisseria gonorrhoeae: origin, evolution, and lessons learned for the future. *Annals of the New York Academy of Sciences,* 1230(E19.

Urvoas, A., Moutiez, M., Estienne, C., Couprie, J., Mintz, E. & Le Clainche, L. 2004. Metal-binding stoichiometry and selectivity of the copper chaperone CopZ from Enterococcus hirae. *European journal of biochemistry,* 271(5)**,** pp 993-1003.

van de Sluis, B. 2019. COMMD1 in Copper Homeostasis. *Clinical and Translational Perspectives on WILSON DISEASE.* Elsevier.

Van den Steen, P. E., Wuyts, A., Husson, S. J., Proost, P., Van Damme, J. & Opdenakker, G. 2003. Gelatinase B/MMP-9 and neutrophil collagenase/MMP-8 process the chemokines

human GCP-2/CXCL6, ENA-78/CXCL5 and mouse GCP-2/LIX and modulate their physiological activities. *European journal of biochemistry,* 270(18)**,** pp 3739-3749.

Van Wart, H. E. & Lin, S. H. 1981. Metal binding stoichiometry and mechanism of metal ion modulation of the activity of porcine kidney leucine aminopeptidase. *Biochemistry,* 20(20)**,** pp 5682-5689.

Vincent, M., Hartemann, P. & Engels-Deutsch, M. 2016. Antimicrobial applications of copper. *International journal of hygiene and environmental health,* 219(7)**,** pp 585-591.

Vita, N., Landolfi, G., Baslé, A., Platsaki, S., Lee, J., Waldron, K. J. & Dennison, C. 2016. Bacterial cytosolic proteins with a high capacity for Cu (I) that protect against copper toxicity. *Scientific reports,* 6(1)**,** pp 1-11.

Vita, N., Platsaki, S., Baslé, A., Allen, S. J., Paterson, N. G., Crombie, A. T., Murrell, J. C., Waldron, K. J. & Dennison, C. 2015. A four-helix bundle stores copper for methane oxidation. *Nature,* 525(7567)**,** pp 140-143.

Volpicella, M., Leoni, C., Manzari, C., Chiara, M., Picardi, E., Piancone, E., Italiano, F., D'Erchia, A., Trotta, M. & Horner, D. 2017. Transcriptomic analysis of nickel exposure in Sphingobium sp. ba1 cells using RNA-seq. *Scientific reports,* 7(1)**,** pp 1-10.

Voulhoux, R., Ball, G., Ize, B., Vasil, M. L., Lazdunski, A., Wu, L. F. & Filloux, A. 2001. Involvement of the twin-arginine translocation system in protein secretion via the type II pathway. *The EMBO journal,* 20(23)**,** pp 6735-6741.

Wagner, D., Maser, J., Lai, B., Cai, Z., Barry, C. E., Zu Bentrup, K. H., Russell, D. G. & Bermudez, L. E. 2005. Elemental analysis of Mycobacterium avium-, Mycobacterium tuberculosis-, and Mycobacterium smegmatis-containing phagosomes indicates pathogen-induced microenvironments within the host cell's endosomal system. *The Journal of Immunology,* 174(3)**,** pp 1491-1500.

Wagner, D., Maser, J., Moric, I., Vogt, S., Kern, W. V. & Bermudez, L. E. 2006. Elemental analysis of the Mycobacterium avium phagosome in Balb/c mouse macrophages. *Biochemical and biophysical research communications,* 344(4)**,** pp 1346-1351.

Waldron, K. J. & Robinson, N. J. 2009. How do bacterial cells ensure that metalloproteins get the correct metal? *Nature Reviews Microbiology,* 7(1)**,** pp 25-35.

Wallis, T. S. & Galyov, E. E. 2000. Molecular basis of Salmonella-induced enteritis: microReview. *Molecular microbiology,* 36(5)**,** pp 997-1005.

Wang, L., Zhu, M., Zhang, Q., Zhang, X., Yang, P., Liu, Z., Deng, Y., Zhu, Y., Huang, X. & Han, L. 2017. Diisonitrile natural product SF2768 functions as a chalkophore that mediates copper acquisition in Streptomyces thioluteus. *ACS chemical biology,* 12(12)**,** pp 3067-3075.

Wang, T. & Guo, Z. 2006. Copper in medicine: homeostasis, chelation therapy and antitumor drug design. *Current medicinal chemistry,* 13(5)**,** pp 525-537.

Ward, S. K., Abomoelak, B., Hoye, E. A., Steinberg, H. & Talaat, A. M. 2010. CtpV: a putative copper exporter required for full virulence of Mycobacterium tuberculosis. *Molecular microbiology,* 77(5)**,** pp 1096-1110.

Weström, L., Joesoef, R., Reynolds, G., Hagdu, A. & Thompson, S. E. 1992. Pelvic inflammatory disease and fertility. A cohort study of 1,844 women with laparoscopically verified disease and 657 control women with normal laparoscopic results. *Sexually transmitted diseases,* 19(4)**,** pp 185-192.

White, C., Lee, J., Kambe, T., Fritsche, K. & Petris, M. J. 2009a. A role for the ATP7A copper-transporting ATPase in macrophage bactericidal activity. *The Journal of biological chemistry,* 284(49)**,** pp 33949-33956.

White, C., Lee, J., Kambe, T., Fritsche, K. & Petris, M. J. 2009b. A role for the ATP7A copper-transporting ATPase in macrophage bactericidal activity. *Journal of Biological Chemistry,* 284(49)**,** pp 33949-33956.

Wickner, W., Driessen, A. J. & Haril, F.-U. 1991. The enzymology of protein translocation across the Escherichia coli plasma membrane. *Annual review of biochemistry,* 60(1)**,** pp 101-124.

Wickner, W. & Schekman, R. 2005. Protein translocation across biological membranes. *Science,* 310(5753)**,** pp 1452-1456.

Wolschendorf, F., Ackart, D., Shrestha, T. B., Hascall-Dove, L., Nolan, S., Lamichhane, G., Wang, Y., Bossmann, S. H., Basaraba, R. J. & Niederweis, M. 2011. Copper resistance is essential for virulence of Mycobacterium tuberculosis. *Proceedings of the National Academy of Sciences,* 108(4)**,** pp 1621-1626.

Wu, X., Leegwater, P. A. & Fieten, H. 2016. Canine models for copper homeostasis disorders. *International journal of molecular sciences,* 17(2)**,** pp 196.

Yen, M.-R., Tseng, Y.-H., Nguyen, E. H., Wu, L.-F. & Saier, M. H. 2002. Sequence and phylogenetic analyses of the twin-arginine targeting (Tat) protein export system. *Archives of microbiology,* 177(6)**,** pp 441-450.

Yu, C. H., Dolgova, N. V. & Dmitriev, O. Y. 2017. Dynamics of the metal binding domains and regulation of the human copper transporters ATP7B and ATP7A. *IUBMB life,* 69(4)**,** pp 226-235.

Zapotoczna, M., Riboldi, G. P., Moustafa, A. M., Dickson, E., Narechania, A., Morrissey, J. A., Planet, P. J., Holden, M. T., Waldron, K. J. & Geoghegan, J. A. 2018. Mobile-genetic-element-encoded hypertolerance to copper protects Staphylococcus aureus from killing by host phagocytes. *MBio,* 9(5)**,** pp e00550-18.

Zhang, Y., Ying, H. & Xu, Y. 2019. Comparative genomics and metagenomics of the metallomes. *Metallomics,* 11(6)**,** pp 1026-1043.

Zhurina, D. 2009. *Identification and partial characterization of transcriptional regulators involved in temperature-dependent expression of levansucrase in Pseudomonas syringae.* Jacobs University Bremen.